2017

Utrecht University

Steenwinkel, N.B.

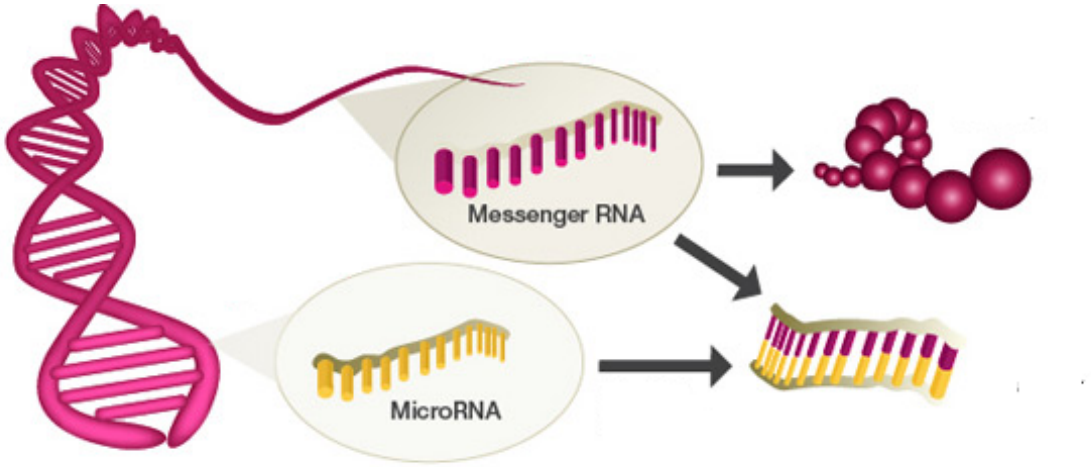

[MICRORNA AND STEMNESS IN CANINE MAMMARY GLAND TISSUE]

TABLE OF CONTENTS

GENERAL INTRODUCTION

Cancer, a disease that has been gaining increasing attention over the years. Not only is the rate of cancer incidences still rising, more is also known with regard to preventive measurements. Smoking has been related to lung cancer, sunray exposure to skin cancer and certain nourishment types are connected to colon or gastric cancer. However, there are also still many tumour types of which the cause is relatively unknown, and thus preventive measurements cannot be part of the remedy. Breast cancer is one of those tumour types, and with being the second most common cancer type found in women from the western world, it is without a doubt a disease worth elucidating.

Over the years, female dogs have tremendously facilitated the investigation of human breast cancer development, due to a strong comparability between canine mammary gland carcinomas and human breast cancer (**Hansen & Khanna, 2004; Pinho et al., 2012; Schneider et al., 1969**). Female dogs are prone to hormone-induced mammary cancer, a cancer type also often seen in women. In fact, spontaneous mammary cancer is the most common type of neoplasm found in female dogs (**Dobson et al., 2002; Merlo et al., 2008; Vascellari et al., 2009**). Additionally, dogs and humans share several environmental factors, which also facilitates comparison (**Wagner et al., 2013**). Until now, a significant role has been assigned to progesterone (P4). P4 expression is inevitable for normal mammary gland development (**Lydon et al., 1995**), so extensive research has been conducted on the working mechanism. For one, P4 leads to an increase in growth hormone (GH) expression, a hormone important to mammary gland development (**Lombardi et al., 2014; Milanese et al., 2006**), and known to cause proliferative events of mammary cells in uncastrated female dogs (**Van Garderen et al., 1999**).

Hormones and other signalling molecules often exert their function through activating or inhibiting certain pathways. One of the pathways attributed to progesterone activity is the Wnt signalling pathway (**Brisken et al., 2000**), a pathway already often linked to proliferation-stimulating and carcinogenic transformations in several organ types (**Pai et al., 2017**). Dogs and humans share this pathway, and in both species seems to be regulated in a comparable manner (**Schneider et al., 1969; Uva et al., 2009**). Through several co-regulators, signalling molecules and effectors the final result of the Wnt pathways comprises increased proliferation, and an enhanced metastatic phenotype. This effect is executed predominantly on stem cells (SC), cells found throughout the body that are immature, and are capable of self-renewal and differentiation (**Reya et al., 2001**). It is this cell type that is held responsible for transformations towards malignancy, and SCs are at present under intensive investigation in an attempt to discover a therapy against the multitude of seemingly incurable carcinogenic diseases.

One approach of cancer investigations is through organoids. Organoids are small cell clusters that originate from SCs. They can be cultured in 3-dimensional culturing systems, and develop into complete mini-organs that can subsequently be used for *ex vivo* disease investigations and drug testing. This *ex vivo* method of investigating circumvents the use of laboratory animals, a method often leading to stress and discomfort for many animals. In light of the fact that The Netherlands is aiming to become the leading country in innovative research methods without using laboratory animals worldwide (**Koëter et al., 2016**), organoids could well form a means for translational research in the medical branch. Eventually, organoids present a means for personalizing cancer treatment. By developing organoids from stem cells obtained from the patient, one is able to investigate drug effect on an organ representation as if in that individual patient. Once this method is widely available and commonly used, it is likely to be employed not only for human medicinal purposes, but may be utilized in veterinary practices as well. Nevertheless, at present research groups are still working to develop and improve on existing organoid models. In fact, there is a large discrepancy between the levels of development between different organ-type based organoids. Liver organoids are ahead of most systems, as they can already be cultured infinitely and have even been applied in interspecies lipid accumulation studies (**Huch M., 2017; Kruitwagen et al., 2017**). Mammary gland models, however, are much less developed, and attempts are still made to determining the optimal culturing conditions for mammary gland organoids. Although focussing on a different tissue type, the Wnt pathway has been found connected to organoid culturing, where higher concentrations of Wnt were linked to increased differentiation status (**Boretto et al., 2017**). Since Wnt has been linked to mammary gland development, and even a connection was found between Wnt levels and induced cancer SC properties (**Skibinski, Kuperwasser, 2015**), in this study the influence of Wnt concentration on canine mammary SC-derived organoids was researched. The aim was to investigate the influence of varying Wnt

concentrations on organoid differentiation level. Additionally, an attempt was made to find a link between mammary gland development level and P4 expression, through studying canine mammary gland tissues immunohistochemically while connecting to blood sample P4 levels. This could aid the research towards the exact role of P4 on mammary gland developmental staging.

Another route towards expanding the knowledge concerning mammary gland development and carcinogenic transformations lies in microRNAs (miRs). MiRs are essential carcinogenic regulators, and have been posed potential risk biomarkers of metastatic developments (**LeBlanc, Morin, 2015**). They are small, 21-24 nucleotides long, non-coding RNA molecules. MiRs are highly conserved between species, and remain stable in several bodily fluids and tissues (**Kakimoto et al., 2015; Mall et al., 2013; Mitchell et al., 2008**). This renders miRs ideal for non-invasive sample acquiring and quantification, something of especially high value in breast cancer since early detection is of crucial importance to a good prognosis and survival chance. Besides, canine and human miRs often connected to disease have been shown to be evolutionary comparable ((**Wagner et al., 2013**)), deeming canine models for miR-related mammary cancer research reliable examples for human breast cancer.

In the cell nucleus, miRs associate with other molecules to constitute a miR-induced silencing complex (miRISC) (**Meister et al., 2004**). This complex ultimately causes alterations in target gene expression through either mRNA degradation or by repressing gene expression at the translational level (**Esquela-Kerscher, Slack, 2006**). MiRs are widely expressed in the mammary gland, although expression levels depend on the developmental stage of the individual. For example, in human beings miRs are most elaborately expressed during puberty. It is during this phase that miRs have been shown to regulate growth, differentiation and apoptosis of mammary cells (**Piao, Ma, 2012**).

A multitude of miRs have shown to be potentially interesting targets for Wnt-pathway related breast cancer research. However, despite the vast number of opted miRs, there is no consensus as to which one, or which selection of miRs from this elaborate pool of possible targets would deem most promising. Thus, after extensive research the choice was made to investigate the miR cluster consisting of miR-96, miR-182 and miR-183. This cluster possessed a significant connection to metastatic breast cancer cells (**Liang & Xi, 2016**), possibly through a relation with the GH receptor, and promotion of epithelial-mesenchymal transition (EMT) (**Zhang et al., 2015**). Research performed on mice yielded evidence of metastasis-promoting characteristics that were attributed to this very same cluster. This has culminated in the selection of miR cluster 96/182/183 as a promising target for breast cancer research, with the aim of connecting miRs related to mammary carcinomas to the Wnt signalling pathway. Subsequently, target genes were chosen based on literature research, with the intention of finding an association between these genes, the Wnt pathway and the selected miRs.

Altogether, this study aims to elucidate the working mechanisms behind the Wnt signalling pathway including related miRs and target genes, to further highlight the role of P4 in mammary gland and cancer development, and additionally to improve upon mammary organoid culturing systems to aid in breast cancer research in future times. Eventually, this study hopes to aid researchers worldwide trying to come up with novel treatment options for cancer victims not responding to the therapies presently available.

Chapter I - miRs, a risk factor for canine mammary cancer metastasis?

Abstract I

Introduction MicroRNAs (miRs) are small, non-coding RNA molecules that facilitate specific mRNA breakdown, thus they may prove to be potential risk biomarkers of breast cancer metastasis. Over the years, the Wnt pathway has been highlighted to exhibit enhancing effects on stem cell proliferation and metastasis formation, aspects closely related to carcinogenic transformation of tissues. These aspects are all connected to one cell type, namely the stem cell. Stem cells exist throughout the body, and are capable of both self-renewal and differentiation. If a cell with these potentials mutates, it has the possibility of shifting towards a cancer stem cell phenotype, a cell that will proliferate without regulation, and is less apt to respond to apoptotic signals. Thus, close research of these stem cells might hold the secret to cancer formation. Female dogs have become established to be of great value in the investigation of breast cancer development. Female dogs are prone to hormone-induced mammary cancer, and early castration results in a decreased incidence of mammary carcinomas. In dogs and humans, progesterone (P4) stimulates the local expression of growth hormone (GH), which has been shown to increase the amount of stem cells in human breast epithelium. P4 also stimulates Wnt expression, contributing to both stemness and metastasis formation.

Aim of the study The aim of this study was to uncover the role of miRs in stemness, by investigating canine mammary carcinoma cell lines. Also, an attempt was made to unravel which miRs are directly connected to the Wnt signalling pathway, to research if these miRs form reliable markers.

Materials and Methods A Dog miFinder microRNA PCR Array was used to screen 12 canine mammary tumour cell lines for miR expression. Based on the outcome of the miR Array, miRs specific for cell lines showing a high basal Wnt signalling were selected, and qPCR was performed on these specific miRs to investigate the influence of Wnt, RSPO and a Src inhibitor, Dasatinib. Both Wnt and RSPO were expected to initiate an increase in Wnt activity, which is believed to be linked to an enhanced likelihood of breast cancer formation, whereas Dasatinib is expected to cause an inhibiting effect on Wnt activity levels. Also an attempt was made to connect the selected miRs to potential target genes.

Results 2 miRs were selected from the miFinder Array results, namely miR-34a and miR-203. These miRs were chosen based on substantial upregulated or downregulated expression in the high basal Wnt active cell lines. Additionally, one miR cluster was chosen based on literature, being the miR cluster 96/182/183. MiR-34a was significantly upregulated after treatment with Wnt CM, and the cluster-96/182/183 showed an explicit increase in expression level in reaction to Dasatinib. miR-203 yielded significant data as well, as the miR both exhibited a significantly upregulating effect on the high Wnt activity cell lines, and miR-203 showed an almost 2.5-fold increase in copy number after the cell lines were treated with Wnt conditioned medium (CM). However, both miR-34a and miR-203 did not respond in a significant manner to Dasatinib treatment. Regarding the target genes, 2 genes displayed significant downregulation in response to Dasatinib, however no effects were obtained resulting from either Wnt or RSPO1 exposure.

Conclusions Contrary to what has been proposed in recent literature, the cluster miR-96/182/183 did not yield significant data after treatment with Wnt. On the other hand, miR-34a did show an increase after Wnt treatment, but contradictory did not respond significantly to Dasatinib. Similar findings were obtained with regard to miR-203. This miR proved a promising target for further investigations. Previous research has already shown that increased circulating miR-203 associated with poor prognosis in breast cancer. Additionally, we found that miR-203 both exerts an important and promising upregulating effect on copy numbers in explicitly the high Wnt cell lines, but the miR also displays a direct connection to the Wnt signalling pathway in subsequent experiments. From this study it can thus be concluded that miR-203 provides the highest potential as marker for Wnt signalling activity, and in order to clarify the exact working mechanism of miR-203 in breast cancer development, further research is warranted. If miRs can indeed be used as cancer markers, or to selectively target cancer cells with seminal new treatment options, this would bring us one step closer to a world without cancer deaths.

Introduction I

Cancer is a disease responsible for many thousands of deaths every year. Although many different types of cancer exist, all tumour formation involves unregulated cell growth, cell division and EMT, often leading to metastasis formation.

However, for tissues to undergo carcinogenic modifications, one specific cell type is required. This is the so called stem cell, an immature cell capable of both self-renewal and differentiation (**Reya et al., 2001**). Stem cells are a necessity in tissue maintenance, and actively participate in the replacement of tissue cells (**Cuiffo et al., 2014**). It is thus thought that these cells form the basis of cancer formation, possibly capable of indefinite proliferation in carcinogenic environments.

As mentioned, unregulated cell proliferation and lack of apoptosis form the essential processes causing breast cancer. These processes originate from gene mutations and dysregulated gene expression. However, the exact mechanism behind these processes remain poorly understood, since many different signalling pathways are involved in regulating cellular functions. Even so, it can be concluded from extensive research that the Wingless-type (Wnt) signalling pathway plays a key role in proliferation, migration and apoptosis (**Pai et al., 2017**).

The Wnt pathway is an evolutionary very stable pathway, with well conserved factors and genes (**Komiya and Habas, 2008**). The pathway is activated under the influence of P4, causing a series of signalling events from the cell wall containing the P4 receptors, to eventually arrive at the nucleus. On its way it encounters several receptors and ligands required for signal transmission, starting off with the frizzled (FZD) receptor in the outer membrane of the cell. The FZD receptor is receptive to lipoprotein receptor related protein 5 or 6 (LPR5/6) (**Kim et al., 2006; Tamai et al., 2000**) to form a FZD/LPR complex. This complex inhibits glycogen synthase kinase 3β (GSK3β), a member of the β-catenin destruction complex comprised of at least GSK3β, Axin, Adenomatous polyposis coli (APC) and Casein kinase 1 a/d (CK1a/d). Thus, when the destruction complex is inhibited, this induces the phosphorylation of β-catenin, the core transducer of the canonical Wnt pathway (**Reya, Clevers, 2005**). Phosphorylated β-catenin leads to stabilization of β-catenin to the destruction complex, saturating all β-catenin binding sites. Newly formed β-catenin will subsequently accumulate in the cytosol, translocate to the nucleus and in turn increase gene expression through T-cell factor (TCF)/Lymphoid enhancer factor (LEF)/β-catenin formation, with altered cell proliferation and differentiation behaviour as final outcome (Fig 1 Wnt signalling pathway) (**Gonzáles-Sancho et al., 2004; Li et al., 2012**).

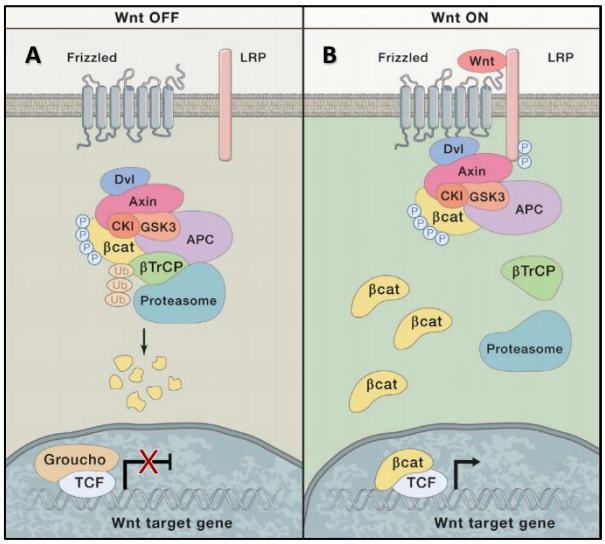

Figure 1 Wnt signalling pathway. (**A**) With the Wnt signalling turned off, the FZD receptor remains unoccupied, which leaves the destruction complex intact. β-cat is phosphorylated and ubiquitinated, rendering it degraded by proteasome. This leaves TCF inactive in the nucleus, resulting in the absence of Wnt target gene transcription; (**B**) Stimulation of the Wnt pathway leading to phosphorylation and stabilisation of β-cat to the destruction complex. Newly produced β-cat accumulates in the cytosol and translocates to the nucleus to form TCF/LEF/β-cat complex.
Nusse, Clevers, 2017

Essentially, the Wnt pathway is of crucial importance to cellular survival and tissue growth. This explicitly highlights the importance of this particular pathway in cell proliferation and differentiation, two aspects clearly associated with stem cells and carcinogenesis.

Still, for any pathway to cause an effect, an initial effector is required. As can be deduced from the previous paragraph, the entire pathway needs first to activate the FZD/LRP5/6 receptor, a function carried out by Wnt proteins. Although there are many Wnt proteins reported, and they may exert slightly varying effects on the pathway, the overall result remains similar in all animals, namely the activation of the Wnt pathway through FZD/LRP receptor complex binding. The ultimate effect of this activation, however, can differ substantially between animals, tissues and may even vary for the same receptor when

activated at a different moment in time. This is due to a variation of co-receptors and their ligands, which may inhibit, stimulate or alter the cascade.

For example, several hormones exert an influence on mammary tissue development, such as growth hormone (GH) and P4. GH is secreted from the pituitary gland, and affects both the epithelial and stromal compartments of the mammary tissue. Stimulation by GH results in elongation and differentiation of the ductal epithelium, leading to end bud formation (**Kleinberg, 1997**; **Walden et al., 1998**). Additionally, several studies have already elucidated a role for GH in aiding oncogenic transformation of epithelial cells through increased cell survival and proliferation (**Mukhina et al., 2004; Zhu et al., 2005**).

Another important co-receptor comprises R-spondin-1 (RSPO1). Notably, accumulating evidence suggests RSPO1 to exert a synergistic effect on Wnt (**Binnerts et al., 2007; Boretto et al., 2017; Kazanskaya et al., 2004; Kim et al., 2006**), by binding to leucine-rich repeat-containing G-protein-coupled receptor 5 (LGR5) (**de Lau et al., 2011; Wang et al., 2013**), thereby enhancing Wnt signalling. LGR5 is the prime receptor mediating RSPO activity (**Carmon et al., 2011**), and seems to employ an adult stem cell marker role in many different tissues (**Barker et al., 2007**).

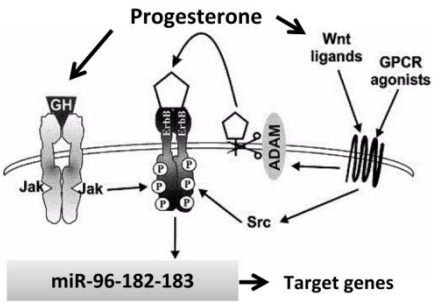

Figure 2 miR-96 cluster mechanism

Yet another important factor in the Wnt signalling pathway involves Src. Src is a known regulator of the Wnt pathway (Fig 2 miR-96 cluster mechanism), and recently published data conveys a role for Src in the regulation of proliferation, migration and invasion of cancer cells (**Sánchez-Bailón et al., 2012; Zhang, Ma et al., 2017**).

Overall it can be stated that the Wnt signalling pathways comprises many different ligands, receptors and co-effectors, and in order to unravel the secrets behind this complex but crucially important pathway, extensive research is required still. Src would seem an interesting target for further investigations, to study the effect of the inhibition of the Wnt pathway through Src inhibitors such as Dasatinib.

In recent years, female dogs have been shown to be of great value in the investigation of breast cancer development, due to a strong similitude between canine mammary gland carcinomas and human breast cancer, both genetically and biologically (**Hansen & Khanna, 2004; Pinho et al., 2012; Schneider et al., 1969**). Also, female dogs are prone to hormone-induced mammary cancer, with early castration leading to a decreased incidence of mammary carcinomas. In fact, in female dogs, the most common type of neoplasm comprises spontaneous cancer of the mammary gland (**Dobson et al., 2002; Merlo et al., 2008; Vascellari et al., 2009**). In addition, dogs are exposed to many similar environmental factors as humans, facilitating comparison between the carcinomas (**Wagner et al., 2013**). In both dogs and humans, stimulation of P4 leads to the local expression of growth hormone (GH). This expression has been shown to increase the number of stem cells in human breast epithelium as well. Causal relations might be sought in the fact that a similarity appears to exist between human and canine regulation of cancer-related pathways, including the Wnt signalling pathway (**Schneider et al., 1969; Uva et al., 2009**). Now the challenge is to determine exactly what part of the pathway can be held responsible for the carcinogenic alterations seen in tumour formation. It is often seen that the effect of a pathway is caused by a modification of gene transcription. The final effector capable of influencing this crucial step in many a pathway is the microRNA (miR).

MiRs were not discovered until the early nineteen nineties (**Lee et al., 1993**), when they were detected in the roundworm *Caenorhabditis elegans*. Until now, over 2000 different miRs have been identified, and since they have shown to be important regulators of carcinogenesis and may form a risk biomarker of cancer metastasis (**LeBlanc, Morin, 2015**), many more are yet to be unveiled.

MiRs are small, non-coding RNA molecules, usually about 21-24 nucleotides long. They are present in nearly all bodily tissues and fluids, including serum, saliva and urine, making them easy targets for non-invasive collection and quantification (**Hanke et al., 2010; Lawrie et al., 2008**). Besides, miRs remain stable in such as in saliva or in formalin-fixed paraffin-embedded (FFPE) tissues conditions (**Kakimoto et al., 2015; Mall et al., 2013; Mitchell et al., 2008**). Mitchell and colleagues also showed that

miRs in plasma are unaffected by up to eight cycles of freeze-thawing (**Mitchell et al., 2008**). Also, miRs are highly conserved between species, but can vary depending on developmental stage and tissue context. Moreover, in the light of the use of miRs in research, Wagner et al showed that most of both human and canine miRs involved in disease are evolutionarily well conserved, deeming female dogs apt models for human breast cancer (**Wagner et al., 2013**). Combined characteristics render miRs ideal targets for both diagnostic testing and hopefully to eventually function as non-invasive biomarkers for both canine and human tumours.

In the nucleus of the cell, mature miRs associate with other proteins to form a miR-induced silencing complex (miRISC) (**Meister et al., 2004**). This complex is then able to bind, through base-pairing, with the targeted transcription factors. Through either destabilisation of messengerRNA (mRNA) sequences or through translational repression the miRISC complex alters target gene expression. The first method functions through cleavage of mRNA by ribonucleases, with mRNA degradation as result. The other approach does not involve cleaving of mRNA. Instead the miRISC binds the targeted mRNA, which ultimately leads to repression of target gene expression at the translational level (**Esquela-Kerscher, Slack, 2006**).

Previous research has demonstrated that miRs are extensively expressed in the mammary gland. In human beings this is seen especially during puberty. In dogs this has unfortunately not been subject of thorough investigation yet. During puberty, miRs act upon the development of the mammary gland by influencing growth, differentiation and cell death (**Piao, Ma, 2012**). Deregulation of miRs in the mammary gland can thus lead to oncogenic transformation, resulting in breast cancer formation.

Breast cancer is one of the main causes of cancer-related deaths in women in the Western World, being the second most common cancer to be diagnosed worldwide (**Ferlay et al., 2015; Siegel et al., 2013**). Metastatic breast cancer causes up to 90% of all breast cancer mortalities (**Gupta, Massagué, 2006**). Over the years it has become clear that early detection and treatment of breast cancer is of invaluable importance. Survival chances decrease drastically with time, even more so than is the case with many other types of cancer. This characteristic of mammary cancer, in addition to the relatively high occurrence in both humans and female dogs, elucidates the importance of novel means of detection and treatment of the disease, in order to improve on both identification speed and treatment efficacy.

Already, several different breast cancer types have been identified, but four main molecular subtypes have unassailably been categorized: luminal A, luminal B, HER2+ and triple negative, with incidence rates of 50–60 %, 10–20 %,, 15–20 %, and 10–20%, respectively (**Borges et al., 2017; Perou et al., 2000**). To uncover the exact role of miRs in relation to this subtype categorisation and carcinogenic transformation properties is the key priority for many researchers. For once discovered, these specific miRs can serve as possible treatment targets for mammary cancer patients. Interestingly, a large number of these investigations have resulted in a promising potential for miRs, in the light of subtype-specific breast cancer detection (**Anfossie et al., 2014; Lowery et al., 2009; McDermott et al., 2014**), for targeting characteristical cancer-related occurrences such as proliferation (**Enerly et al., 2011**), or even prognosis (**Li et al., 2013**), risk of recurrence (**Anfossie et al., 2014; Hoppe et al., 2013; Li et al., 2013**) and metastatic potential (**Avery-Kiejda et al., 2014**). Additionally, miRs have been opted as predictors of treatment response for several cancer types, including breast cancers (**Chen, Tian et al., 2012; Frères et al., 2015; Hoppe et al., 2013**)

A multitude of miRs have already been proposed as interesting targets for Wnt-pathway related breast cancer research. MiR-17 was proposed by **O'Bryan and colleagues**, supposedly causing upregulation of Wnt/β-catenin signalling (**Li et al., 2011; O'Bryan et al., 2017**). In the same review, miR-301 was also suggested, through multiple pathways leading to increased motility and invasion (**Shi et al., 2011**), and miR-374a through promotion of EMT and repression of several Wnt proteins (**Cai et al., 2013**). **Onyido et al** opted for different miRs to investigate. MiR-31 is described to attribute to several important signalling pathways **(Valastyan, Weinberg, 2010)**, and according to Kim and colleagues miR-145 inhibits multiple tumour survivor effectors (**Sachdeva, Mo, 2010; Kim, Oh et al., 2011**). Many more miRs can be suggested to investigate in connection to Wnt-related breast cancer.

Clearly, there is an urgent need for functional, specific biomarkers to enhance breast cancer detection rates. However, despite the vast number of miRs opted as potential biomarkers, both for breast

cancer in general, and even for a variation of subtypes, no conclusive evidence has been obtained regarding one specific miR, or one cluster of specific miRs to further investigate.

Thus, solely based on literature research it would be nearly impossible to ensure an appropriate and accurate selection of miRs related to breast cancer. Chances are one might overlook some potentially very important and valuable miRs, while spending time and effort on other miRs that may prove unfit for this study. So instead of choosing a selection from the many possibilities, we decided on testing all abundantly expressed and characterized miRs available for dogs. The tests were performed on 12 canine mammary tumour cell lines readily available at the lab. These cell lines were particularly suitable for this study, since previous research had elucidated 3 of these 12 cell lines to possess both a high Wnt activity levels (**Gracanin et al., 2014**), positivity for LEF1 and positivity for LGR5, the receptor for the ligand RSPO. These cells contained many characteristics also observed in stem cells, making them appealing targets for breast cancer research.

One potential subject for investigation was already selected beforehand, after extensive literature research performed by my predecessors and supervisors. Namely the miR cluster consisting of miR-96, miR-182 and miR-183, which seemed to possess a direct and strong relation to metastatic breast cancer cells (**Liang & Xi, 2016; Zhang et al., 2015**). Investigations on this cluster not only yielded EMT promoting data, a connection with the GH receptor (GHR) was also observed (**Zhang et al., 2015**), and miR-96/182/183 appeared to initiate distant metastases in mice injected with breast cancer cells. Zhang and colleagues even provided novel evidence that inhibition of the cluster resulted in a remarkable decrease of both colony number and size of cancer cells cultured in matrigel, and also inhibition of cell migration and invasion. These findings all culminate in the believe that miR cluster 96/182/183 poses a promising target for breast cancer treatment, and opt for further investigations into this cluster with regard to working mechanism, target genes, and clinical relevance.

In short, our goal was to perform research on this cluster, and any other miRs related to breast cancer and the Wnt pathway, and investigate its potential in developing a novel diagnostic tool for mammary cancer. Eventually, this study hopes to aid researchers worldwide searching for a new treatment option for cancer victims not responding to the therapies presently available.

Outline of the study

On the basis of recent publications (**Li et al., 2014**; **Zhang et al., 2015**) it seems that the miR cluster 96-182-183 is stimulated by GH and canonical Wnt signalling. Thus this Honours study focused on this cluster as a potential biomarker for breast cancer metastases, and as a means to develop new treatments for cancer patients.

Materials & Methods I

Cell culture & Transfections

12 canine mammary cell lines were used in this study: 7 were established from primary tumours diagnosed as carcinomas (CMT1, CMT-U27 (CMT5), CMT9, P114, CIPp, CHMp, CNMp), three were metastases (CIPm, CHMm, CNMm), one was a benign mixed tumour (CMT3 (CMT-U229)) and one an osteosarcoma-like tumour (CMT-U335) (**Hellmen, 1992**; **Van Leeuwen et al., 1996**; **Uyama et al., 2006**). The cell lines were a generous gift from Prof Dr Hellmen (SLU, Uppsala, Sweden) and Prof. N. Sasaki (Laboratory of Veterinary Surgery, University of Tokyo, Japan).

3 cell lines (CMT1, CMT-U27 (CMT5), CMT9) showed high Wnt activity, 4 (P114, CHMp, CNMp, CNMm) showed moderate Wnt TCF reporter activity and in 5 cell lines (CMT-U229, CMT-U335, CIPp, CIPm and CHMm) Wnt activity was absent (**Gracanin et al., 2014**).

Cell lines were cultured in DMEM/F12 (#11320-074, Gibco, Life technologies, Bleiswijk, The Netherlands)) supplemented with 10% Fetal Bovine Serum (FBS) (#10270-106, Gibco, Life technologies) and 1% Penicillin & Streptomycin (P/S) (#15140-122, Gibco, Life technologies). All cell culture activities were performed in a vertical flow cabinet. The cells were first collected from liquid nitrogen, thawed, and cultured in T75 culture flasks (#658175, Greiner Bio-One, Kremsmünster, Austria). During the first 2 weeks, the cell lines were passaged twice a week, whereas after P3, this was reduced to once a week. Experiments were executed with cells in the growing phase. In order to detach the cell cultures, medium was removed, 10 ml Hank's Balanced Salt Solution (HBSS) (#14025-050, Gibco, Life technologies) was added, swirled around the flask, removed, and 2 ml TrypLE Express (#12604-013, Gibco, Life technologies) was added. Cells were incubated in an Innova CO_2 Incubator (New Brunswick Scientific, Edison, New Jersey, USA) at 37°C and 5% CO_2 for 10 minutes, after which 10 ml culture medium (DMEM/F12 + 10% FBS + 1% P/S) was added.

Due to variance in growth speed and morphology, the cell density and viability were analysed by microscope before each passage. The cells were subsequently passaged at the appropriate seeding concentrations.

TCF-reporter assay

TOPflash, a luciferase reporter plasmid, was used to investigate Wnt activity. Cells were seeded in 24-well plates (#353847, Corning, Primaria, BD Biosciences, Breda, The Netherlands). The cells were seeded at a concentration adjusted to reach 80% density before transfection, being 100.000 cells per well for CMT-U27, and CIPm cells were seeded at 55.000 cells per well. CIPm cells were transfected to ensure the results of the transfection were specific for high basal Wnt activity cell lines. 1 ml DMEM/F12 + 10% FBS + 1% P/S was added. 24 hours later, the cells were washed with 1 ml HBSS, and 400 µl DMEM/F12 was added to each well. Transfection was performed in FBS-free medium, using Lipofectamine 2000 Transfection Reagent (#11668019, Invitrogen, Life technologies), and either pTOPFLASH (TOP) or pFOPFLASH (FOP) (gift from Prof. dr. H Clevers, Hubrecht Institute, The Netherlands). Lipofectamine was added to the TOP and FOP mixes, and 100 µl final mix was added to each well, resulting in a final concentration of 2 µl Lipofectamine, 400 ng TOP or FOP and 1 ng β-actin-promoter-renilla construct (**Doleshaw et al., 2007**) per well. The β-actin-promoter-renilla construct was added as an internal control. The cells were incubated for 5 hours at 37°C at 5% CO_2. After 5 hours the transfection was terminated by adding 100 µl FBS, and the cells were treated with Wnt3a CM (prepared as in **Willert et al., 2003**) 50 µl at 125 µl/ml, Dasatinib (#S1021, Selleck Chemicals, Munich, Germany) 2 µl of 10 mM in DMSO, and RSPO1 CM (the Rspo1-Fc-expressing cell line was a kind gift from Calvin J. Kuo, Stanford University, California) 20 µl at 50 µl/ml, in a final volume of 1 ml.

48 hours after treatment, the cells were washed, and 100 µl 5 times diluted Passive Lysis Buffer (#E1910, Promega, Leiden, The Netherlands) was added to each well. The plates were stirred for 15 minutes and subsequently transferred to a -70°C freezer for 30 minutes. After 30 minutes, the plates were thawed and the lysate was transferred to a V-shape 96-wells plate (#651191, Greiner Bio-one). The plate was centrifuged for 15 minutes at 2900 rpm (rounds per minute). Firefly and renilla luciferase activities were measured using a Dual-Luciferase Assay System (Promega, Leiden, The Netherlands) in a Centro LB 960 luminometer (Berthold Technologies, Vilvoorde, Belgium). 36 µl Luciferase (#E1910, Promega) and 36

µl 50 times diluted Stop & Glo Substrate, 50X) (#E1910, Promega) were added to each well. Depending on treatment, either 5 or 20 µl of the supernatant was pipetted into a white 96-wells plate with a flat bottom (#3600, Corning). From cells treated with Wnt3a CM 5 µl per well was used, due to unreliable high TOP levels when using 20 µl supernatant (the Dual-Luciferase Assay System only gives reliable results up to 1.000.000 RLU (relative light units)).

Differences in TOP and FOP levels were assessed using an unpaired, two-tailed Student's t test in Microsoft Excel 2010. The data were corrected for transfection efficiency by dividing both TOP and FOP data by the β-actin-promoter-renilla construct levels. The TOP/FOP ratio was then calculated by dividing the TOP levels by the FOP levels. All transfection experiments were performed 2 to 4 times, in either threefolds or quadruplicates to obtain more reliable results.

RNA isolation & cDNA synthesis

RNA was isolated using the miRCURY™ RNA Isolation Kit (Exiqon, Vedbaek, Denmark). RNA concentration was measured using Nanodrop spectrophotometer (Thermo Scientific NanoDrop ND-1000, Isogen Life Sciences). Isolated RNA was stored at -20°C.

Wnt signalling was inhibited using the Src inhibitor Dasatinib, or stimulated with Wnt3a CM and RSPO1 CM, and qPCR was performed to measure the effect on miR expression of all 5 miRs.

cDNA synthesis was performed using the miScript II RT Kit (Qiagen, Hilden, Germany), according to the manufacturers protocol. For this purpose, 250 ng total RNA was employed. cDNA was stored either in the fridge or at -20°C, depending on the time until use. Eventually this cDNA was used in the miFinder Array and for specific miR assays.

Resulting from the Array data, target genes were selected in an attempt to uncover a direct connection between these target genes and the chosen miRs. The selection was based on literature research (**Aval et al., 2017**), and cDNA was synthesized using the iScript cDNA Synthesis Kit (Bio-Rad, Veenendaal, The Netherlands), according to manufacturer's protocol.

Gene expression

qPCR was performed on 8 cell lines, 3 of which with high basal Wnt activity (CMT1, CMT-U27, CMT9) and 5 with either moderate (P114, CNMm) or low Wnt activity (CIPp, CIPm, CNMm). A miScript miR PCR Array Dog miFinder (Qiagen) was performed on a total of 84 most abundantly expressed and best characterized miRs in miRBase (www.qiagen.com/nl/shop/pcr/primer-sets/miscript-miR-pcr-arrays/?catno=MIFD-001Z#geneglobe), in order to select miR's unique (either upregulated or downregulated) for the high basal Wnt activity cell lines. The relative expression was measured using the miScript II RT Kit on 384-well plates using the miScript SYBR Green PCR kit (#218160, Qiagen), and a standard amplification protocol according to the manufacturer. qPCR was performed on a 384 Real-Time System (Bio-Rad). Each reaction was performed with 10 µl reaction volume. All reactions were performed in fourfold.

The selected miRs were subsequently tested on all 12 tumour cell lines, with inclusion of an exogenous control for normalisation, to control for variations in for example RNA input differences. As an exogenous control lyophilized *C. elegans* Ce_miR-39_1 miR mimic was used (miRNeasy Serum/Plasma Spike-In Control (10 pmol) (Qiagen)) (for sequences and product numbers, see Table 1 Primer sequences used in quantitative RT-PCR). The relative expression was measured with the miScript II RT Kit, on 386 well plates using the miScript SYBR Green PCR kit and a standard amplification protocol according to the manufacturer. qPCR was performed on a 384 Real-Time System (Bio-Rad). Each reaction was performed with 10 µl reaction volume. All reactions were performed either in duplicate (samples) or in threefold (Spike-In Control) (see Protocol I miRNA pipetting protocol).

Target gene expression was analysed using iQ™ SYBR® Green Supermix (#170-8885, Bio-Rad). PCR was performed following manufacturer's recommendations (iQ™ SYBR® Green Supermix Instruction Manual, Bio-Rad). Relative target gene expression was normalized to a set of 7 reference genes (Table 2 Gene table for Q-PCR primers).

Data analysis for the remaining reactions was performed using CFX Manager 3.1 software (Bio-Rad). The amplification efficiency was selected between 95%-105% for reference genes, and between 90%-110% for target genes. Melt curve temperatures were inspected to ensure single-peak curves, and the No Template Controls were checked to show non available (N/A) Cq-values.

Statistical analysis

Statistical analysis was performed using RStudio (Version 0.99.90, 2009-2016, RStudio, Inc.) Transfection studies were performed in three independent experiments (n = 4 for each transfected/incubation compound). The Wnt-signalling and protein levels were calculated as a percentage of the non-treated cells. A P-value of less than 0.05 was considered significant.

Data analysis of the miScript miR PCR Array Dog miFinder was performed online (http://pcrdataanalysis.sabiosciences.com/miR), following the ΔΔCt method, according to manufacturer's protocol. This included cluster analysis and corresponding heat map formation (http://pcrdataanalysis.sabiosciences.com/miR/arrayanalysis.php?target=clustergram).

With regard to the Wnt, Dasatinib & RSPO1 experiments no alpha-adjustment has been applied, since only a limited number of tests was performed. Thus it was deemed unnecessary to make use of the Bonferroni correction.

Reference genes were tested using the geNorm implementation of the SLqPCR package in R using RStudio (version 3.3.1) (Fig 33 Stability and Variance). Relative expression of the target genes was assessed with the ΔΔCT method (Livak & Schmittgen, 2001).

Results I

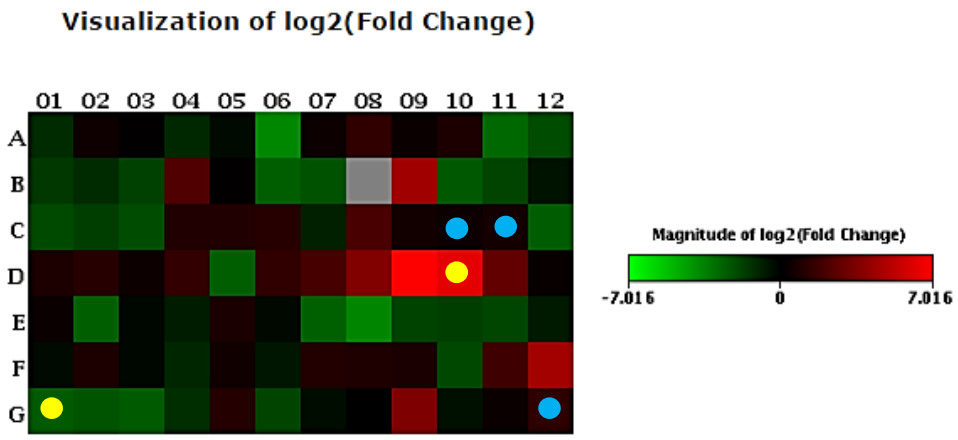

Layout	01	02	03	04	05	06	07	08	09	10	11	12
A	cfa-let-7a **-2.20** OKAY	cfa-let-7b **1.31** OKAY	cfa-let-7c **1.02** OKAY	cfa-let-7f **-2.12** OKAY	cfa-let-7g **-1.20** OKAY	cfa-miR-1 **-13.55** B	cfa-miR-101 **1.25** A	cfa-miR-103 **2.54** OKAY	cfa-miR-106a **1.20** OKAY	cfa-miR-106b **1.71** OKAY	cfa-miR-10b **-7.39** OKAY	cfa-miR-122 **-4.23** B
B	cfa-miR-124 **-2.87** B	cfa-miR-125a **-2.23** OKAY	cfa-miR-125b **-3.41** OKAY	cfa-miR-126 **4.55** A	cfa-miR-130a **1.05** OKAY	cfa-miR-133a **-6.00** B	cfa-miR-133b **-4.85** B	cfa-miR-137 **-4.55** C	cfa-miR-141 **21.93** A	cfa-miR-143 **-5.42** B	cfa-miR-145 **-3.63** B	cfa-miR-146a **-1.43** B
C	cfa-miR-146b **-4.13** B	cfa-miR-148a **-3.32** OKAY	cfa-miR-150 **-4.34** B	cfa-miR-15a **1.84** OKAY	cfa-miR-15b **1.84** OKAY	cfa-miR-16 **2.07** OKAY	cfa-miR-17 **-1.85** B	cfa-miR-181a **3.97** OKAY	cfa-miR-181b **1.41** OKAY	cfa-miR-182 **1.25** OKAY	cfa-miR-183 **1.49** OKAY	cfa-miR-184 **-5.77** B
D	cfa-miR-18a **1.73** OKAY	cfa-miR-191 **2.04** OKAY	cfa-miR-192 **1.28** A	cfa-miR-195 **2.61** OKAY	cfa-miR-196a **-5.91** OKAY	cfa-miR-19a **2.53** OKAY	cfa-miR-200a **3.83** A	cfa-miR-200b **12.11** A	cfa-miR-200c **129.46** OKAY	cfa-miR-203 **80.73** A	cfa-miR-204 **6.41** OKAY	cfa-miR-205 **1.18** A
E	cfa-miR-20a **1.21** OKAY	cfa-miR-21 **-5.95** OKAY	cfa-miR-210 **-1.10** A	cfa-miR-214 **-1.72** B	cfa-miR-218 **1.66** A	cfa-miR-22 **-1.19** OKAY	cfa-miR-222 **-6.35** OKAY	cfa-miR-223 **-13.02** B	cfa-miR-224 **-3.48** B	cfa-miR-23a **-3.22** OKAY	cfa-miR-23b **-3.73** OKAY	cfa-miR-24 **-1.67** OKAY
F	cfa-miR-25 **-1.19** OKAY	cfa-miR-26a **1.70** OKAY	cfa-miR-27a **-1.12** OKAY	cfa-miR-27b **-2.06** OKAY	cfa-miR-29b **1.36** A	cfa-miR-29c **-1.53** OKAY	cfa-miR-30b **1.88** OKAY	cfa-miR-30c **1.77** OKAY	cfa-miR-30d **1.67** OKAY	cfa-miR-31 **-3.92** B	cfa-miR-335 **3.25** A	cfa-miR-342 **23.03** A
G	cfa-miR-34a **-5.59** OKAY	cfa-miR-34b **-5.05** B	cfa-miR-34c **-5.53** B	cfa-miR-375 **-2.42** OKAY	cfa-miR-378 **2.01** OKAY	cfa-miR-451 **-3.69** B	cfa-miR-499 **-1.24** A	cfa-miR-7 **-1.01** OKAY	cfa-miR-9 **11.21** OKAY	cfa-miR-92a **-1.35** OKAY	cfa-miR-93 **1.22** OKAY	cfa-miR-96 **2.36** A

Figure 3 Heat map. (**L**) Cluster analysis of the expression of miRs in high Wnt cell lines relative to low Wnt expression cell lines; (**R**) corresponding miRs; yellow dots represent selected miRs based on the miFinder Array, blue dots represent the cluster miRs

MiRNA Screen

Based on the data derived from the miScript miR PCR Array Dog miFinder, and following extensive literature research, 5 miRs were selected to be investigated in more detail. These miRs were chosen based on either substantial upregulation or downregulation specific for the cell lines showing elevated Wnt activity (Fig 3 Heat map). Clustergram analysis (Figure 34 Clustergram for miFinder PCR Array) performed on the data set more clearly distinguished between the uniqueness of altered miR expression in the 12 cell lines. Combined data analysis resulted in the selection of the cluster miR-96 (upregulated), miR-182 (upregulated) and miR-183 (upregulated), and furthermore miR-34a (downregulated), and miR-203 (upregulated).

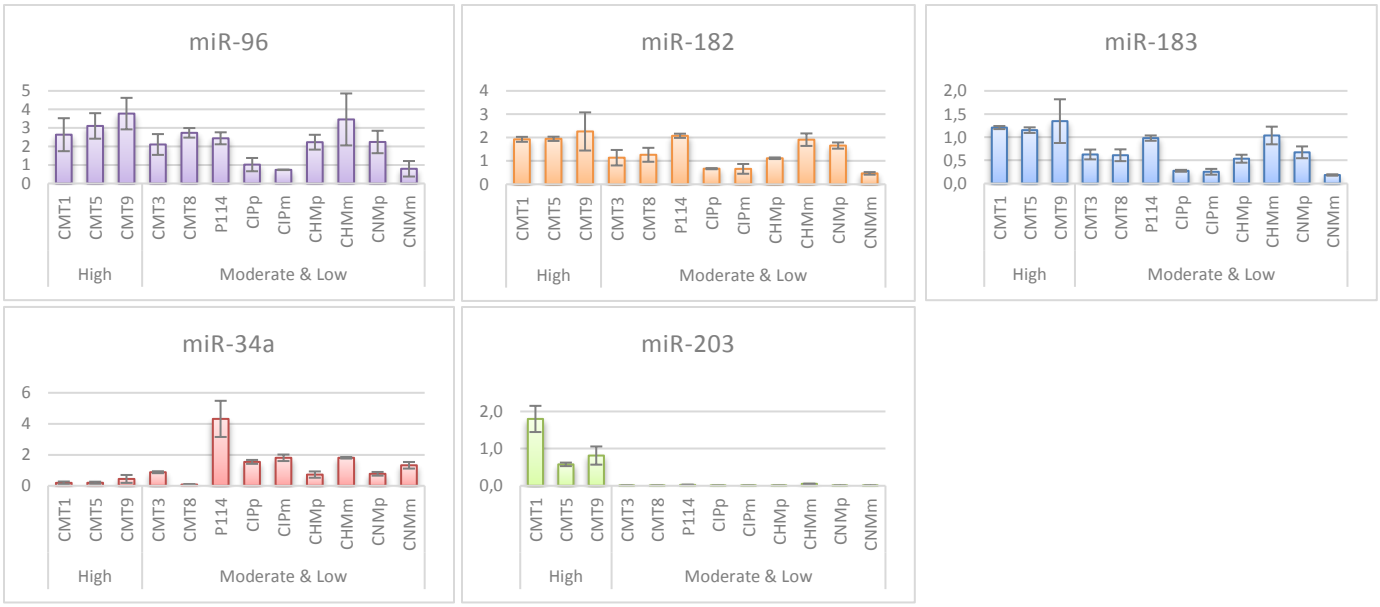

Figure 4 miR expression level in 12 cell lines; Numbers displayed in average copy number (+/- s.e.m.), normalized to Ce miR-39 miR mimic; miR-96 in 1000; miR-182 in 100.000; miR-183 in 100.000; miR-34a in 10.000; miR-203 in 100.000.

Specific qPCR

Based on the miFinder Array results, follow-up studies were performed. qPCR was performed on the 5 miRs to evaluate the exact miR level in each of the 12 cell lines. This was done to ensure only miRs were selected that showed an up- or downregulation in high Wnt cell lines, distinct from th e moderate and low Wnt cell lines. The miRs were tested against a Spike-In Control as normalisation. Despite an increased expression of the miR cluster 96/182/183 displayed in the miFinder Array, none of the 3 miRs showed clear upregulation in the high Wnt activity cell lines (Fig 4 miR expression level in 12 cell lines). The average copy numbers totalled 3171 in the high against 1972 in the moderate/low cell lines of miR-96, 204394 and 121641 in miR-182 and 123550 versus 57490 in miR-183.

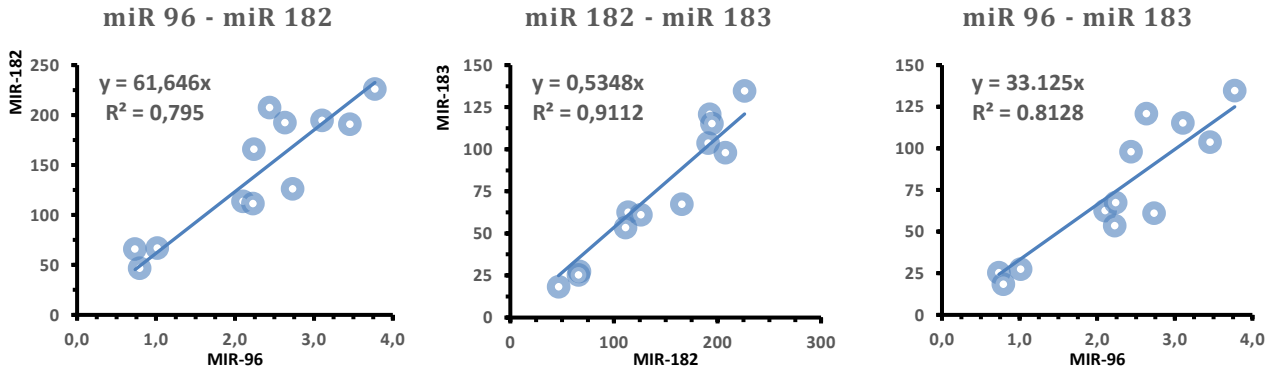

Figure 5 Correlation analysis of cluster miR-96/182/183; Numbers in copy number x 1000

However, a correlation did seem to exist between the 3 miRs, so this was investigated by comparing all 3 miRs from the cluster against each other. The obtained results clearly describe a strong correlation between both miR-96 and miR-182, miR-182 with miR-183 and miR-96 with miR-183, with an R^2 of 0.80, 0.91 and 0.81, respectively (Fig 5 Correlation analysis of cluster miR-96/182/183).

MiR-34a did display a tendency for lower miR levels in the high basal Wnt activity cell lines, with an average of 2758 average copy numbers in the high basal Wnt cell lines against 14725 in the moderate and low cell lines combined. However this was not a unique feature of these cell lines, as cell line CMT8 showed insignificant miR levels comparable to the high Wnt cell lines.

MiR-203, on the other hand, did present with a substantial increase in miR levels in the high Wnt cell lines. With an average of 106268 average copy numbers in the high Wnt cell lines against 1002 in the moderate and low cell lines, these were significant value differences worth pursuing.

Effect of Wnt, Dasatinib & RSPO1

Figure 6 Expression level in CMT-U27 cells; Numbers are percentages (+/- s.e.m.) in relation to Control (100%). * indicates P<0.05, ** indicates P<0.01

Subsequently, one high basal Wnt activity cell line was selected, namely CMT-U27. This cell line was then treated with Wnt signalling pathway regulators Wnt, Dasatinib and RSPO, to identify any possible connection between miR levels and target gene expression.

The cluster miR-96/182/183 showed a distinct increase in expression level when treated with Dasatinib, however Wnt and RSPO had varying effects on the miR expression level, showing an increase for Wnt in miR-96 and 183, a decrease after Wnt treatment for miR-182, and an increase after treatment with RSPO only in miR-96, the other two miRs displaying a slight decrease (Fig 6 Expression level in CMT-U27 cells).

MiR-34a did present with a significant increase after exposure to Wnt CM. Although miR expression also increased compared to the control when treated with Dasatinib, this enhancing effect was found to be insignificant. RSPO posed no effect on miR-34a expression.

Comparable data was obtained for miR-203, however with a substantially larger and significant increase after Wnt treatment, 425% versus 186% for miR-203 against miR-34a, respectively. Both Dasatinib and RSPO1 yielded no significant results, reaching only 133% in miR-203. RSPO yielded infinitesimal miR enhancing data in miR-203.

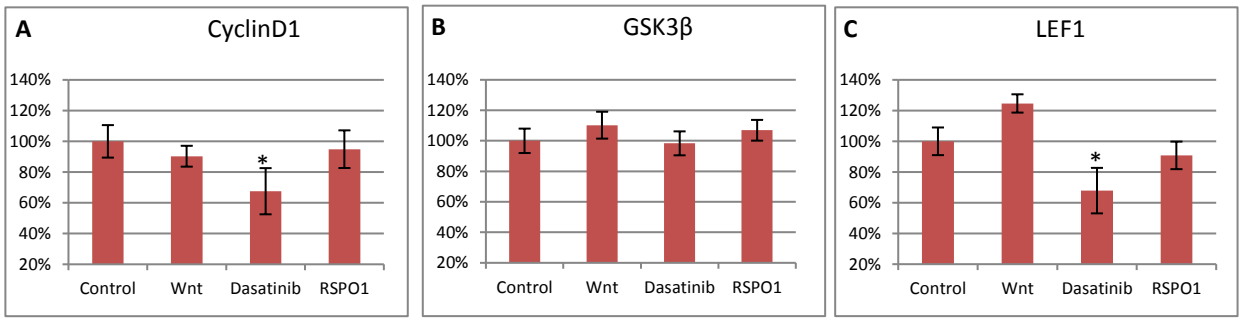

Figure 7 qPCR data after treatment with Wnt CM, Dasatinib and RSPO CM (**A**) CCND1 levels; (**B**) GSK3β levels; (**C**) LEF1 levels. All levels are percentages (+/- s.e.m.) relative to the control sample. * indicates P<0.05

Target gene expression

To further elucidate the connection between the miRs and the Wnt pathway, an attempt was made to find a connection between the miRs and several potential target genes. These genes included Cyclin D1 (CCND1), GSK3β and LEF1.

CCND1 obtained significant target gene reducing effects, with a decrease from 100% in the control samples to 68% after Dasatinib treatment. Although Wnt and RSPO yielded reducing effects as well, decreasing to 90% and 95%, respectively, these changes were not found significant (Fig 7 qPCR data after treatment with Wnt CM, Dasatinib and RSPO CM. (A) CCND1 levels).

GSK3β did not follow this line, with only a slight decrease to 98% after Dasatinib exposure compared to the control samples. Both Wnt and RSPO resulted in increased target gene expression, reaching 110% after Wnt medium culturing and 107% when exposed to RSPO1 (Fig 7 qPCR data after treatment with Wnt CM, Dasatinib and RSPO CM. (B) GSK3β levels). However, none of the responses were significant.

LEF1 showed again a different pattern from the other 2 target genes. Treatment with Wnt resulted in a considerable although insignificant increase, reaching 125% relative to the control samples. Dasatinib yielded exact opposite results, declining to 70%. Contrary to Wnt and RSPO response, this inhibiting effect was found to be significant. RSPO reduced only to 91% compared to control (Fig 7 qPCR data after treatment with Wnt CM, Dasatinib and RSPO CM. (C) LEF1 levels).

Discussion I

Prior work has elucidated the importance of the Wnt signalling pathway in mammary development. Not only does this pathway play a role in tissue development during puberty, it is also likely to encompass a major target behind mammary tumour formation. Cell growth, proliferation, EMT and metastasis formation are all under influence of the Wnt pathway (**Mukhina et al., 2004**), and activation of this pathway leads to an increased likelihood of developing breast cancer.

Extensive research has already been conducted on the Wnt signalling pathway. However, information is still scarce as to exactly how this pathway exerts its influence on the carcinogenic transformation of mammary tissue. Nonetheless, it is highly likely that these changes can, to a large extend, be attributed to miRs. MiRs can be found throughout the body, and are said to be involved in many, if not all, cellular functions (**Piao & Ma, 2012**). Yet until recently it has remained unclear which miRs in particular were responsible for the carcinogenic shift necessary for tumour formation.
Thus, in order to investigate this subject we tested twelve tumour cell lines, which were divided into two groups, being the high basal Wnt activity, and the moderate and low/absent basal Wnt activity groups. These groups were then investigated on canonical miR expression, for which a miFinder array was used which encompassed the 84 most abundantly expressed miRs in dogs. This resulted in the selection of five miRs, four of which were significantly and uniquely upregulated in the high Wnt activity group, while one was unambiguously downregulated in these same cell lines. The five miRs were subsequently tested on their response to treatment with two Wnt pathway activators, namely Wnt and RSPO1, and additionally one Wnt pathway inhibitor called Dasatinib.

MiR-96/182/183 cluster

Despite a clear upregulation in the original cluster analysis, none of the constituents of the miR-96/182/183 cluster displayed an evident relation to the Wnt pathway. Surprisingly, the entire cluster expressed a substantial and, in the case of miR-182 and miR-183 highly significant, increase in miR copy number after treatment with Dasatinib, which is in contrast to our expectations. Literature research led to believe that high miR-96-182-183 expression is correlated to increased tumour metastasis *in vivo* in mice and humans (**Zhang et al., 2015**), and that the cluster is in general regarded as oncogenic miR cluster (**Guttilla & White, 2009**). Although often the 3 miRs exert similar and conjugated effects on target gene expression or RNA transcription, the miRs do not always function as a triplet. Lin et al found that miR-96 seems to promote proliferation in human breast cancer cells (**Lin et al., 2010**). However, they solely investigated miR-96, without taking into consideration the remaining cluster members. Thus it remains unclear if the proliferative tendency is exclusively attributed to miR-96.

It has occurred, that cancer cell screenings for miRs resulted in only one of the cluster members being selected to investigate further (e.g. in a study of lung cancer cells by Wang and colleagues (2008)). Subsequently, if investigators based their miR-selection on such articles they would continue investigating only one member of the cluster (**Lowery et al., 2010**). Thus, although Lowery et al state that a dysregulation of miR-183 causes inhibition of breast cancer cell migration, one cannot exclusively attribute this role to miR-183, and the influence the other cluster members should also be taken into consideration.

This is confirmed by our correlation analysis of the miR-cluster, which showed that despite no distinctive alteration of miR levels in the high Wnt cell lines, a significant correlation was evidenced between the 3 miRs. This is not surprising, since in humans the entire cluster is situated on chromosome 7q32.2, and was previously observed to possess a strong correlation (**Zhang et al., 2015**). Endorsing this, Leung and colleagues found the entire cluster expression to be upregulated in hepatocellular carcinoma (**Leung et al., 2015**). Additionally, the 3 cluster members have also been identified separately to be connected to carcinogenic effects of human breast cancer (**Macedo et al., 2017; Moazzeni et al., 2017; Shi et al., 2017; Zhang et al., 2017**). Even when knocked down individually, the 3 miRs all showed reduced cell motility and enhanced invasive properties, although the effects were more pronounced when the combined cluster was investigated (**Leung et al., 2015**). And though often only miR-96 and miR-182 are found to be upregulated in human cancer patients, some studies find evidence that miR-183 individually plays a significant role as well (**Cheng et al., 2016**).

Transfection results, however, did yield significant increase after Wnt stimulation (See ***Chapter II*** Fig 10 CMT-U27 Wnt3a CM & RSPO1 CM optimization; y-axis in 1.000), so it seems as though Wnt treatment does effect the β-catenin construct, although it does not seem to exert an influence at gene expression level.

It remains as yet unknown how the upregulation of the miRs by Dasatinib can be explained. Both miR-182 and miR-183 showed a tremendous and highly significant increase in expression level after Dasatinib treatment, and although it was not found significant in miR-96, this miR did display a similar tendency. An explanation for miR-96 not yielding similarly significant data could be sought in the fact that the deviation in miR-96 is much larger. This could be attributed to the relatively low expression levels of miR-96 in comparison to the other 2 cluster members, wherein small deviations are resultantly magnified in relation to miRs showing higher expression levels. There are several possibilities as to why miR-96 is expressed in such low numbers compared to the other 2 cluster members. Firstly, the possibility exists that, although originating from the same chromosomal location, the splicing that occurs down miR-96 expression pathway is of relatively lower efficiency compared to miR-182 and -183 splicing. This would ultimately lead to a decreased expression of this miR. Another option is that miR-96 is relatively more instable, resulting in quicker miR degradation and lower numbers to be measured after any period of time. A third, more drastic explanation might be that miR-96 actually doesn't develop from the same precursor as miR-182 and miR-183, but instead is independently regulated. This is the least likely option, seen the correlation found during this study, and the extensive evidence that often the miR cluster responds simultaneously and comparably. So far, no definitive statement can be made with regard to the varying expression levels. However, for future research it might pose an interesting topic to investigate exactly how miRs present inside cells, since it has been known that miRs remain in quite stable condition when in plasma since they are transported in specialized vesicles. But how miRs move from the nucleus to the cell wall is yet unknown, and if investigated this could either rule out or substantiate the possibility that miR-96 presents with lower stability in comparison to the other miR cluster members.

To the best of our knowledge, no research has yet been conducted on any of the cluster members in relation to Src. Src has repeatedly been reported to enhance carcinogenic properties such as proliferation, invasion and metastasis formation in a multitude of carcinomas, such as colorectal cancer (**Zhang, Ma et al., 2017**) and melanoma (**Girotti et al., 2015; Spender et al., 2016**). Furthermore, increased Src activity has been related to reduced differentiation in embryonic stem cells (**Przybyla et al., 2016**), further promoting a role for Src in cancer development and cellular differentiation. However, it is universally known that the Wnt pathway is not the sole pathway for Src to exert an influence. Neither is it likely that, in relation to the Wnt signalling pathway, the complete effect of Src activation has already been uncovered. It might exert an extensive influence on different ligands and co-effectors, where the net effect differs per organ, tissue or even cellular state. On the other hand, there is a possibility that Dasatinib not only inhibits Src, but exerts its effects on other receptors and ligands as well. In relation to this study however, it can be concluded that Dasatinib is not directly related to basal Wnt activity, but does seem to pose a stimulating effect on cluster miR-96/182/183.

MiR-34a

MiR-34a is known to yield tumour suppressor abilities in breast cancer cells (**Achari et al., 2014**; **Javeri et al., 2013**; **Yang et al., 2013**). However, in spite of the considerable downregulation of miR-34a in the high basal Wnt activity cell lines, it failed to pursue this trend in subsequent experiments. No decrease in miR-34a expression level was observed in the 3 high Wnt activity tumour cell lines when compared to the 9 cell lines with moderate or low Wnt activity (Fig 4 miR expression level in 12 cell lines). Moreover, stimulation of the high Wnt active cell line with Wnt medium caused an especially significant increase in miR expression (Fig 6 Expression level in CMT-U27 cells). However, an opposite response was expected if miR-34a truly exerts a suppressive influence on Wnt signalling. These results are also in contrast to literature studies, of which numerous state that miR-34a has a significant role as tumour suppressor in many different tumour types (**Bu et al., 2013**; **Chen et al., 2015**; **Kim et al., 2011**; **Li et al., 2009; Shen et al., 2012**). However, according to many of these articles, miR-34a seems to exert its effect predominantly through the Notch signalling pathway (**Kang et al., 2015**; **Li et al., 2009**), or the MAPK pathway (**Chen et al., 2010**; **Shen et al., 2012**). Still, there are several investigations demonstrating a negative regulatory

connection between miR-34a and the Wnt signalling pathway (**Bu et al., 2013**; **Chen et al., 2015**; **Kim et al., 2011; Rathod et al., 2014**). This was, however, not substantiated by this study, since the miR was upregulated after Wnt treatment, and both Dasatinib and RSPO1 yielded no significant data. Thus the effect of both Dasatinib and RSPO1 on miR-34a expression has not been elucidated by this study. Either RSPO1 was expected to follow the line of Wnt on the miR, or an effect opposite to that of Dasatinib was predicted. However, RSPO1 didn't show either, exerting almost no effect on miR-34a expression levels. This was not entirely opposite our expectations, as RSPO1 is known to exhibit Wnt stabilizing characteristics (**Binnerts et al., 2007; Boretto et al., 2017; Kazanskaya et al., 2004; Kim et al., 2006**). Thus when applied in the absence of Wnt, little effect is anticipated.

In order to elucidate the connection between miR-34a and the Wnt signalling pathway, further research is warranted. Nevertheless, the importance of miR-34a in tumour formation is indisputable, since multiple studies have found miR-34a to pose a promising biomarker for malignancy. This is only substantiated by the fact that MRX34, a miR-34a mimic, treatment already reached phase I Study level in 2013, researching the effect of MRX34 on several different types of solid tumours (**Beg et al., 2017**).

MiR-203

While miR-34a failed to show a direct connection to the Wnt pathway, accumulating evidence does propose a role for miR-203 in relation to Wnt signalling. When testing all 12 cell lines against this miR, a significant increase in miR copy number was found in the high basal Wnt active cell lines (Fig 4 miR expression level in 12 cell lines). When CMT-U27 was subsequently treated with Wnt, Dasatinib and RSPO, the cells treated with Wnt revealed an almost 2.5-fold increase in miR-203 copy number compared to the control cells, increasing to 425% in comparison to the control sample (Fig 6 Expression level in CMT-U27 cells). However, Dasatinib did not display the suppressing effect expected from a Src inhibitor. Little is certain on the exact role of miR-203 in cellular signalling, and much can be said for a tumour-, organ- or tissue-specific role for miR-203. For both breast cancer and colorectal cancer, a link appears to exist between elevated miR-203 levels measured in the circulation, and poorer prognosis (**Bovell et al., 2013; Hur et al., 2017; Shao et al., 2017**), increased breast cancer metastasis (**Madhavan et al., 2016**) or colorectal metastasis (**Hur et al., 2017**). On the contrary, decreased levels of miR-203 correspond to poor prognosis in other types of cancers, including melanoma (**van Kempen et al., 2012**; **Wang, Zhang, 2015**), oesophageal cancer (**Hezova et al., 2015; Liu et al., 2016**) and liver cancer (**Chen et al., 2012; Li et al., 2015**). This would counter a carcinogenesis promoter role for miR-203. In line with these data, some researchers found that silencing of miR-203 leads to increased EMT (**Taube et al., 2013**), and Wang et al found miR-203 to significantly inhibit cell proliferation in triple-negative breast cancer (TNBC) cell lines (**Wang et al., 2012**). In prostate cells, miR-203 seems to be completely repressed during EMT (**Qu et al., 2013**). These articles all support the statement of miR-203 being a tumour suppressor gene. In fact, much evidence exists on a differentiation-promoting role for miR-203 in human skin cells (**Nissan et al., 2011**).

Concludingly, little can yet be ascertained concerning the exact role of miR-203, both in cancer formation in general and in breast cancer development in particular. From the data obtained in this study however, there appears to be a positive correlation between a stimulation of the Wnt signalling pathway and increased levels of miR-203, suggesting a tumour promotor role in mammary cancer cell lines. This is in line with **Shao et al., 2017**, and resultantly the assumption can be made that miR-203 indeed potentiates a role as basal Wnt activity marker**.** Although Src inhibiting did not respond accordingly, there is a multitude of possible explanations, including simultaneous Wnt pathway inhibition/stimulation of effectors other than Src, or co-participation in different pathways concerned with cellular proliferation. Since no research has been performed on miR-203 levels in dogs in relation to mammary carcinomas, this investigation appears to be pioneering in relating canine mammary cancer to the prognostic level of miR-203.

Target genes

GSK3β

In order to relate one or more of the 5 miRs to target gene expression, 3 potential gene targets were selected, namely GSK3β, LEF1 and CCND1. GSK3β is a protein kinase, and a member of the β-catenin destruction complex. Thus, if the miRs would function through targeting the Wnt pathway, an effect on GSK3β would be expected. As can been seen from Fig 7, GSK3β does show a slight increase after stimulation by Wnt CM, and an inconsequential decrease when the Wnt pathway is inhibited by Dasatinib. Also, RSPO1 treatment yields minor elevating effects (Fig 7 qPCR data after treatment with Wnt CM, Dasatinib and RSPO1 CM (B) GSK3β levels). However, neither of the effects were found to be significant, thus based on these data no conclusions can be drawn concerning the relation between GSK3β and the Wnt signalling pathway. A possible explanation for this could be that GSK3β is found throughout the body, not only forming a co-effector in the Wnt signalling pathway but in many other biological functions as well. The combined results of these pathways together might cause specific carcinogenic effects, however when investigated separately this connection is not found.

LEF1 shows a direct response to Wnt stimulation and Dasatinib inhibition

LEF1 has been proposed by many researchers to be of valuable influence in the Wnt signalling pathway (**Aval et al., 2017; Thatcher et al., 2008**). Thatcher et al provided a link between miR-203 and LEF1 levels, where miR-203 seems to repress LEF1 and loss of miR-203 causes a LEF1 excess, leading to abnormally high cell proliferation levels. Concordantly, LEF1 seems connected to cell growth, migration and invasion in breast cancer cells (**Hsieh et al., 2012**) and promotes EMT (**Kim et al., 2002**). In this study similar results were obtained. LEF displayed slight upregulation after Wnt treatment, whereas the target gene expression levels greatly and significantly reduced when treated with Dasatinib. Unfortunately, LEF1 cannot be linked to any of the miRs investigated in this study, since gene expression levels do not compare to any of the miR expression levels. However, it can be stated that LEF1 expression is closely related to Wnt activity, a result that is supported by literature on LEF1 in relation to the canonical Wnt pathway (**Gracanin et al., 2014**).

CCND1 does not seem directly correlated with miR-34a

Studies have proposed a downregulating effect of miR-34a on CCND1 (**Chen et al., 2014**; **Kastl et al., 2012; Sun et al., 2008**). Contradictory, others invert this statement by attributing a controlling role of CCND1 over miR-34a activity (**Pulikkan et al., 2010**). However, during this investigation a connection between CCND1 expression and miR-34a levels was not found.

Although Dasatinib exhibited reducing effects on both CCND1 and LEF1, it is as yet unknown if these effects are linked to a specific miR. It could be linked to the effects of the cluster miR-96/182/183, since all miRs show considerably increased expression after Dasatinib treatment. With miR upregulation often being connected to inhibition of target gene transcription, increased miR-96/182/183 levels could lead to a decrease of CCND1 and LEF1 expression. However, this remains to be investigated in more detail before any final conclusion can be drawn. Additionally, Wnt connection to CCND1 expression is further questionable seen the level of variance observed in CCND1 levels following Dasatinib treatment. Thus the cluster is more likely to be directly connected to LEF1 expression compared to CCND1.

Altogether, promising results were obtained when testing target genes GSK3β, LEF1 and CCND1, although further research is warranted. One promising target gene for the miR-96-182-183 cluster may be FOXO1 (**O'Bryan et al., 2017; Guttilla & White, 2009**), and for miR-34a FOXQ1 could be a potential research target (**Christensen et al., 2013**). FOXQ1 has recently been shown to increase tumorigenesis of both colon (**Kaneda et al., 2010**) and breast cancer (**Zhang et al., 2011**). In breast cancer, another research group found FOXQ1 to be associated with increased EMT (**Qiao et al., 2011**), and also related this gene to the aggressiveness of the carcinomas. Thus, FOXQ1 could be an interesting target gene to further examine.

Conclusion I

In conclusion, 5 potential miRs were uncovered, one of which showed highly promising results in subsequent testing. This is the first study to examine in such great detail the role of miR-203 in mammary cancer development and the Wnt pathway. From these investigations, it can be concluded that miR-203, out of the investigated 5 miRs, seems to be the most promising marker for Wnt activity, and is highly likely to play a significant role in the carcinogenic transformation of mammary tissue. Future work should look into the options of using this miR as a potential risk biomarker for mammary cancer. If this miR can also be detected in blood samples, it should be considered to investigate a role for miR-203s as diagnostic tool for breast cancer. However, future research should also elucidate the exact effect of Dasatinib on cells, cell lines and tissues, if Dasatinib is ever to be considered a treatment option for inhibiting the Wnt pathway and thus targeting breast cancer formation. Nevertheless, this research has brought us one step closer to unveiling the exact working mechanism behind tumour formation, and hopefully eventually to a cure for cancer in general, and breast cancer in particular.

Chapter II - Mammary Organoids, culturing and application

As has been elucidated by the previous chapter, the Wnt signalling pathway plays a crucial role in tissue development and differentiation. This is not only of interest when studying tumour formation, it is also widely used by researchers in an entirely different field, the microbiologists studying organoid systems (Clevers, 2016).

Introduction II

Over the last few decades, three-dimensional (3D) systems have gained popularity in the world of cell culturing and microbiology, with the most recent method being the organoid culturing system. Organoids, or mini organs, are small cell clusters. They originate from stem cells, cells found in all organs that are undifferentiated, specialized and capable of self-renewal.

The first 3D tissue culture derived from human cells was already developed in 1975 by Rheinwald & Green (**Rheinwald & Green, 1975**). Yet, it wasn't until a decade ago that the term 'organoid' was applied to a 3D culture of stem cells, consisting of multiple organ-specific cell types.

The invention of these mini organs has already proved to be seminal, and of invaluable importance to the medical branch. Not only do organoids allow us to study organ function in close detail without the cost of donor organs or laboratory animals, they also provide an accessible tool for translational research, studying potential drug options or treatment effects at organ level. Organoids bridge the gap between 2D petri dish circumstances and *in vivo* investigations, in all research tracks testing drugs for both human and animal medicine. Also, patient-derived organoids provide personalized drug response options, avoiding sometimes lengthy treatments with disappointing or even toxic consequences. In fact, rectal organoids have already successfully been applied in personalized treatment experiments with patients suffering from rare cystic fibrosis transmembrane conductance regulator (CFTR) regulator mutations (**Dekkers et al., 2016**). Thus, this new ex vivo testing of drug responses could well mean a revolutionary step in personalized medicine.

Since the emergence of 3D culturing systems in 1987, researchers have attempted to grow many different types of organoids. At present, medical researchers have succeeded in growing various organs, from cerebral organoids to kidneys, lungs and different types of gut tissue. However, worldwide laboratory teams are working to improve on the 3D systems in many aspects, including innervation, growth speed, efficacy, and organ size. Not all organ systems are yet available as organoid models, neither are all organoid systems equally well-developed. For example, liver organoids derived from mouse liver stem cells can be sustained for over a year (**Huch M., 2017**), and liver organoids from various hosts, dogs, cats, mice and humans, are already used to study interspecies lipid accumulation variance (**Kruitwagen et al., 2017**). However, significantly fewer progress has been made in the development and application of mammary organoids. Investigators worldwide are still researching the exact working mechanism of intercellular signalling pathways, and thus much still remains unclear as to the optimal culturing conditions for the mammary gland. Yet, the Wnt pathway seems again to be of importance in stem cell differentiation and proliferation. For example, Boretto et al. revealed that, although in different tissues, organoid culturing in relatively high Wnt concentrations resulted in increased differentiation levels (**Boretto et al., 2017**).

P4 is known to play a crucial role in mammary gland development (**Macias, Hinck, 2012**). It has been known for decades that P4 is required for normal mammary gland development (**Lydon et al., 1995**), and has been proposed to promote Wnt and GH signalling (**Brisken et al., 2000; Lombardi et al., 2014**). However, the mechanism behind this development is more complicated, starting with the existence of two isotopes of the P4 receptor (PRs), PRA and PRB. These isotopes are the result of gene splicing, and each regulates its own scale of biological functions (**Macias, Hinck, 2012**). However, much of the PR isotype experiments have been conducted *in vitro*, since *in vivo* testing is complex due to simultaneous expression of both isotypes in human mammary epithelial tissue. Additionally, many experiments have been carried out using mice. In these animals only PRA is expressed in pubertal and adult mammary glands, while PRB expression is related to pregnancy (**Aupperlee et al., 2005; Mote et al., 2006**).

Interestingly, the two mammary gland types have been shown to respond differently to P4 stimulation, as murine mammary glands solely expressing PRA reveal decreased P4-induced proliferation as opposed to PRB-expressing mammary glands (**Fendrick et al., 1998**). However, mice lacking the PRB also present with defective morphogenesis (**Mulac-Jericevic et al., 2003**). Overall, mice have thus proved to be aiding in researching the role of PRA in mammary gland development. However, as mentioned in the previous chapter, dogs provide with mammary cancer characteristics much closer related to human breast cancer. For example, they share signalling pathways resulting in tissue proliferation and cellular migration (**Liu et al., 2014; Uva et al., 2009**), and equally important is the initial hormone-dependence seen in both humans and dogs that rodents are devoid of. However, the effect on the canine PR seems to be executed solely through PRA, while PRB showed very limited gene transcription potential (**Gracanin, Voorwald et al., 2014**). Still research into canine mammary gland development and cancer formation is deemed more valuable in gaining an understanding of the exact mechanism behind human carcinogenic transformations of the mammary gland.

P4 poses a risk factor for mammary carcinomas (**Axlund, Sartorius, 2012; Kuhl, Schneider, 2013; Santos et al., 2009**), and has been known to do so for over a century (**Beatson, 1896**). However, since then most research focused on the role of oestrogens in mammary gland development and carcinogenesis. It wasn't until early 21st century that a clear connection was made between P4 and increased risk of human breast cancer (**Rossouw et al., 2002**). In depth research to the exact role of P4 has since then been realized, with seminal and crucial outcomes. For example, increased PRA over PRB expression has been associated with a more aggressive human breast cancer type, including a poorer prognosis (**Mote et al., 2002; Jacobsen et al., 2005**). Thus, research in dogs, where PRA is predominantly expressed, could lead to an insight in PRA signalling and its relation to carcinogenetic changes in the mammary gland.

In mice, P4 exposure has been known to result in stem cell activation, that is: recruitment and differentiation of mammary stem cells (MaSC) (**Joshi et al., 2010**). This is proposed to happen through increased Wnt signalling to the basal cells of the mammary gland. The relevance of the Wnt signalling pathway is only reinforced by the fact that P4 increases Wnt signalling in humans, dogs and mice (**Rao et al., 2009; Weber-Hall et al., 1994**). Additionally, in a majority of human breast cancers an increase in β-catenin activity was observed (**Lin et al., 2000**), which, as can be deduced from the previous chapter, is related to an increase in Wnt signalling. Accordingly, similar results were obtained from *in vivo* studies in dogs, showing an upregulation of Wnt mRNA in dogs with spontaneous mammary carcinomas (**Gracanin et al., 2014**). Wnt has already directly been linked to induced CSC properties by regulating MaSCs (**Skibinski, Kuperwasser, 2015**). Altogether, this deems MaSCs prominent targets for causing the transformational events seen in breast cancer development (**Eden, 2010**).

Through organoid models of canine mammary cells, an attempt can be made to study stem cell properties, for example in relation to Wnt level effect on differentiation. By subjecting mammary organoids to culturing conditions consisting of varying concentrations of Wnt CM and RSPO CM, and assessing their effect on proliferation, differentiation and apoptosis, it is possible to deduce the optimal culturing solution for organoids derived from the mammary gland. Thereafter, we would have at our disposal a means to study the mammary gland without the unnecessary and much debated animal experiments. Also, by closely evaluating organoid differentiation levels in relation to Wnt/RSPO concentrations the effect of Wnt on stem cell differentiation would be elucidated, which might aid the understanding of the Wnt signalling pathway on carcinogenic actions in stem cell development. This could be linked to P4 influence on stem cells by assessing its expression in relation to malignancy characteristics such as proliferation and differentiation.

Another route to studying canine P4 lies in immunohistochemistry (IHC) on dog tissue. Healthy dogs can be utilized to study P4 effect by correlating circulating P4 levels to specific target tissues or even target genes. This might further elucidate the role of P4 in mammary gland development, and suggest specific targets for breast cancer treatment. However, caution should be applied when relating P4 blood levels to canine tissue IHC. Blood levels often vary, and are under influence of innumerable factors and circumstances, including hormone concentrations (of great relevance when taking into consideration the oestrus cycle). Additionally, drawing conclusions based on IHC should be done with care, since quantification of IHC remains a subjective and challenging task.

Outline of the study II

The aim of this study was to optimize culturing conditions for organoids derived from MaSCs, in order to stabilize the stem cell-derived structures for extensive usage in various experiments on the mammary gland, including much warranted oncology research. Additionally, P4 effects on organoid characteristics were investigated, and an effort was made to relate P4 expression to various targets. Furthermore a connection between P4 levels and organoid behaviour was sought, and the effects of Wnt concentration levels on organoid differentiation and proliferation was assessed to attempt to link Wnt signalling, P4 levels and carcinogenesis-related effects.

Materials & Methods II

Cell culture

Organoids were obtained from a pool of 5 different mammary gland tissue suspensions, thawed from liquid nitrogen on November 25, 2016 following **3D Mammary Gland Derived Organoid Isolation & Culturing** (*Protocol II 3D Mammary Gland Derived Organoid Isolation & Culturing*).

They were plated on 24-well Cell Culture Plate, Cellstar® (#662160, Greiner Bio-one, Alphen Aan Den Rijn), whereupon they were cultured in DMEM/F12 (#11320-074, Gibco, Life technologies, Bleiswijk, The Netherlands) supplemented with several growth factors (Table 3 Culture medium for Organoid culturing, 25/11/2016).

After culturing, the organoids were left to grow for one week, while growth medium was refreshed on Tuesday November 29. One week after the organoids had been plated, they were passaged following the **Organoid Passaging Protocol** (*Protocol III Organoid Passaging*). Henceforth, the organoids were passaged once a week or once every two weeks, depending on the assessment of organoid growth speed, number of organoids and contamination level (these same variations also required modification of the passaging protocol, hence the margin left in the Organoid Passaging Protocol).

Also, 7 days after the organoids were obtained from liquid nitrogen, 3 different types of culture media were introduced, being the High, Medium and Low culturing media. The names were derived from the percentage of Wnt CM added to the culture media, which amounted to 50, 25 and 5%, respectively. Also, the percentage of the growth factor RSPO CM varied likewise, with the High, Medium and Low media containing 25, 10 and 2% RSPO, respectively. This led to the formation of the culture medium schedule found in **Appendice D** (Table 3 Culture medium for Organoid culturing, 25/11/2016).

At reaching passage 5, the organoids were divided into three groups. Firstly, some organoids were passaged on to passage 6, following the standard **Organoid Passaging Protocol** (*Protocol III*). Moreover, some organoids were fixated in paraffin following the **Organoid Embedding in Paraffin** (*Protocol V*), later to be sectioned and stained. Lastly, the remaining organoids were treated with RLT, transferred to microcentrifuge tubes and stored at -20°C for RNA isolation.

TCF-reporter assay

See TCF-reporter assay Chapter I. For optimization purposes, cells were treated with 8 different solutions, all including either Wnt CM, RSPO CM or a combination of both (Table 5 Transfection solutions).

Imaging

Organoids were photographed every week and before and after every passaging, to ensure sufficient data was available for growth comparison. The photos were taken on a using Leica Application Suite V4.2 (Leica Microsystems B.V., Amsterdam, The Netherlands). They were cropped using Adobe Photoshop CC, Version: 2014.1.0. For growth speed estimation, measurements were obtained using ImageJ analysis version 1.4.7.

Canine tissue obtainment

Tissue was collected from dogs euthanized at the Department of Clinical Sciences of Companion Animals, Faculty of Veterinary Science, Utrecht University, following the **Tissue Obtainment Protocol** (*Protocol IV*). The dogs came from the common laboratory for animals (Gemeenschappelijk Dierenlaboratorium, GDL) at the Utrecht University, faculty for Veterinary Medicine, and were used for educational and research purposes. All included dog tissue was obtained from Beagle dogs of approximately two years of age, thus rendering these tissues comparable for research purposes. Tissue from a total of 5 dogs was fixated, and brought to the DMPC (Dutch Molecular Pathology Centre) to be sectioned and fixated on microscope slides. The dogs used were 100642 (dog 1), 104762 (dog 2), 105109 (dog 3), 105393 (dog 4) and 108619 (dog 5).

Stainings

Both the dog mammary gland tissues and the organoids at passage 5 and 11 were stained, not only to ensure the correct tissue type was dissected, but also to investigate the possible existence of a correlation between P4 levels found in the blood, and possible predominant tissue and/or cell types found on the stained slides. The organoids were stained with a total of five different staining antibodies, concerning αSMA, CK7, CK19, P-cad (**Gama et al., 2004; Meuten, 2016; Peña et al., 2014**) and E-cad.

The αSMA staining was applied to visualize both smooth muscle and myoepithelial cells (**Vos et al., 1993**), detecting primarily the contractile apparatus of the mammary gland.

CK7 and CK19 were included to differentiate between the inner, secretory luminal epithelial cells and the outer basal/myoepithelial cell layer (Fig 8 Breast cancer; CK19 staining).

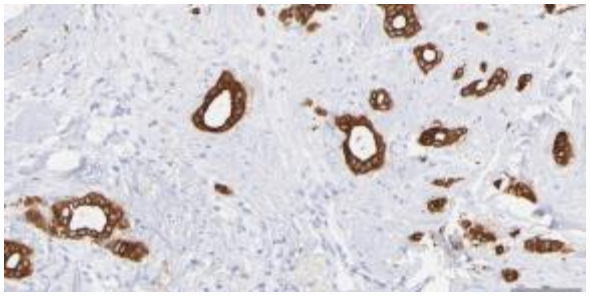

Figure 8 Breast cancer; CK19 staining; HPA002465 Female, age 27; Breast (T-04000); Duct carcinoma (M-85003) ; Patient id: 2392 - Tumor cells; Staining: High; Intensity: Strong; Quantity: >75%; Location: Cytoplasmic/membranous http://www.proteinatlas.org/ENSG00000171345-KRT19/cancer/tissue/breast+cancer#imid_1065350

P-cad antibody staining is generally observed in myoepithelial cells, usually at cell-cell contact sites (**Gama et al., 2004**). So P-cad predominantly envisions cell junctions just below the luminal lining. Contradictory though, according to The Human Protein Atlas the P-cad AB is predominantly expressed in membranous squamous epithelial cells (Fig 9 Breast cancer; P-cad staining) (http://www.proteinatlas.org/ENSG00000062038-CDH3/tissue).

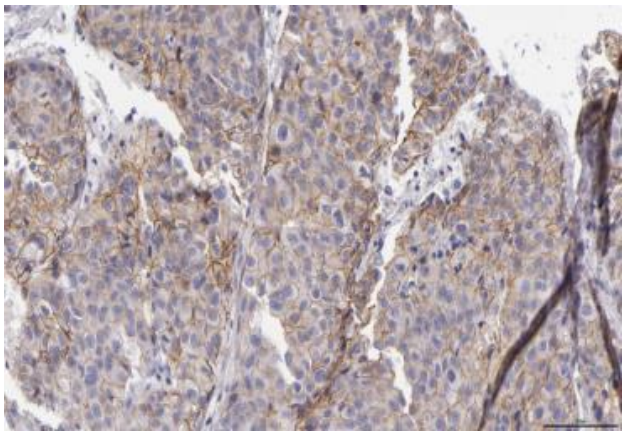

Figure 9 Breast cancer; P-cad staining; CAB002487 Female, age 68; Breast (T-04000); Duct carcinoma (M-85003); Patient id: 261; - Tumor cells; Staining: Medium; Intensity: Moderate; Quantity: >75%; Location: Cytoplasmic/membranous http://www.proteinatlas.org/ENSG00000062038-CDH3/cancer/tissue/breast+cancer#imid_993693

The E-cad staining visualizes the plasma membrane and cell junctions of epithelial cells (**Rakha et al., 2013**), but also the golgi-apparatus (http://www.proteinatlas.org/ENSG00000039068-CDH1/cell). Both cadherin stainings are ways of projecting the myoepithelial tissue layer found in the mammary gland.

By including several different antibody stainings one can, with increased certainty, determine the tissue or cell type. With the ultimate goal of the staining being the determination of the organoid tissue type, a higher number of different antibody stainings is directly correlated to the trustworthiness of the cell type determination. All organoid samples were included in the staining, resulting in 6 organoid slides (two Passage numbers, namely 5 and 11, in High, Medium and Low culture medium). Added were: a positive control to ensure the staining succeeded even if no colour was found on the organoid slides, two types of negative control to check for non-specific binding, and finally the five slides with tissue from the euthanized dogs. Negative control comprised normal canine mammary tissue in the case of αSMA and P-cad, canine mammary carcinoma tissue for the CKS, and canine colon tissue in the case of E-cad. Based on previous experiments performed by our group, these tissues were opted by our lab as most suitable negative control samples for these particular stainings, corresponding with applied staining protocol.

Experimental procedure

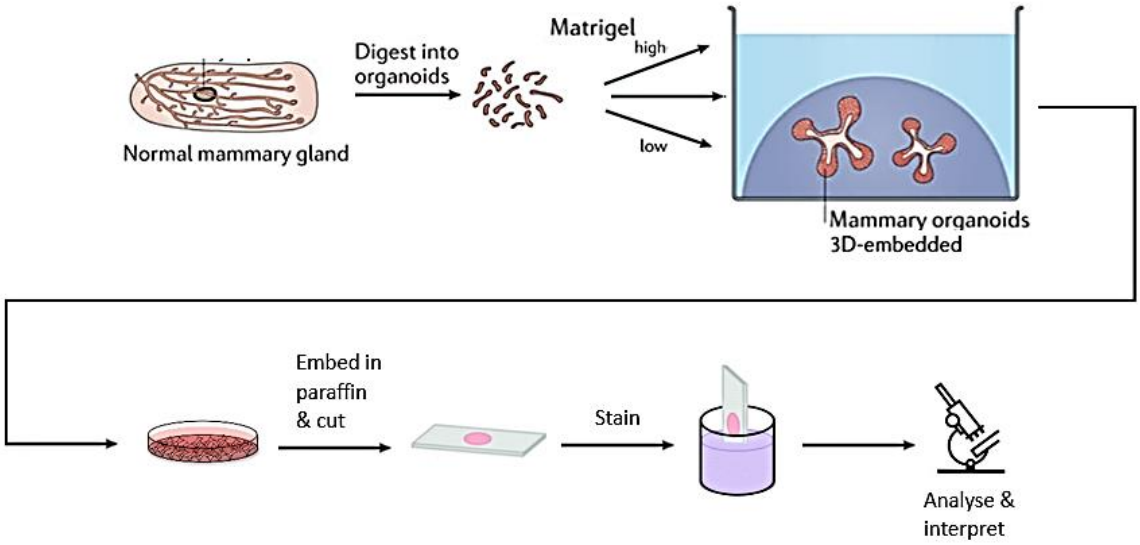

Overview 1 **Experimental procedure.** Schematic overview of experimental procedure. Mammary tissue is collected from liquid nitrogen in small blocks, washed and centrifuged. The organoids are cultured in 3 different culture media: high Wnt culturing medium, medium Wnt culturing medium and low Wnt culturing medium, and embedded in matrigel. At passage 5 and 11 the organoids are divided into groups, and one group is selected to be embedded in paraffin. The paraffin embedded organoids are subsequently cut, and stained following the staining protocols (see Appendice C, Protocol VI – X). Finally, the stained slides are analysed and interpreted through microscopic use and with the aid of experienced pathologists (adapted from **Shamir, Ewald, 2014**).

Statistical analysis

Since research on mammary-derived organoids is still in its early stages at our lab, the investigations are merely of a descriptive nature. With the focus on optimizing culturing conditions and investigating the response to certain growing media, the numbers applied are as yet too small for statistical analysis purposes.

Results II

TCF-reporter assay

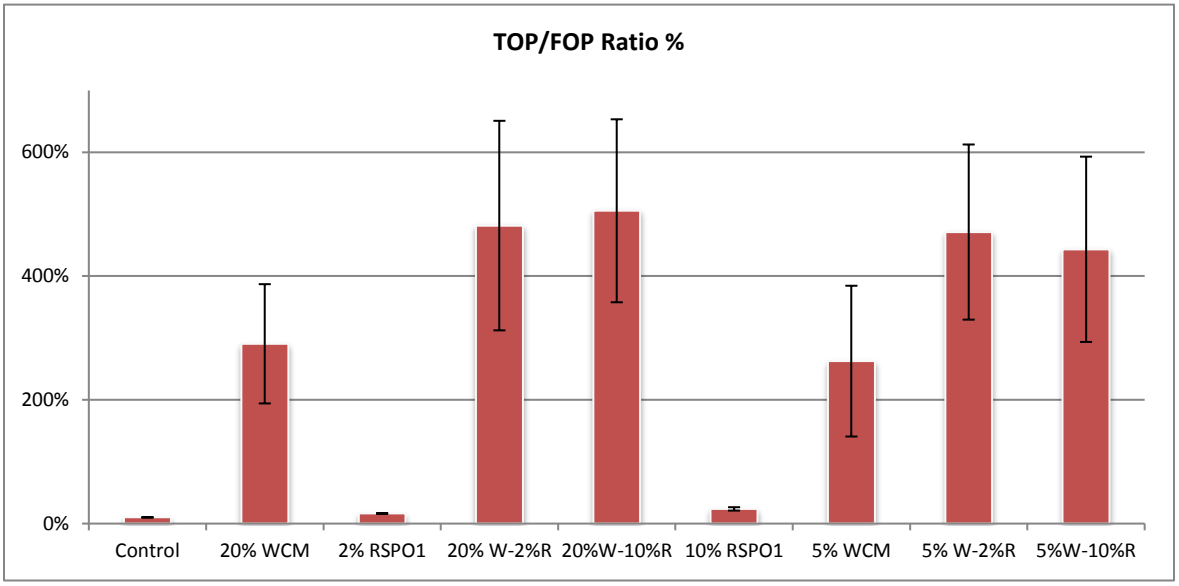

Figure 10 CMT-U27 Wnt3a CM & RSPO1 CM optimization; y-axis in 1.000 (+/- s.e.m.)

A series of transfections was performed to optimize culturing conditions. Although it was already known for RSPO to exert a synergistic effect on Wnt pathway activation (see ***Chapter I***), the optimum concentration combination remained unknown. This study revealed the cost-effective to be at 5% Wnt CM in combination with 2% RSPO CM (Fig 10 CMT-U27 Wnt3a CM & RSPO1 CM optimization), reaching an enhancement of 470% compared to the control sample. Although TCF-reporter activity does not reach its highest level when applying this combination, but instead would suggest a 20% Wnt CM – 10% RSPO1 CM combination thereby reaching 510% increase, stimulation differences are negligible and are compensated for by being able to use ¼th of Wnt CM. The Control solution did not contain any Wnt CM or RSPO1 CM but was otherwise of similar composition as all other solutions. For the Ratio percentage, the control was set at 100%.

Imaging

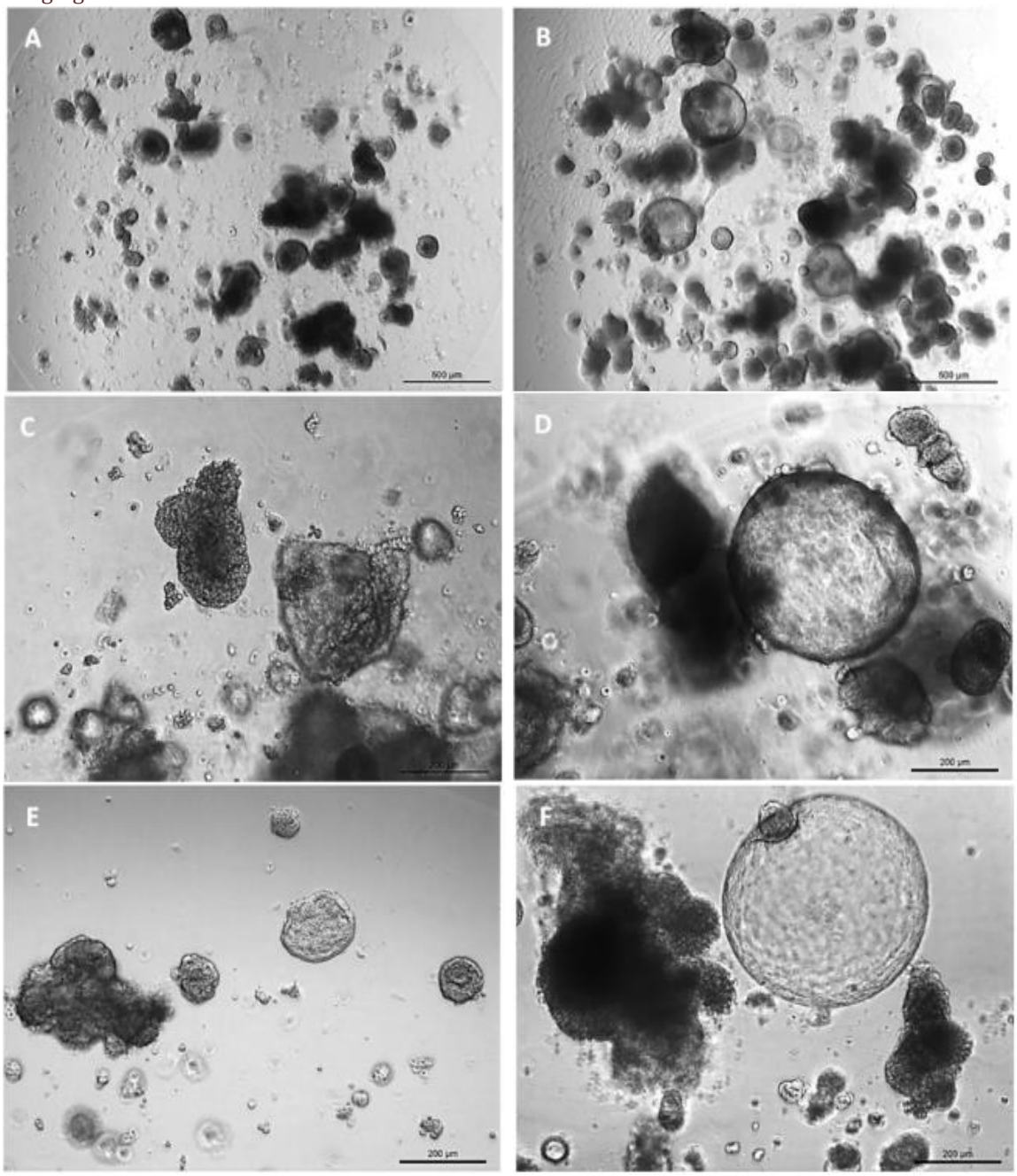

Figure 11 Organoids (**A**) Low Wnt culturing medium P7 day 0; (**B**) Low Wnt culturing medium, P7, day 14; (**C**) Low Wnt culturing medium, P10, day 0; (**D**) Low Wnt culturing medium, P10, day 7; (**E**) Medium Wnt culturing medium, P11, day 0**;** (**F**) Medium Wnt culturing medium, P11, day 16

Although it is challenging to make a definitive statement solely based on imaging, the Low Wnt culture medium did seem to yield the fastest growing organoids (Fig 11 (A) Low Wnt culturing medium, P7, day 0; (B) Low Wnt culturing medium, P7, day 14). Also, this culture condition seems to best facilitate novel organoid formation, compared to the other culturing conditions (Fig 11 (B) Low Wnt culturing medium, P7, day 14; (F) Medium Wnt culturing medium, P11, day 16).

In addition, Low Wnt culturing medium gave rise to quite typical, large, spherical cell formations (Fig 11 (D) Low Wnt culturing medium, P10, day 7). These could also sporadically be seen in Medium Wnt culturing conditions (Fig 11 (F) Medium Wnt culturing medium, P11, day 16), but remained completely absent from the High Wnt condition.

Stainings

αSMA

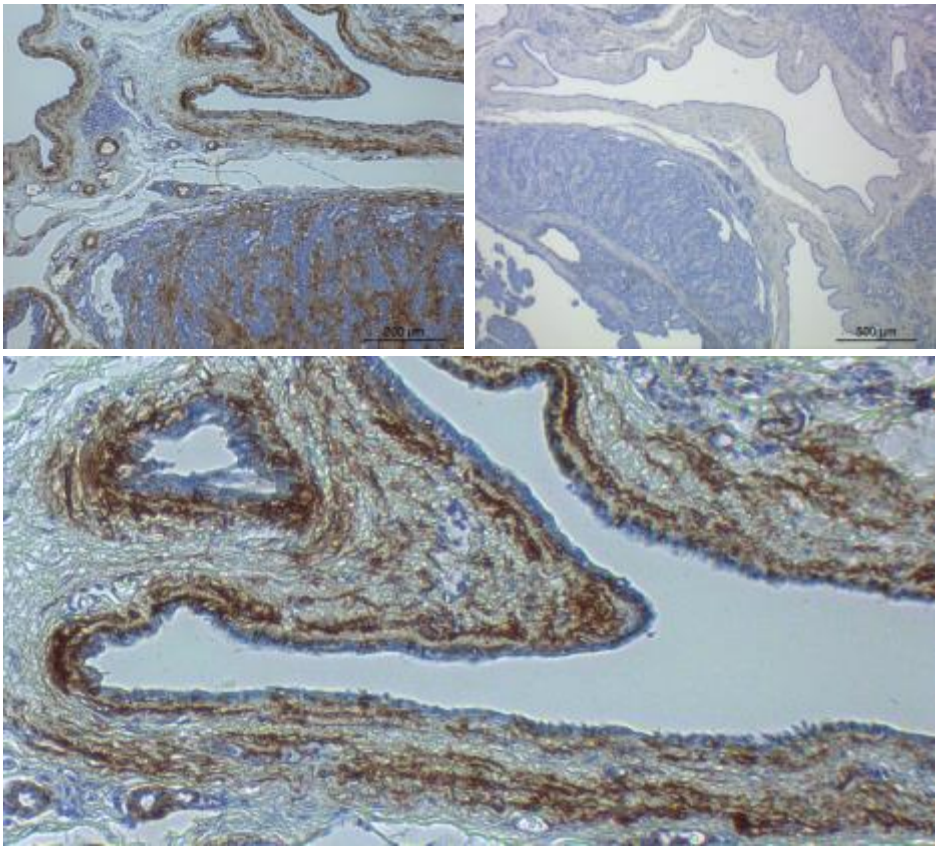

Figure 12 αSMA staining, Control Tissues (**L**) Mammary carcinoma tissue, αSMA AB; (**R**) Mammary carcinoma negative control, IgG AB; (**Below**) Close-up of (L)

αSMA is a smooth muscle and myoepithelial cell protein. This was also observed in the stainings performed both on control tissue and the euthanized dog tissue. As can be seen in the microscopic picture of canine mammary carcinoma tissue (Fig 12 αSMA staining. (L) Mammary carcinoma tissue, αSMA AB; (R) Mammary carcinoma negative control, IgG) staining (brownish colour) can mainly be observed just below the epithelial lining.

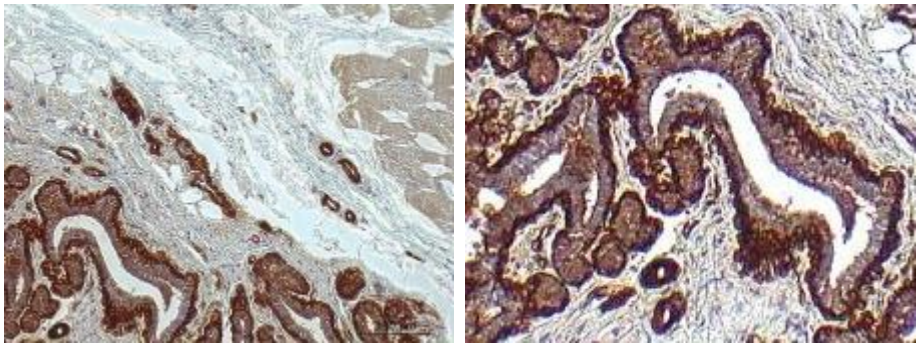

Figure 13 αSMA Staining; Canine mammary tissue; 108619; (**L**) 20 x; (**R**) Close-up

Similar results were obtained from the dog tissue stainings, with the majority of the slides showing clear staining of non-luminal cells bordering the epithelial lining (Fig 13 αSMA staining).

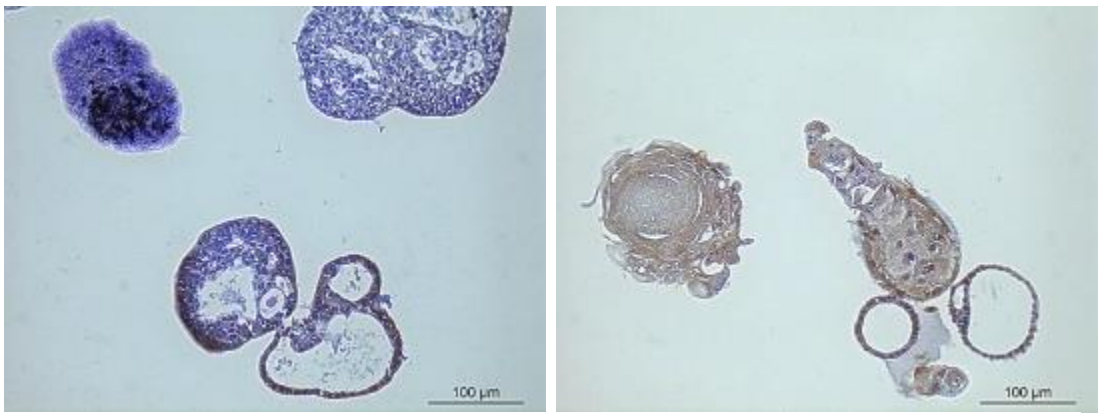

Figure 14 αSMA Staining, Organoids; (**L**) P5 Low; (**R**) P11 High; 20 x

With regard to the organoids, both passages and all culturing conditions resulted in an amount of αSMA staining (Fig 14 Organoids, αSMA staining). Although intensity varied slightly, one cannot with certainty single out one passage number or Wnt/RSPO concentration to produce stronger or more widespread staining.

CK7

CK7 staining was performed to differentiate the inner, glandular epithelium from the basal/myoepithelial layer by colouring solely the epithelium lining ductal or duct-derived structures. As can be derived from the control tissues, CK7 stained positive exclusively in cells bordering ductal-like structures (Fig 15 CK7 Staining, Mammary carcinoma tissue).

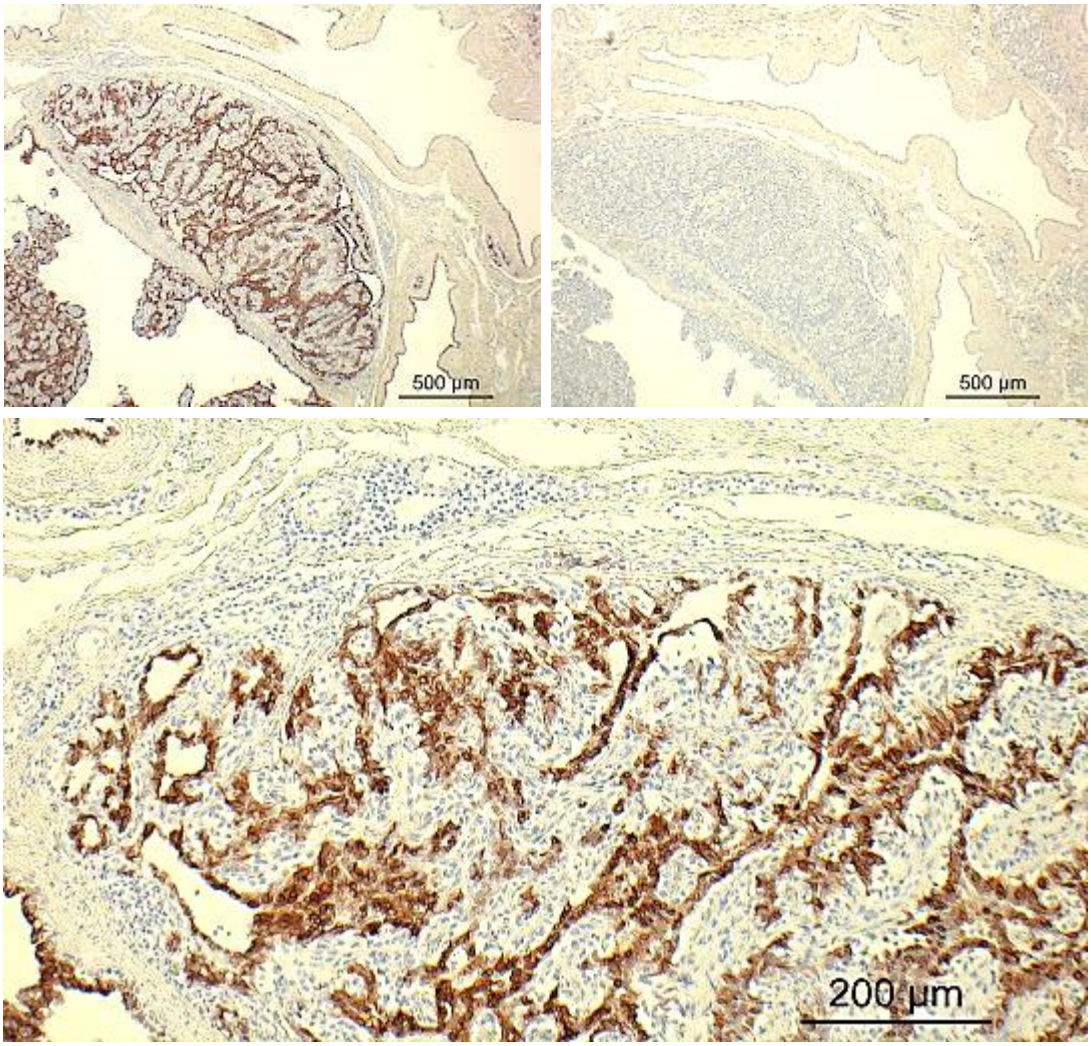

Figure 15 CK7 Staining, Mammary carcinoma tissue, Top row, 4x: (**L**) Positive control, CK7 AB; (**R**) Negative control, IgG1 AB; Bottom row, 10x: Positive control, CK7 AB

In figure 16, an explicitly luminal staining can be observed, colouring solely the ductal epithelium without showing any traces in the tissue layers below (Fig 16 CK7 Staining, Canine mammary tissue). However, some slides from the canine dog tissues did not come out positive, even though they do appear to contain luminal structures. Still, as can be derived from aforementioned figure, even in the slides staining highly positive, large areas appear where all colouring is absent. It might be the case that no ductal structures were sectioned in these slides, or the possibility exists that from these dogs the majority of the obtained tissue comprised of fat cells, which would not display luminal CK staining, thus presence of the CK protein in this part of the tissue is unlikely.

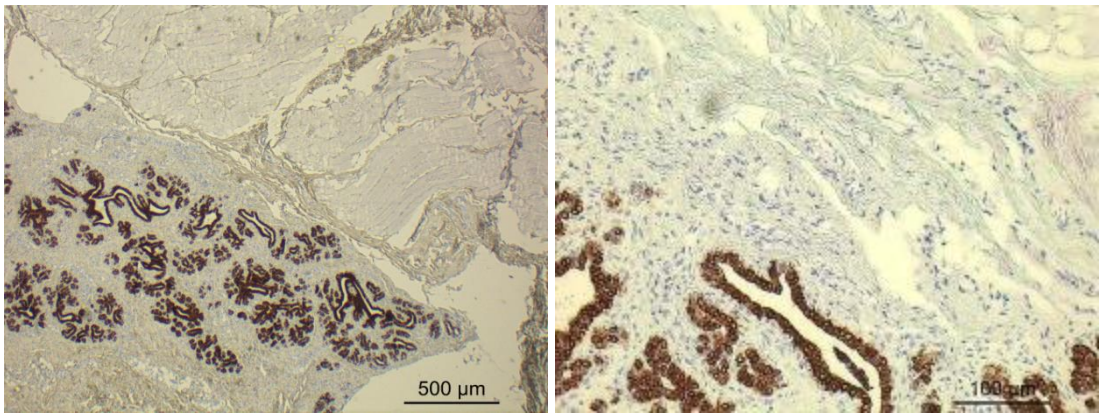

Figure 16 CK7 Staining, Canine mammary tissue, 108619: (**L**) 4x magnification; (**R**) 20x magnification

Regarding the organoids, although less obvious, there still is positive staining visible in both passage numbers, and in all culturing conditions. However, no certainty can be applied when localizing the staining, since it is not clearly situated near ductal structures or epithelial linings (Fig 17 CK7 Staining, Organoids). However, given that the organoid staining was performed simultaneously with all other CK7 stainings, and in the control tissues CK-specific signal was solely detected in luminal epithelium, it can be stated that the organoids also contain analogous ductal epithelium.

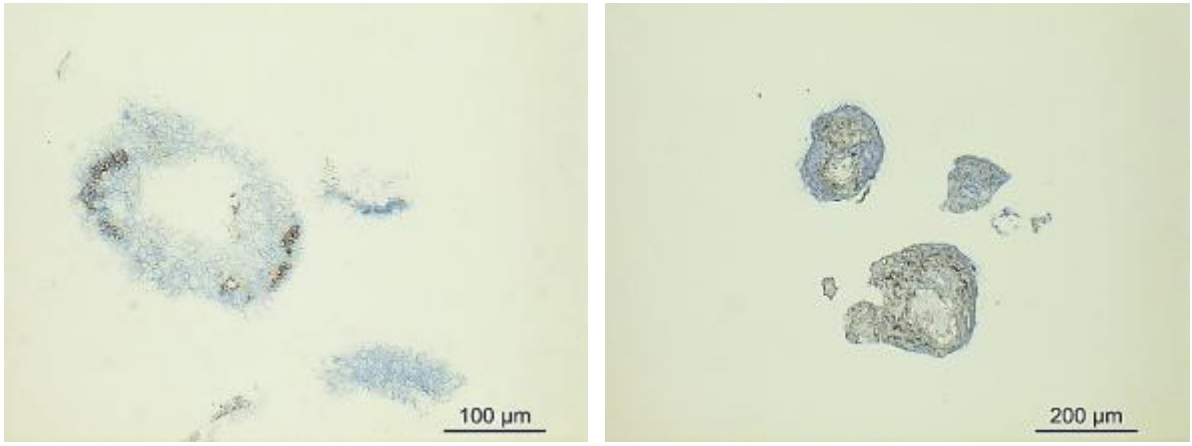

Figure 17 CK7 Staining, Organoids (**L**) P5 Medium, 20x; (**R**) P11 Medium; 10 x

CK19

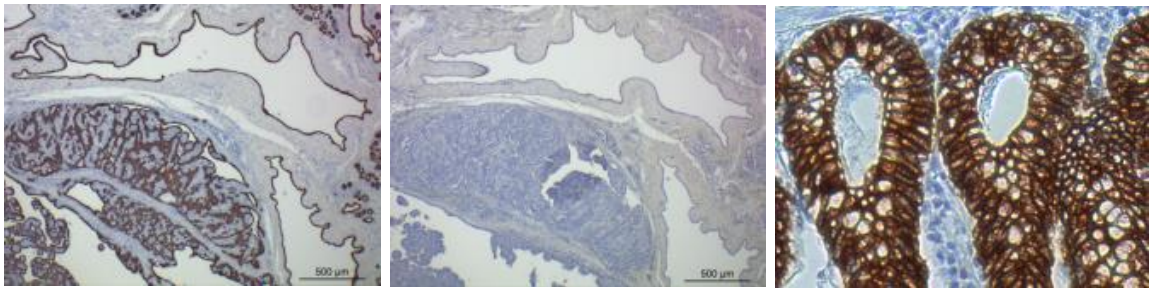

Figure 18 CK19 Staining Mammary carcinoma (**L**) Positive control: CK19 AB, 4x; (**M**) Negative control: IgG AB; 4x (**R**) Colon positive control, 20x

From Fig 18 CK19 Staining Mammary carcinoma, it can clearly be deduced that CK19 staining was performed appropriately, with no colouring visible in the negative control slide. Also, at higher magnifications (Fig 18 CK19 Staining (R) Colon positive control, 20x), a clear contrast between staining of luminal epithelium and absence of staining in all underlying tissues is evident.

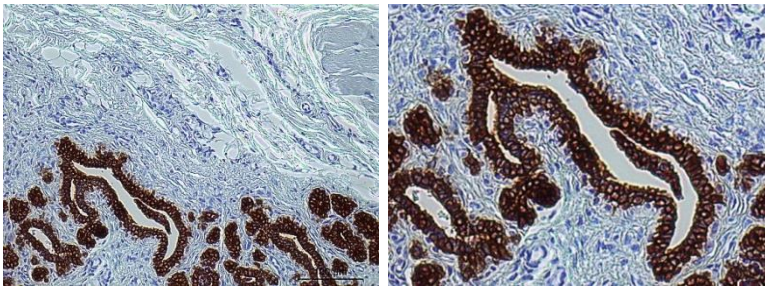

Figure 19 CK19 Staining, Canine mammary tissue, 108619 (**L**) 20x; (**R**) Enlargement

Similarly, most canine mammary tissue slides showed a positive outcome for the CK19 staining. Again the staining was distinctly observed in the epithelial lining of luminal structures, without a colouring signal visible in underlying tissues (Fig 19 CK19 Staining, Canine mammary tissue).

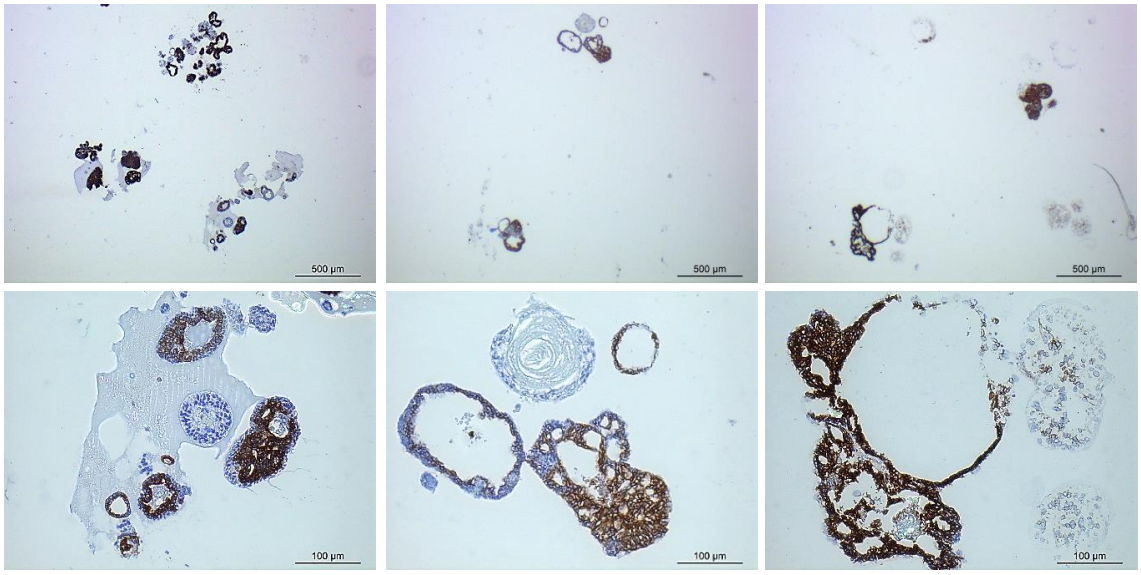

Figure 20 CK19 Staining, Organoids; Top row, P5, 4x: (**L**) High; (**M**) Medium; (**R**) Low; Bottom row, P5, 20x: (**L**) High; (**M**) Medium; (**R**) Low

Most organoid structures presented with positive CK19 staining as well, although not as distinctly localized as seen in the mammary tissues. Furthermore, the Medium culturing condition seemed to display reduced staining intensity compared to both High and Low culturing conditions, and also seemed more diffusely coloured (Fig 21 CK19 Staining, Organoids).

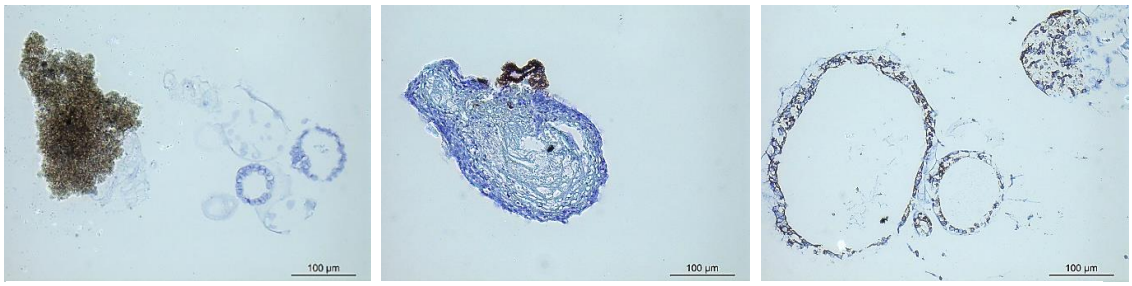

Figure 21 CK19 Staining, Organoids, P11, 20x (**L**) High; (**M**) Medium; (**R**) Low

In contrast, progression of passage number showed an inhibitory effect on staining quality. P11 clearly generated less positive staining, both location and intensity wise. Little can now be concluded on differences in culturing conditions, since no distinct structures have been stained, nor has a sufficient number of organoids been stained to provide reliable comparison (Fig 21 CK19 Staining, Organoids).

P-cad

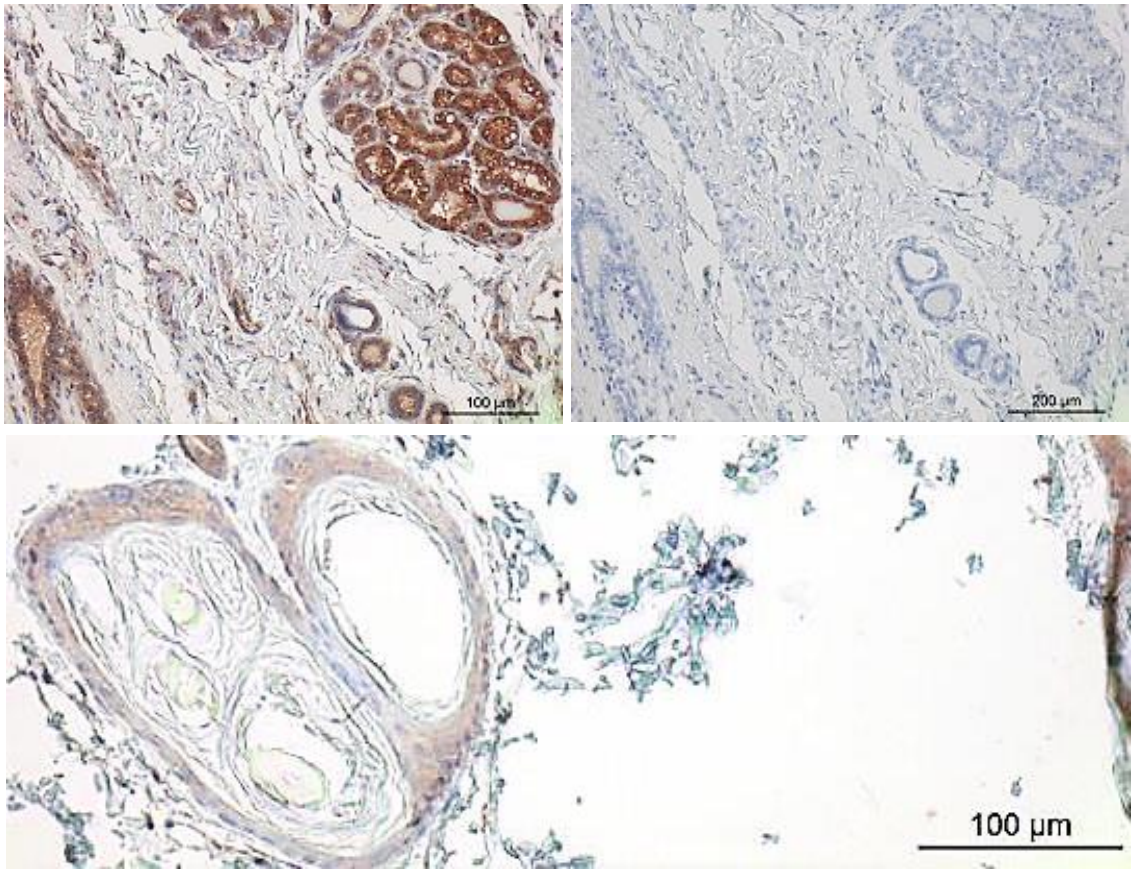

Figure 22 P-cad Staining, Control tissue, 20x, Top row: (**L**) Normal mammary tissue, P-cad AB (**R**) Normal mammary tissue, IgG1 AB; Bottom: Positive control Skin, P-cad AB

In the control mammary tissues, P-cad-specific antibodies highlighted predominantly the epithelial lining of ductal structures, however in the skin control sample colouring is more evident in the layer underlying the epithelium bordering the lumen (Fig 22 P-cad Staining, Control tissue).

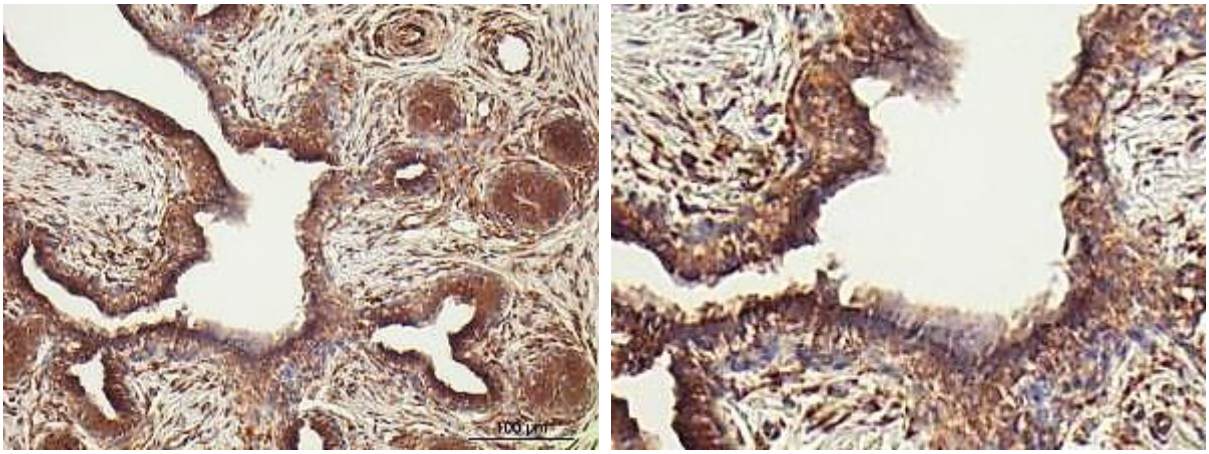

Figure 23 Canine mammary tissue, 105393 (**L**) 20x (**R**) Enlargement

Staining characteristics in the canine mammary tissues most closely resembled the skin control tissue, with predominant colouring in the cell line just below the epithelial lining (Fig 23 Canine mammary tissue).

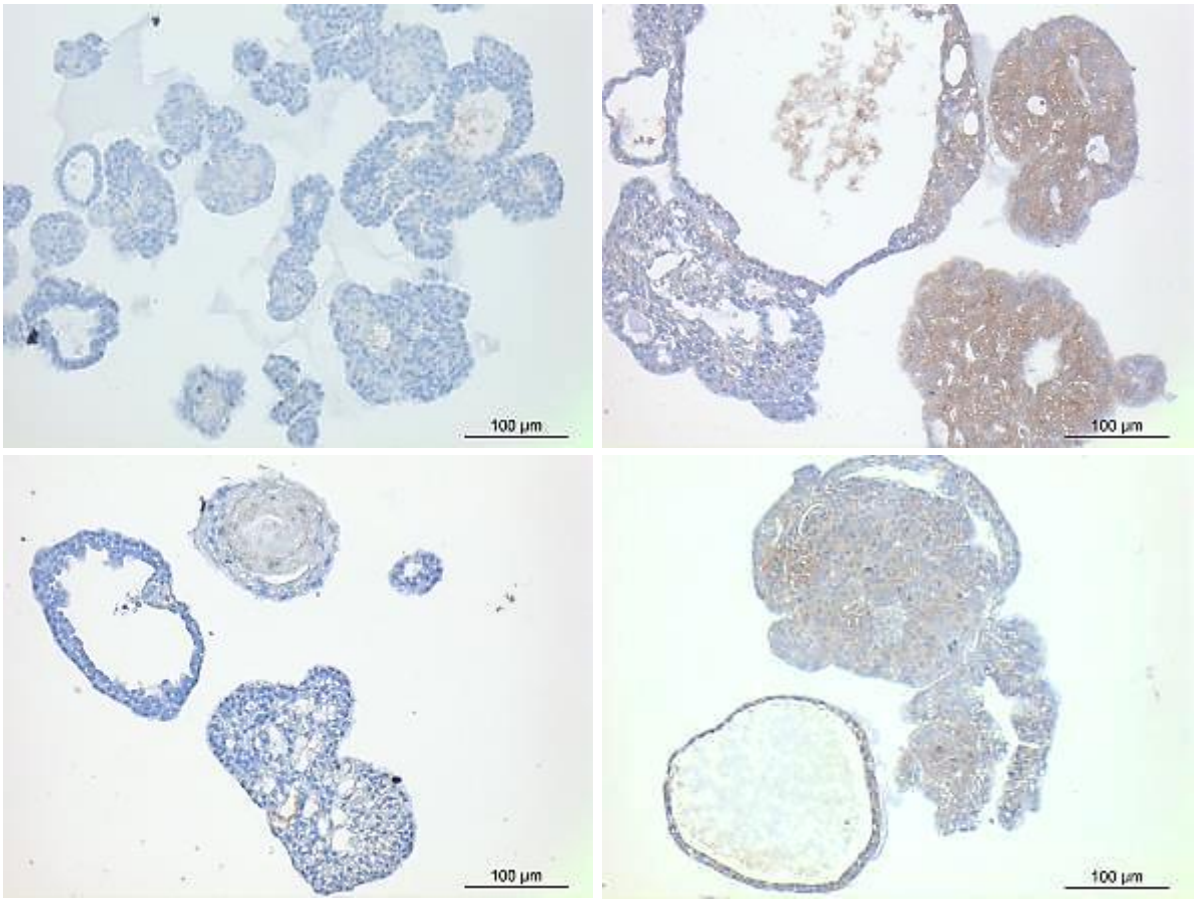

Figure 24 P-cad Staining, Organoids, Top row: P5, 20x (**L**) High; (**R**) Low; Bottom row: P11, 20x (L) Medium; (R) Low

In the lower passage number, P-cad staining was almost exclusively observed in the Low culturing condition. However, with regard to location little can be concluded, as the slides were quite diffusely stained, with no preference for specific cell types or linings (Fig 24 P-cad Staining, Organoids).

Passage 11 yielded comparable results, with the highest staining intensity observed in the Low culturing condition. Little colouring could however also be detected in the Medium condition, whereas the High culturing condition was again devoid of P-cad AB staining.

E-cad

Figure 25 E-cad Staining, Control tissues, Top row, 10x: (**L**) Positive control colon; (**R**) Negative control colon; Bottom row, 20x: Positive control colon

In figure 25 an epithelial staining can indisputably be recognized. All cells bordering the lumen of ductal structures are coloured, whereas no positivity can be detected in underlying tissue (Fig 25 E-cad Staining, Control tissues).

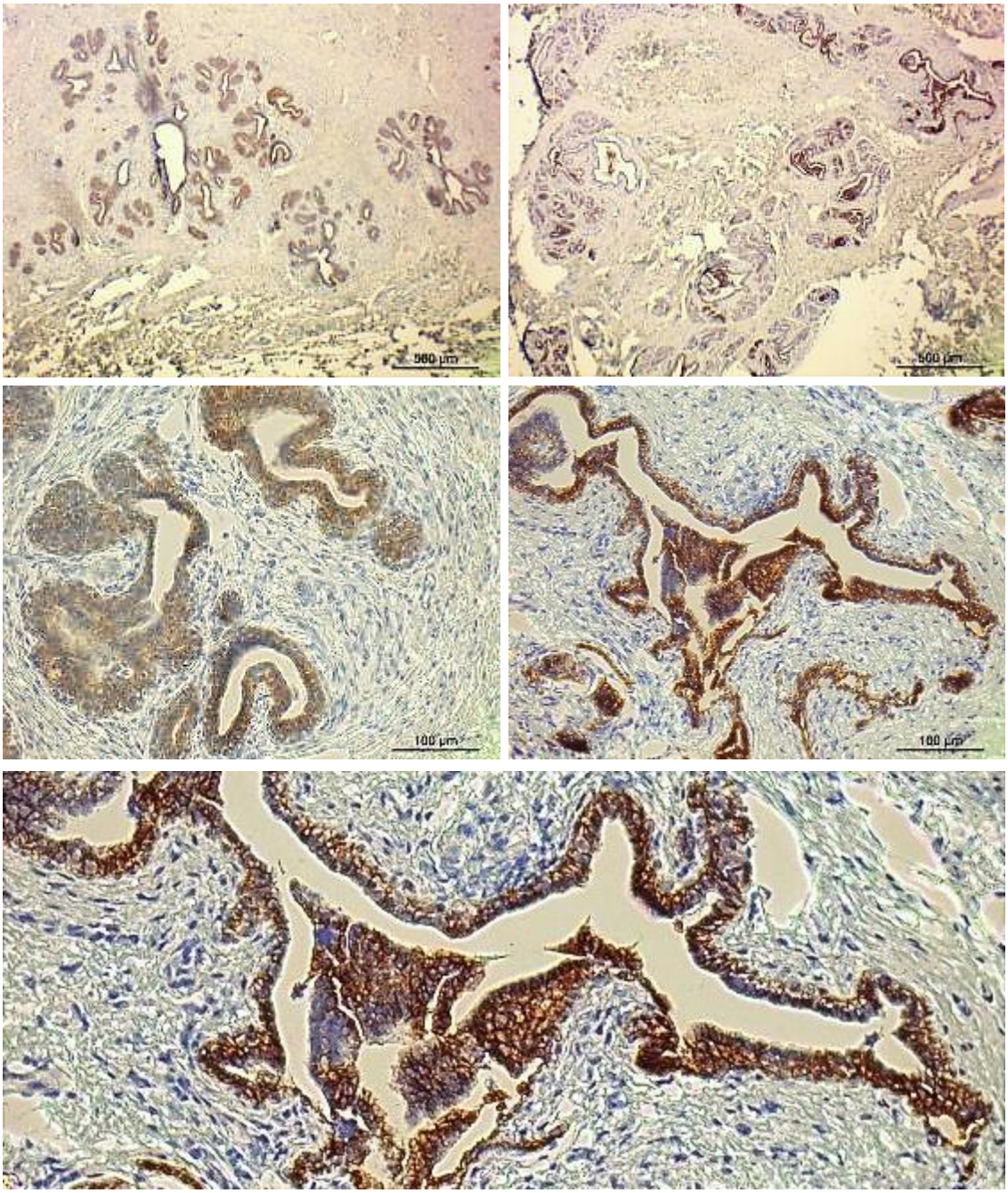

Figure 26 E-cad Staining, canine mammary tissue, Top row, 4x: (**L**) 105393; (**R**) 108619; Middle row, 20x: (**L**) 105393; (**R**) 108619; Bottom row: 108619 enlargement

Surprisingly, only 2 of the 5 euthanized dogs presented with distinct E-cad colouring. Additionally, with regard to the predominant location it remains unclear if E-cad proteins are principally found in the epithelial lining or the cells just below the lumen-bordering tissue. In both slides which presented with the most intense staining, these being the slides from dog 4 and 5, both locations could be opted. Nevertheless, the enlargement suggests E-cad appears to mainly present in the sub epithelial lining, although many cells directly bordering the lumen also stain positive (Fig 26 E-cad Staining, canine mammary tissue).

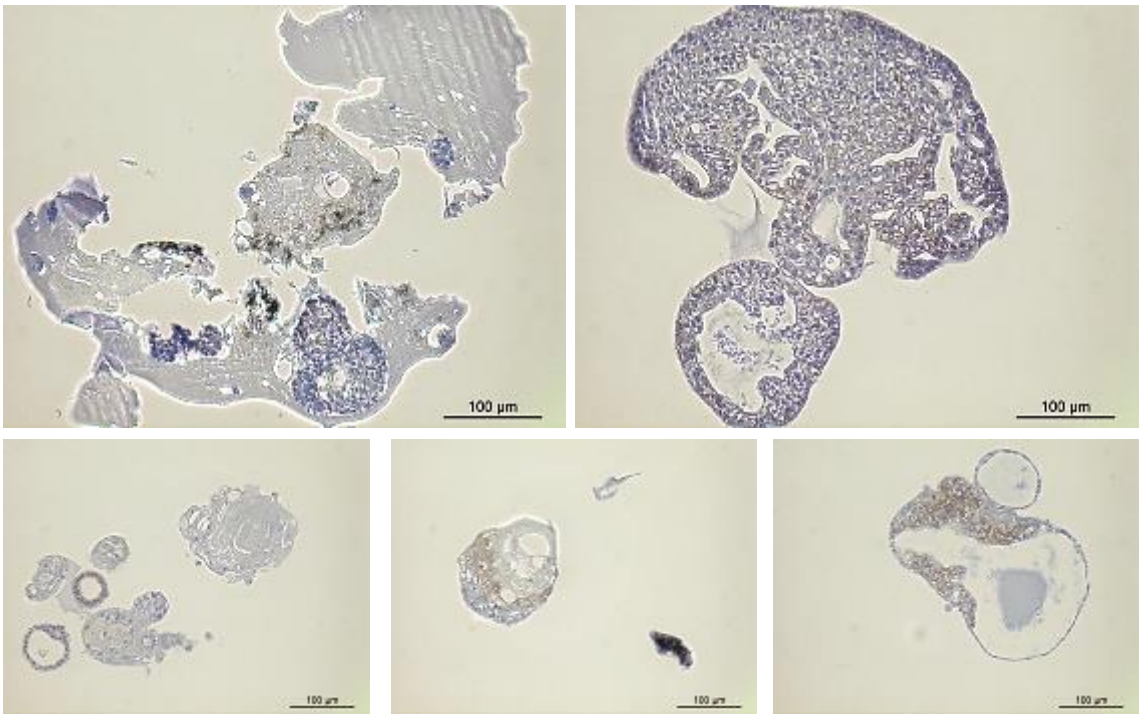

Figure 27 P-cad Staining, Organoids, 20x, Top row, P5: (**L**) High; (**R**) Medium; Bottom row, P11: (L) High; (M) Medium; (R) Low

The organoid slides hardly responded to E-cad staining. In passage 5, E-cad remained completely absent from the Medium culturing condition slides. Although both the High and Low condition presented with marginal colouring, no conclusions can be drawn on the subject of E-cad expression (Fig 27 P-cad Staining, Organoids, 20x, Top row, P5: (L) High; (R) Medium). In the higher passage number, E-cad was detected in all culturing conditions, however, location wise only the High culturing condition gave rise to relative distinct cell types, namely those bordering the lumen of seemingly ductal structures (Fig 27 P-cad Staining, Organoids, 20x, Bottom row, P11: (L) High). All remaining slides presented with diffuse staining of low intensity.

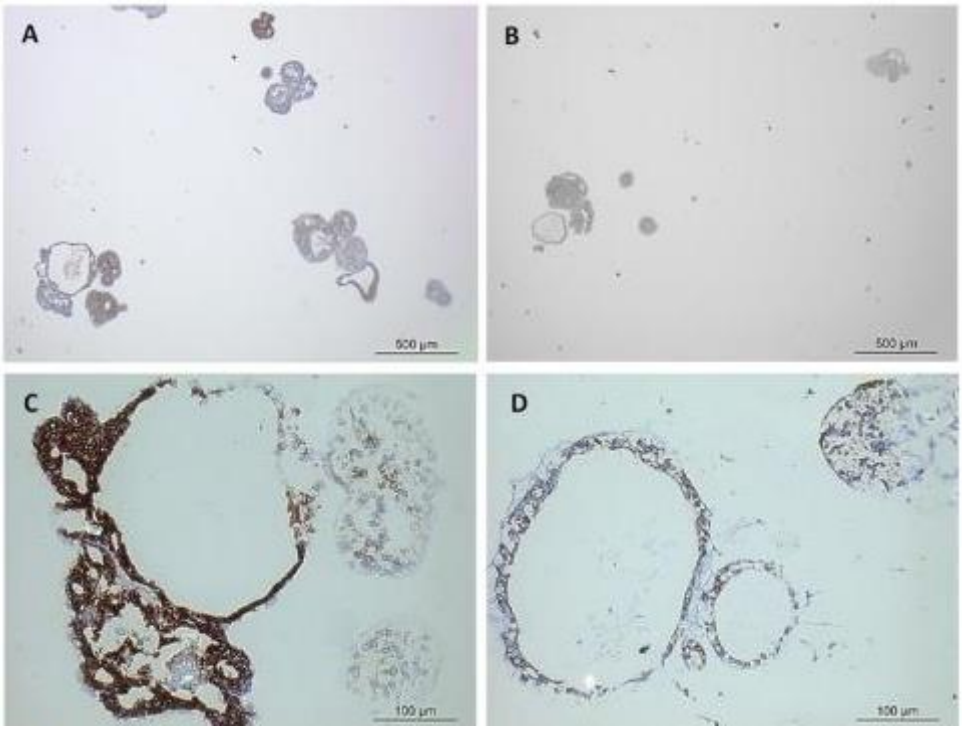

Figure 28 Organoid staining (**A**) P-cad P5 Low Wnt culture medium**;** (**B**) P-cad P11 Low Wnt culture medium; (**C**) CK19 P5 Low Wnt culture medium; (**D**) CK19 P11 Low Wnt culture medium

Passaging seems to impair organoid condition

P5 seemed to provide better staining conditions compared to P11. Although both passage numbers show similar tendencies in staining level, all antibody stainings seem to have affixed better to the lower passage number (Figure 28 Organoid staining).

High Wnt culturing medium seemed to cause preservation of stem cell qualities, whereas the organoids in the Medium Wnt culturing condition display more differentiation characteristics. Overall, these organoids most explicitly present with luminal structures.

P4

From the euthanized dogs P4 levels were also determined. This resulted in one individual showing relatively high P4 levels of 19,4, whereas all other samples remained comparatively low, with an average of 0,9 ng/ml. Subsequently a connection was sought between these P4 levels and the amount of staining observed in the canine mammary tissues. However, 4 out of 5 stainings used did not yield directly comparable data.

Dog	No. #	P4 levels (ng/ml)
1	100642	0.2
2	104762	0.4
3	105109	2.7
4	105393	19.2
5	108619	0.4

αSMA staining in the obtained dog tissues did not link directly to P4 levels. For example, stained tissue slides from dog 2 displayed equal amounts of αSMA signals as did dog 4, although P4 levels varied greatly between the two samples (Fig 29 Top row, αSMA Staining).

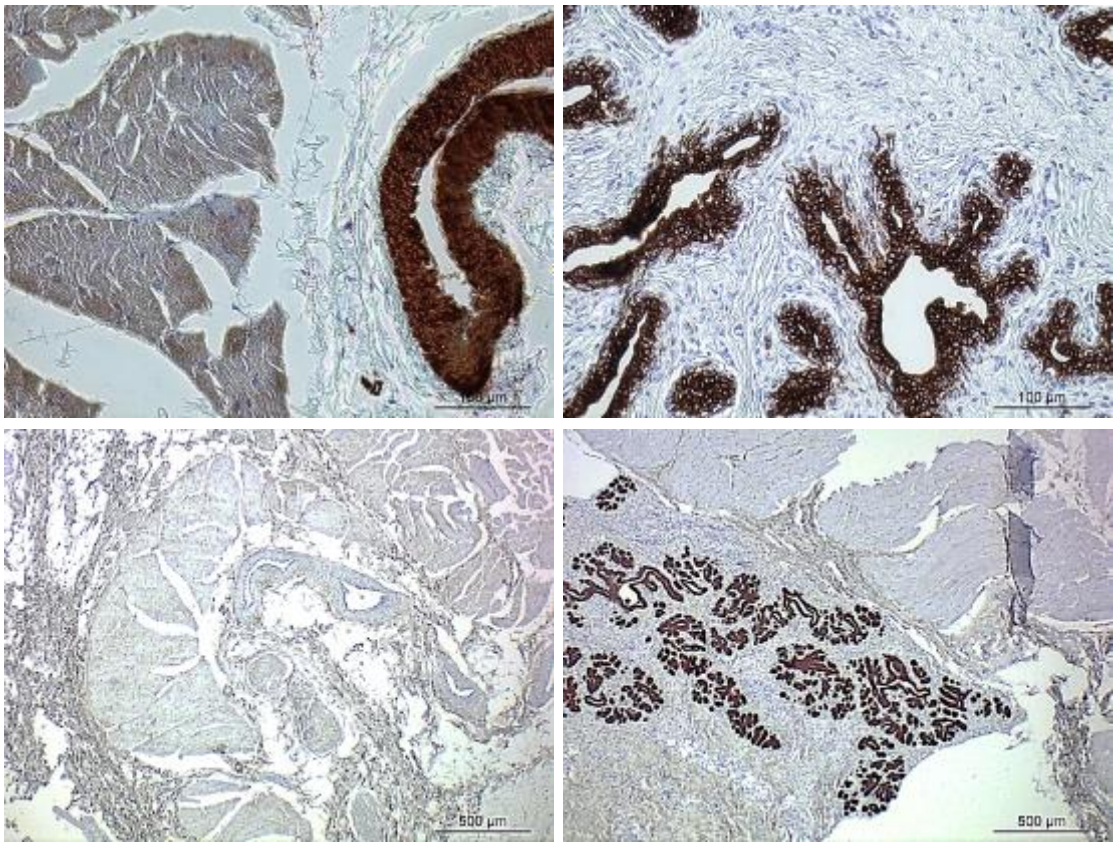

Figure 29 Top row: αSMA Staining, 20x: (**L**) 104762; (**R**) 105393; **Bottom row, CK19 Staining**, 4x: (**L**) 104762; (R) 108619

Similarly incomparable results were obtained when assessing CK expression, with both CK7 and CK19 yielding staining signalling unmatched to P4 levels. Both dog 2 and dog 5 yielded similar P4 levels, namely 0,4 ng/ml, whereas the stained slides from dog 2 displayed no colouring whatsoever while the dog 5 slides were highly positive (Fig 29 Bottom row, CK19 Staining).

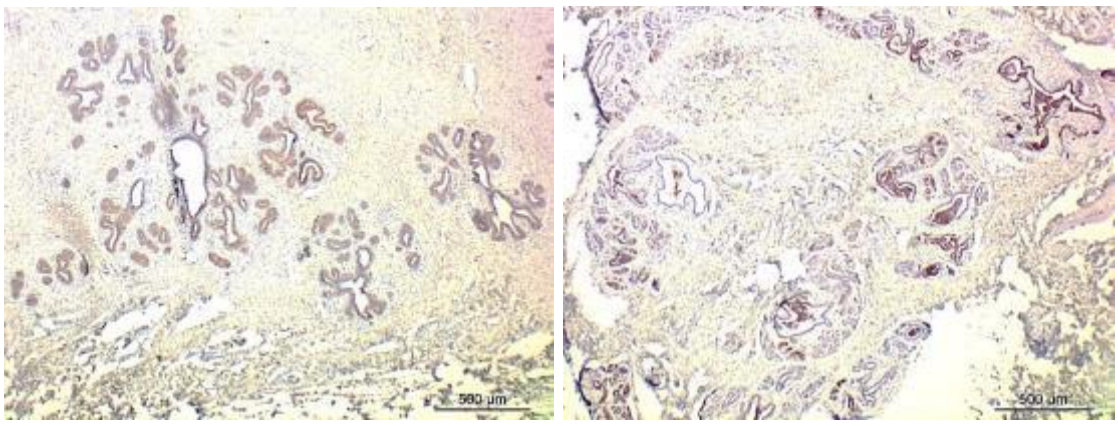

Figure 30 E-cad Staining, Canine mammary tissue, 4x; (L) 105393 (R) 108619

For E-cad the opposite was applicable, with similar staining levels observable in both dog 4 and dog 5, whereas P4 levels comprised 19,2 and 0,4, relatively (Fig 30 E-cad Staining, Canine mammary tissue).

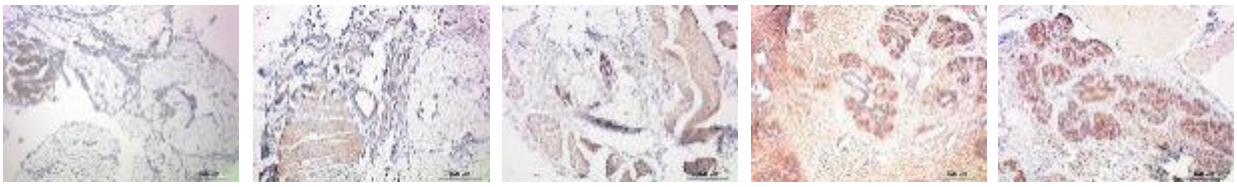

Figure 31 P-cad Staining, 4x, from left to right: 100642, 104762, 105109, 105393, 108619

Lastly, P-cadherin levels did yield staining intensity variations comparable to P4 level differences. From Fig 31 the strongest positivity is imminent in dog 4, who also presented with the highest P4 value of 19,2 ng/ml (Fig 31 P-cad Staining). When viewed at higher magnification it becomes clear that any further relations are questionable, since dog 2 and 5 matched with regard to P4 levels but show very distinct reactions to P-cad staining, with dog 5 displaying a more widespread and intense colour compared to dog 2 (Fig 32 P-cad Staining, canine mammary tissue).

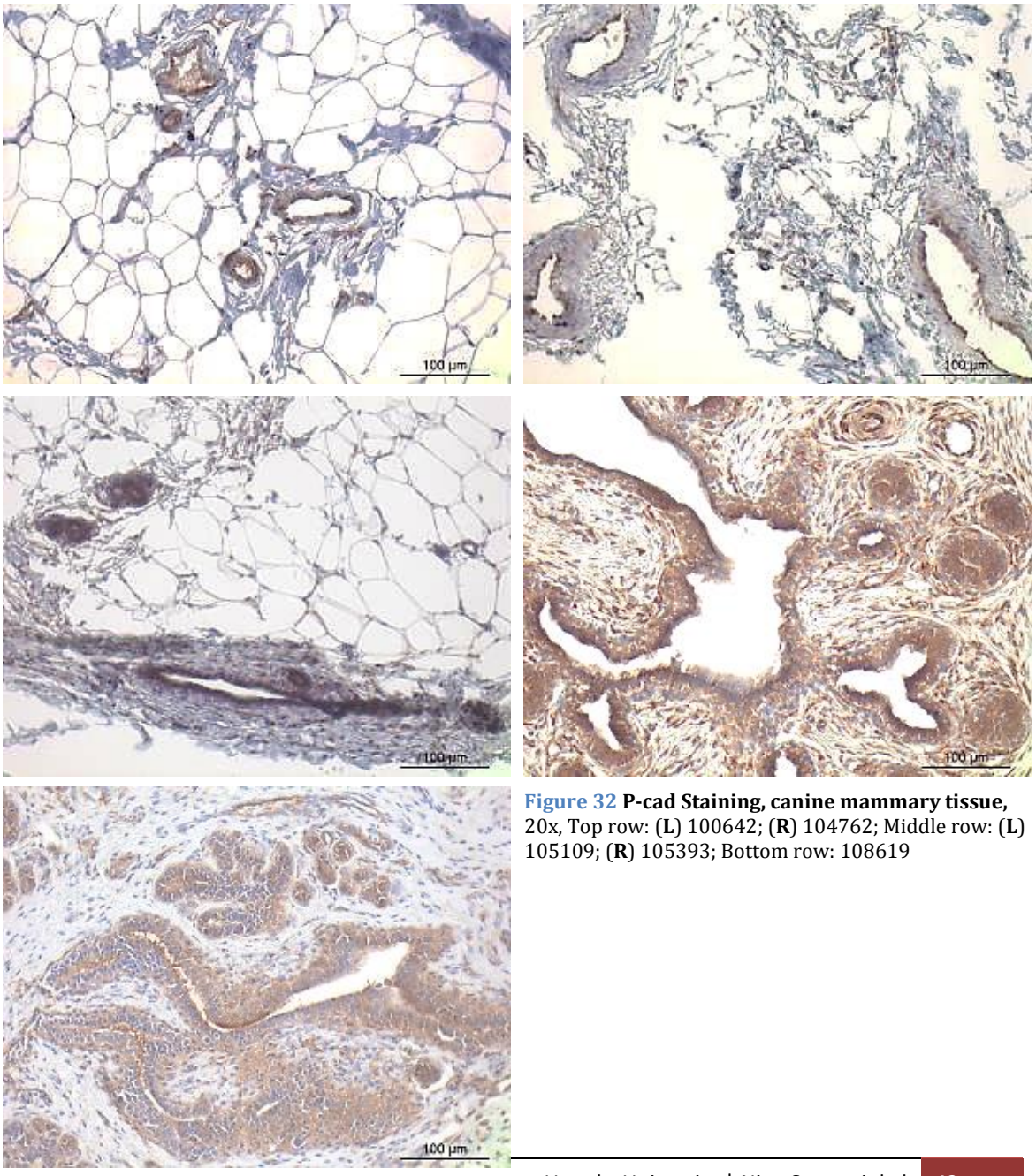

Figure 32 P-cad Staining, canine mammary tissue, 20x, Top row: (**L**) 100642; (**R**) 104762; Middle row: (**L**) 105109; (**R**) 105393; Bottom row: 108619

Discussion II

Organoids have been aiding cancer research extensively over the last decade. However, with mammary gland derived organoids still lagging behind in stability and (thus) application, an attempt was made to improve on culturing conditions, and simultaneously investigate the effects of the several conditions on stem cell development.

Since organoids develop from stem cells, and stem cells are known to be regulated by the Wnt pathway, the choice was made to subject the organoids to 3 culturing conditions containing varying levels of Wnt CM and RSPO1 CM, and investigate the effects on differentiation versus stem cell property preservation.

With αSMA yielding positive results in both passage numbers under all conditions, it can be stated that all organoid formations contain some sort of myoepithelial layer, or muscle-like cell types. However, no clear structural organisation can yet be recognized, except for some distinct colouring of cells surrounding luminal structures. This is not entirely surprising, since αSMA has been proposed to play a role in the contraction of mesenchymal stem cells (**Kinner et al., 2002**). Also, αSMA is found near wound margins during the healing process, opting for a proliferative role under these conditions as well (**Yoshiba et al., 2012**). In general, αSMA is considered a marker for myoepithelial differentiation (**Shan et al., 2016**), however in this study we find no evidence of αSMA staining variations of conditions that are otherwise considered to be in diverse differentiation stages.

CK7 and 19 are both low molecular weight CKs expressed specifically in the luminal epithelial cells, and the stainings have proven to be consistent and fully functional in canine mammary gland tissues (**Griffey et al., 1993**). According to the Human Protein Atlas (http://www.proteinatlas.org), the CK19 staining is well-nigh similar to the CK7 staining in that they both stain the cytoplasm and membrane of glandular epithelium. Additionally, for CK19 respiratory and squamous epithelium can be added, as well as renal tubules, exocrine pancreas and trophoblasts (http://www.proteinatlas.org/ENSG00000171345-KRT19/tissue). Both CKs were found present under all Wnt/RSPO1 circumstances, and although they often showed quite diffuse expression throughout the organoid structures, they also showed a tendency to accumulate around ductal structures. From this the assumption might perchance be made that the organoids are well capable of self-structuring, and it is surprising to see that the structures manage to do so in such short notice. Additionally, a decrease in CK staining was observed in both the High and Low culturing condition at P11, accompanied by incredibly diffuse and unorganized staining, whereas in the Medium condition one quite unmistakably luminal structure was profoundly coloured. Whether this is due to imbalanced decrease of organoid quality, or because of distinct ongoing differentiation in the Medium culturing condition remains to be determined.

E-cad AB staining was nigh absent from all passages under all culturing conditions. To assess whether the remote colouring perceived was caused by non-specific binding or indeed the presence of E-cad-positive cells further research is warranted.

Since P-cad has closely been related to preserving the undifferentiated state of stem cells, and seems to limit proliferation (**Vieira, Paredes, 2015**), it would appear that due to elevated P-cad staining in the Low culturing condition, this condition is most likely to be suitable for the preservation of stem cell properties, at Wnt CM and RSPO CM percentages of 5% and 2%, respectively. The organoids in the Medium Wnt culturing condition display more differentiation characteristics, since the Medium culturing condition most explicitly present with luminal structures. Based on the comparison between the 3 conditions, tentatively it can be stated that the medium condition seemed to yield the most differentiated structures. It is thus suggested to apply concentrations of around 25% Wnt CM with 10% RSPO1 CM, when aiming for differentiating mammary gland derived organoids.

Regarding the High culturing condition, little can be stated with certainty. This is due to a relatively small number of organoids present in this condition, while previous research on this lab highlighted the importance of organoids being cultured in ample numbers. This seemed to have beneficial effects on organoid growth and quality. However, after dividing the organoids in 3 groups the High condition was left with relatively few structures, and due to unfortunate culturing circumstances these organoids never managed to proliferate similarly to the organoids in the remaining conditions. Thus, the effect of the culturing concentrations used for the High condition remain undefined, and in depth research is required to elucidate its exact role.

Despite widespread knowledge on P4 in relation to the mammary gland, the details of this connection have, to a large extend, remained obscure. Here we present evidence that P4 levels might be related to P-cad, with extensive P-cad staining observed in canine tissues yielding extremely high P4 levels in the corresponding blood sample. Unfortunately, no further statements can be made regarding the remaining stainings applied in relation to P4 working mechanism.

According to Vieira and Paredes (2015), P-cad is a cell junction adhesion molecule, conserving epithelial tissue structure. Presence of the molecule has been observed in the basal layer of e.g. epidermis, prostate, cornea and breast tissues (**Vieira, Paredes, 2015**). Additionally, in mammary gland tissue, P-cad was localized in stem cells that give rise to the myoepithelial layer (**Knudsen, Wheelock, 2005**). However, they also found that expression of P-cad is dependent on developmental stage, with P-cad expression having been observed in human alveolar cells in the lactating gland (**Soler et al., 2002**), and even a soluble form of P-cad was measured in human breast milk. Despite the uncertainty still existing with regard to the exact localisation of P-cad, its role in the conservation of structural integrity has been widely accepted. P-cad, like many other cadherins, unmistakeably regulates cell structuring and growth (**Cavallaro, Dejana, 2011**), explicitly limiting proliferation and migration of mammary epithelial cells. Thus, since P-cad has closely been related to preserving the undifferentiated state of stem cells, it is not surprising that P-cad has been proposed as promising stem cell marker.

A close connection between P-cadherin levels and breast cancer has actually been published earlier this year, although in combination with increased E-cadherin expression (**Brilliant et al., 2017**). They also found that either cadherin expression, β-catenin and p120 catenin (another cell adhesion molecule) release into the tumour cell cytoplasm, or a combination of these two processes provided a link with increased EMT, resulting in progressive cancer and metastasis formation. This is in accordance with the present findings, where increased P4 levels appeared related to both P-cadherin expression and maintenance of stem cell properties. Overall, the combined research on healthy canine mammary tissue and MaSC derived organoids has yielded some promising results, and although much is left to investigate, this study has hopefully aided in the research on carcinogenic mechanisms in general, and canine mammary cancer more specifically.

Conclusion II

Concludingly, this investigation has contributed to the ever-expanding knowledge regarding the organoid culturing system. Mammary stem cell-derived systems can now be grown for up to 15 passages, and greater insight has been obtained concerning the culturing medium to be applied depending on the preferred results. These could either be stem cell property maintenance or, contrarily, differentiation of the organoid structures. As the importance of the Wnt pathway in retaining stem cell predicates has been widely accepted, it brings no surprise that distinct Wnt concentrations yield varying developmental stages. An outline has been created on a defined culturing solution where organoid quality is kept intact, and proliferation speed is not restrained, but where the organoids can still be steered into the preferred direction. This should aid all research conducted on mammary tissue, or any mammary gland-related topic. However, in this case the focus was laid on mammary carcinomas, since this remains one of the most common diseases found in many species, including dog and human. Much research in this area is still warranted, and with the dog forming a useful model of human breast cancer, organoids derived from canine stem cell will prove of invaluable assistance in the fight against one of the most common cancers worldwide.

References

Articles

A

Achari et al., 2014 Achari C, Winslow S, Ceder Y, Larsson C (2014) *Expression of miR-34c induces G2/M cell cycle arrest in breast cancer cells*. BMC Cancer. 2014 Jul 26;14:538. doi: 10.1186/1471-2407-14-538.

Anfossie et al., 2014 Anfossi S, Giordano A, Gao H, Cohen EN, Tin S, Wu Q, Garza RJ, Debeb BG, Alvarez RH, Valero V, Hortobagyi GN, Calin GA, Ueno NT, Woodward WA, Reuben JM (2014) *High serum miR-19a levels are associated with inflammatory breast cancer and are predictive of favorable clinical outcome in patients with metastatic HER2+ inflammatory breast cancer*. PLoS One. Jan 8;9(1):e83113. doi: 10.1371/journal.pone.0083113.

Aupperlee et al., 2005 Aupperlee MD, Smith KT, Kariagina A, Haslam SZ (2005) *P4 receptor isoforms A and B: temporal and spatial differences in expression during murine mammary gland development*. Endocrinology. Aug;146(8):3577-88.

Aval et al., 2017 Aval SF, Lotfi H, Sheervalilou R, Zarghami N (2017) *Tuning of major signaling networks (TGF-β, Wnt, Notch and Hedgehog) by miRs in human stem cells commitment to different lineages: Possible clinical application*. Biomed Pharmacother. Jul;91:849-860. doi: 10.1016/j.biopha.2017.05.020.

Avery-Kiejda et al., 2014 Avery-Kiejda KA, Braye SG, Mathe A, Forbes JF, Scott RJ (2014) *Decreased expression of key tumour suppressor microRNAs is associated with lymph node metastases in triple negative breast cancer*. BMC Cancer. Jan 31;14:51. doi: 10.1186/1471-2407-14-51.

Axlund, Sartorius, 2012 Axlund SD, Sartorius CA (2012) *P4 regulation of stem and progenitor cells in normal and malignant breast*. Mol Cell Endocrinol. Jun 24;357(1-2):71-9. doi: 10.1016/j.mce.2011.09.021.

B

Barker et al., 2007 Barker N, van Es JH, Kuipers J, Kujala P, van den Born M, Cozijnsen M, Haegebarth A, Korving J, Begthel H, Peters PJ, Clevers H (2007) *Identification of stem cells in small intestine and colon by marker gene Lgr5*. Nature. Oct 25;449(7165):1003-7.

Beatson, 1896 Beatson GT (1896) *On the treatment of inoperable cases of carcinoma of the mamma: suggestions for a new method of treatment with illustrative cases.* Lancet. Volume 148, No. 3803, p162–165, 18 July;ii:104–107.

Beg et al., 2017 Beg MS, Brenner AJ, Sachdev J, Borad M, Kang YK, StoudemiRe J, Smith S, Bader AG, Kim S, Hong DS (2017) *Phase I study of MRX34, a liposomal miR-34a mimic, administered twice weekly in patients with advanced solid tumors*. Invest New Drugs. Apr;35(2):180-188. doi: 10.1007/s10637-016-0407-y.

Binnerts et al., 2007 Binnerts ME, Kim KA, Bright JM, Patel SM, Tran K, Zhou M, Leung JM, Liu Y, Lomas WE 3rd, Dixon M, Hazell SA, Wagle M, Nie WS, Tomasevic N, Williams J, Zhan X, Levy MD, Funk WD, Abo A (2007) *R-Spondin1 regulates Wnt signaling by inhibiting internalization of LRP6*. Proc Natl Acad Sci U S A. Sep 11;104(37):14700-5.

Boj et al., 2015 Boj SF, Hwang CI, Baker LA, Chio II, Engle DD, Corbo V, Jager M, Ponz-Sarvise M, Tiriac H, Spector MS, Gracanin A, Oni T, Yu KH, van Boxtel R, Huch M, Rivera KD, Wilson JP, Feigin ME, Öhlund D, Handly-Santana A, Ardito-Abraham CM, Ludwig M, Elyada E, Alagesan B, Biffi G, Yordanov GN, Delcuze B, Creighton B, Wright K, Park Y, Morsink FH, Molenaar IQ, Borel Rinkes IH, Cuppen E, Hao Y, Jin Y, Nijman IJ, Iacobuzio-Donahue C, Leach SD, Pappin DJ, Hammell M, Klimstra DS, Basturk O, Hruban RH, Offerhaus GJ, Vries RG, Clevers H, Tuveson DA (2015) *Organoid models of human and mouse ductal pancreatic cancer*. Cell. Jan 15;160(1-2):324-38. doi: 10.1016/j.cell.2014.12.021.

Boretto et al., 2017 Boretto M, Cox B, Noben M, Hendriks N, Fassbender A, Roose H, Amant F, Timmerman D, Tomassetti C, Vanhie A, Meuleman C, Ferrante M, Vankelecom H (2017) *Development of*

organoids from mouse and human endometrium showing endometrial epithelium physiology and long-term expandability. Development. May 15;144(10):1775-1786. doi: 10.1242/dev.148478.

Borges et al., 2017 Borges US, Costa-Silva DR, da Silva-Sampaio JP, Escórcio-Dourado CS, Conde AM Jr, Campelo V, Gebrim LH, da Silva BB, Lopes-Costa PV (2017) *A comparative study of Ki-67 antigen expression between luminal A and triple-negative subtypes of breast cancer*. Med Oncol. 2017 Sep;34(9):156. doi: 10.1007/s12032-017-1019-x.

Bovell et al., 2013 Bovell LC, Shanmugam C, Putcha BD, Katkoori VR, Zhang B, Bae S, Singh KP, Grizzle WE, Manne U (2013) *The prognostic value of microRNAs varies with patient race/ethnicity and stage of colorectal cancer*. Clin Cancer Res. Jul 15;19(14):3955-65. doi: 10.1158/1078-0432.CCR-12-3302.

Brilliant et al., 2017 Brilliant YM, Brilliant AA, Sazonov SV (2017) *Epithelial cadherins and associated molecules in invasive lobular breast cancer*. Arkh Patol.;79(1):12-18. doi: 10.17116/patol201779112-18.

Brisken et al., 2000 Brisken C, Heineman A, Chavarria T, Elenbaas B, Tan J, Dey SK, McMahon JA, McMahon AP, Weinberg RA (2000) *Essential function of Wnt-4 in mammary gland development downstream of P4 signaling*. Genes Dev. Mar 15;14(6):650-4.

Bu et al., 2013 Bu P, Chen KY, Chen JH, Wang L, Walters J, Shin YJ, Goerger JP, Sun J, Witherspoon M, Rakhilin N, Li J, Yang H, Milsom J, Lee S, Zipfel W, Jin MM, Gümüş ZH, Lipkin SM, Shen X (2013) *A microRNA miR-34a-regulated bimodal switch targets Notch in colon cancer stem cells*. Cell Stem Cell. May 2;12(5):602-15. doi: 10.1016/j.stem.2013.03.002.

C

Cai et al., 2013 Cai J, Guan H, Fang L, Yang Y, Zhu X, Yuan J, Wu J, Li M (2013) *MicroRNA-374a activates Wnt/β-catenin signaling to promote breast cancer metastasis*. J Clin Invest. Feb;123(2):566-79. doi: 10.1172/JCI65871.

Carmon et al., 2011 Carmon KS, Gong X, Lin Q, Thomas A, Liu Q (2011) *R-spondins function as ligands of the orphan receptors LGR4 and LGR5 to regulate Wnt/beta-catenin signaling*. Proc Natl Acad Sci U S A. Jul 12;108(28):11452-7. doi: 10.1073/pnas.1106083108.

Cavallaro, Dejana, 2011 Cavallaro U, Dejana E (2011) *Adhesion molecule signalling: not always a sticky business*. Nat Rev Mol Cell Biol. Mar;12(3):189-97. doi: 10.1038/nrm3068.

Chen et al., 2010 Chen Y, Zhu X, Zhang X, Liu B, Huang L (2010) *Nanoparticles modified with tumor-targeting scFv deliver siRNA and miR for cancer therapy*. Mol Ther. Sep;18(9):1650-6. doi: 10.1038/mt.2010.136.

Chen et al., 2012 Chen HY, Han ZB, Fan JW, Xia J, Wu JY, Qiu GQ, Tang HM, Peng ZH (2012) *miR-203 expression predicts outcome after liver transplantation for hepatocellular carcinoma in cirrhotic liver*. Med Oncol. Sep;29(3):1859-65. doi: 10.1007/s12032-011-0031-9.

Chen, Tian et al., 2012 Chen J, Tian W, Cai H, He H, Deng Y (2012) *Down-regulation of microRNA-200c is associated with drug resistance in human breast cancer*. Med Oncol. Dec;29(4):2527-34. doi: 10.1007/s12032-011-0117-4.

Chen et al., 2014 Chen L, Holmstrøm K, Qiu W, Ditzel N, Shi K, Hokland L, Kassem M (2014) *MicroRNA-34a inhibits osteoblast differentiation and in vivo bone formation of human stromal stem cells*. Stem Cells. Apr;32(4):902-12. doi: 10.1002/stem.1615.

Chen et al., 2015 Chen WY, Liu SY, Chang YS, Yin JJ, Yeh HL, Mouhieddine TH, Hadadeh O, Abou-Kheir W, Liu YN (2015) *MicroRNA-34a regulates WNT/TCF7 signaling and inhibits bone metastasis in Ras-activated prostate cancer*. Oncotarget. Jan 1;6(1):441-57.

Cheng et al., 2016 Cheng Y, Xiang G, Meng Y, Dong R (2016) *MiR-183-5p promotes cell proliferation and inhibits apoptosis in human breast cancer by targeting the PDCD4*. Reprod Biol. Sep;16(3):225-233. doi: 10.1016/j.repbio.2016.07.002.

Christensen et al., 2013 Christensen J, Bentz S, Sengstag T, Shastri VP, Anderle P (2013) *FOXQ1, a novel target of the Wnt pathway and a new marker for activation of Wnt signaling in solid tumors*. PLoS One.;8(3):e60051. doi: 10.1371/journal.pone.0060051.

Clevers, 2016 Clevers H (2016) *Modeling Development and Disease with Organoids*. Cell. Jun 16;165(7):1586-97. doi: 10.1016/j.cell.2016.05.082.

Crea et al., 2011 Crea F, Duhagon MA, Farrar WL, Danesi R (2011) *Pharmacogenomics and cancer stem cells: a changing landscape*? Trends Pharmacol Sci. Aug;32(8):487-94. doi: 10.1016/j.tips.2011.03.010.
Cuiffo et al., 2014 Cuiffo BG, Campagne A, Bell GW, Lembo A, Orso F, Lien EC, Bhasin MK, Raimo M, Hanson SE, Marusyk A, El-Ashry D, Hematti P, Polyak K, Mechta-Grigoriou F, Mariani O, Volinia S, Vincent-Salomon A, Taverna D, Karnoub AE (2014) *MSC-regulated microRNAs converge on the transcription factor FOXP2 and promote breast cancer metastasis*. Cell Stem Cell. Dec 4;15(6):762-74. doi: 10.1016/j.stem.2014.10.001.

D
Dekkers et al., 2016 Dekkers JF, Berkers G, Kruisselbrink E, Vonk A, de Jonge HR, Janssens HM, Bronsveld I, van de Graaf EA, Nieuwenhuis EE, Houwen RH, Vleggaar FP, Escher JC, de Rijke YB, Majoor CJ, Heijerman HG, de Winter-de Groot KM, Clevers H, van der Ent CK, Beekman JM (2016) *Characterizing responses to CFTR-modulating drugs using rectal organoids derived from subjects with cystic fibrosis*. Sci Transl Med. Jun 22;8(344):344ra84. doi: 10.1126/scitranslmed.aad8278.
Dobson et al., 2002 Dobson JM, Samuel S, Milstein H, Rogers K, Wood JL (2002) *Canine neoplasia in the UK: estimates of incidence rates from a population of insured dogs*. J Small Anim Pract. Jun;43(6):240-6.
Doleshaw et al., 2007 Doleshaw M, Mayer B, Cervenak J, Kacskovics I (2007) *Cloning, expression and characterisation of the bovine p65 subunit of NFkappaB*. Dev Comp Immunol ;31(9):945-961. 10.1016/j.dci.2006.12.007

E
Eden, 2010 Eden JA (2010) *Breast cancer, stem cells and sex hormones: part 1. The impact of fetal life and infancy*. Maturitas. Oct;67(2):117-20. doi: 10.1016/j.maturitas.2010.05.005.
Enerly et al., 2011 Enerly E, Steinfeld I, Kleivi K, Leivonen SK, Aure MR, Russnes HG, Rønneberg JA, Johnsen H, Navon R, Rødland E, Mäkelä R, Naume B, Perälä M, Kallioniemi O, Kristensen VN, Yakhini Z, Børresen-Dale AL (2011) *miR-mRNA integrated analysis reveals roles for miRs in primary breast tumors*. PLoS One. Feb 22;6(2):e16915. doi: 10.1371/journal.pone.0016915.
Esquela-Kerscher, Slack, 2006 Esquela-Kerscher A, Slack FJ (2006) *OncomiRs - microRNAs with a role in cancer*. Nat Rev Cancer. Apr;6(4):259-69.

F
Fendrick et al., 1998 Fendrick JL, Raafat AM, Haslam SZ (1998) *Mammary gland growth and development from the postnatal period to postmenopause: ovarian steroid receptor ontogeny and regulation in the mouse*. J Mammary Gland Biol Neoplasia. Jan;3(1):7-22.
Ferlay et al., 2015 Ferlay J, Soerjomataram I, Dikshit R, Eser S, Mathers C, Rebelo M, Parkin DM, Forman D, Bray F (2015) *Cancer incidence and mortality worldwide: sources, methods and major patterns in GLOBOCAN 2012*. Int J Cancer. Mar 1;136(5):E359-86. doi: 10.1002/ijc.29210.
Frères et al., 2015 Frères P, Josse C, Bovy N, Boukerroucha M, Struman I, Bours V, Jerusalem G (2015) *Neoadjuvant Chemotherapy in Breast Cancer Patients Induces miR-34a and miR-122 Expression*. J Cell Physiol. Feb;230(2):473-81. doi: 10.1002/jcp.24730.

G
Gama et al., 2004 Gama A, Paredes J, Albergaria A, Gartner F, Schmitt F (2004) *P-cadherin expression in canine mammary tissues*. J Comp Pathol. Jan;130(1):13-20.
Van Garderen et al., 1999 van Garderen E, van der Poel HJ, Swennenhuis JF, Wissink EH, Rutteman GR, Hellmén E, Mol JA, Schalken JA (1999) *Expression and molecular characterization of the growth hormone receptor in canine mammary tissue and mammary tumors*. Endocrinology. Dec;140(12):5907-14.
Girotti et al., 2015 Girotti MR, Lopes F, Preece N, Niculescu-Duvaz D, Zambon A, Davies L, Whittaker S, Saturno G, Viros A, Pedersen M, Suijkerbuijk BM, Menard D, McLeary R, Johnson L, Fish L, Ejiama S, Sanchez-Laorden B, Hohloch J, Carragher N, Macleod K, Ashton G, Marusiak AA, Fusi A, Brognard J, Frame M, Lorigan P, Marais R, Springer C (2015) *Paradox-breaking RAF inhibitors that also target SRC*

are effective in drug-resistant BRAF mutant melanoma. Cancer Cell. Jan 12;27(1):85-96. doi: 10.1016/j.ccell.2014.11.006.

Gonzáles-Sancho et al., 2004 González-Sancho JM, Brennan KR, Castelo-Soccio LA, Brown AM (2004) *Wnt proteins induce dishevelled phosphorylation via an LRP5/6- independent mechanism, irrespective of their ability to stabilize beta-catenin*. Mol Cell Biol. Jun;24(11):4757-68.

Gracanin et al., 2014 Gracanin A, Timmermans-Sprang EP, van Wolferen ME, Rao NA, Grizelj J, Vince S, Hellmen E, Mol JA (2014) *Ligand-independent canonical Wnt activity in canine mammary tumor cell lines associated with aberrant LEF1 expression*. PLoS One. Jun 2;9(6):e98698. doi: 10.1371/journal.pone.0098698.

Gracanin, Voorwald et al., 2014 Gracanin A, Voorwald FA, van Wolferen M, Timmermans-Sprang E, Mol JA (2014) *Marginal activity of P4 receptor B (PR-B) in dogs but high incidence of mammary cancer*. J Steroid Biochem Mol Biol. Oct;144 Pt B:492-9. doi: 10.1016/j.jsbmb.2014.08.016.

Griffey et al., 1993 Griffey SM, Madewell BR, Dairkee SH, Hunt JE, Naydan DK, Higgins RJ (1993) *Immunohistochemical reactivity of basal and luminal epithelium-specific cytokeratin antibodies within normal and neoplastic canine mammary glands*. Vet Pathol. Mar;30(2):155-61.

Gupta, Massagué, 2006 Gupta GP, Massagué J (2006) *Cancer metastasis: building a framework*. Cell. Nov 17;127(4):679-95.

Guttilla, White, 2009 Guttilla IK, White BA (2009) *Coordinate regulation of FOXO1 by miR-27a, miR-96, and miR-182 in breast cancer cells*. J Biol Chem. Aug 28;284(35):23204-16. doi: 10.1074/jbc.M109.031427.

H

Hanke et al., 2010 Hanke M, Hoefig K, Merz H, Feller AC, Kausch I, Jocham D, Warnecke JM, Sczakiel G (2010) *A robust methodology to study urine microRNA as tumor marker: microRNA-126 and microRNA-182 are related to urinary bladder cancer*. Urol Oncol. Nov-Dec;28(6):655-61. doi: 10.1016/j.urolonc.2009.01.027. Epub 2009 Apr 17.

Hansen & Khanna, 2004 Hansen K, Khanna C (2004) *Spontaneous and genetically engineered animal models; use in preclinical cancer drug development.* Eur J Cancer. Apr;40(6):858-80.

Hellmen, 1992 Hellmen E. (1992) *Characterization of four in vitro established canine mammary carcinoma and one atypical benign mixed tumor cell lines.* In Vitro Cell Dev Biol 28A: 309–319.

Hezova et al., 2015 Hezova R, Kovarikova A, Srovnal J, Zemanova M, Harustiak T, Ehrmann J, Hajduch M, Svoboda M, Sachlova M, Slaby O (2015) *Diagnostic and prognostic potential of miR-21, miR-29c, miR-148 and miR-203 in adenocarcinoma and squamous cell carcinoma of esophagus*. Diagn Pathol. Apr 28;10:42. doi: 10.1186/s13000-015-0280-6.

Hoppe et al., 2013 Hoppe R, Achinger-Kawecka J, Winter S, Fritz P, Lo WY, Schroth W, Brauch H (2013) *Increased expression of miR-126 and miR-10a predict prolonged relapse-free time of primary oestrogen receptor-positive breast cancer following tamoxifen treatment*. Eur J Cancer. Nov;49(17):3598-608. doi: 10.1016/j.ejca.2013.07.145. Epub 2013 Aug 19.

Hsieh et al., 2012 Hsieh TH, Tsai CF, Hsu CY, Kuo PL, Hsi E, Suen JL, Hung CH, Lee JN, Chai CY, Wang SC, Tsai EM (2012) *n-Butyl benzyl phthalate promotes breast cancer progression by inducing expression of lymphoid enhancer factor 1*. PLoS One. 7(8):e42750. doi: 10.1371/journal.pone.0042750.

Huch, 2017 Presentation: Huch M. *Liver organoids for the study of liver biology and disease*. IRB Barcelona, Oncology Programme Seminar. 2017, June 22.

Huch et al., 2013 Huch M, Bonfanti P, Boj SF, Sato T, Loomans CJM, van de Wetering M, Sojoodi M, Li VSW, Schuijers J, Gracanin A, Ringnalda F, Begthel H, Hamer K, Mulder J, van Es JH, de Koning E, Vries RGJ, H Heimberg and Clevers H (2013) *Unlimited in vitro expansion of adult bi-potent pancreas progenitors through the Lgr5/R-spondin axis* EMBO J. Oct 16; 32(20): 2708–2721. doi: 10.1038/emboj.2013.204.

Hur et al., 2017 Hur K, Toiyama Y, Okugawa Y, Ide S, Imaoka H, Boland CR, Goel A (2017) *Circulating microRNA-203 predicts prognosis and metastasis in human colorectal cancer*. Gut. Apr;66(4):654-665. doi: 10.1136/gutjnl-2014-308737. Epub 2015 Dec 23.

I

Isobe et al., 2014 Isobe T, Hisamori S, Hogan DJ, Zabala M, Hendrickson DG, Dalerba P, Cai S, Scheeren F, Kuo AH, Sikandar SS, Lam JS, Qian D, Dirbas FM, Soml o G, Lao K, Brown PO, Clarke MF, Shimono Y (2014) *miR-142 regulates the tumorigenicity of human breast cancer stem cells through the canonical WNT signaling pathway*. Elife. Nov 18;3. doi: 10.7554/

J

Jacobsen et al., 2005 Jacobsen BM, Schittone SA, Richer JK, Horwitz KB (2005) *P4-independent effects of human P4 receptors (PRs) in estrogen receptor-positive breast cancer: PR isoform-specific gene regulation and tumor biology*. Mol Endocrinol. Mar;19(3):574-87.

Javeri et al., 2013 Javeri A, Ghaffarpour M, Taha MF, Houshmand M (2013) *Downregulation of miR-34a in breast tumors is not associated with either p53 mutations or promoter hypermethylation while it correlates with metastasis*. Med Oncol. Mar;30(1):413. doi: 10.1007/s12032-012-0413-7.

Joshi et al., 2010 Joshi PA, Jackson HW, Beristain AG, Di Grappa MA, Mote PA, Clarke CL, Stingl J, Waterhouse PD, Khokha R (2010) *P4 induces adult mammary stem cell expansion*. Nature. Jun 10;465(7299):803-7. doi: 10.1038/nature09091

K

Kakimoto et al., 2015 Kakimoto Y, Kamiguchi H, Ochiai E, Satoh F, Osawa M (2015) *MicroRNA Stability in Postmortem FFPE Tissues: Quantitative Analysis Using Autoptic Samples from Acute Myocardial Infarction Patients*. PLoS One. Jun 5;10(6):e0129338. doi: 10.1371/journal.pone.0129338. **Kaneda et al., 2010** Kaneda H, Arao T, Tanaka K, Tamura D, Aomatsu K, Kudo K, Sakai K, De Velasco MA, Matsumoto K, Fujita Y, Yamada Y, Tsurutani J, Okamoto I, Nakagawa K, Nishio K (2010) *FOXQ1 is overexpressed in colorectal cancer and enhances tumorigenicity and tumor growth*. Cancer Res. Mar 1;70(5):2053-63. doi: 10.1158/0008-5472.CAN-09-2161..

Kang et al., 2015 Kang L, Mao J, Tao Y, Song B, Ma W, Lu Y, Zhao L, Li J, Yang B, Li L (2015) *MicroRNA-34a suppresses the breast cancer stem cell-like characteristics by downregulating Notch1 pathway*. Cancer Sci. Jun;106(6):700-8. doi: 10.1111/cas.12656.

Kastl et al., 2012 Kastl L, Brown I, Schofield AC (2012) *miR-34a is associated with docetaxel resistance in human breast cancer cells*. Breast Cancer Res Treat. Jan;131(2):445-54. doi: 10.1007/s10549-011-1424-3.

Kazanskaya et al., 2004 Kazanskaya O, Glinka A, del Barco Barrantes I, Stannek P, Niehrs C, Wu W (2004) *R-Spondin2 is a secreted activator of Wnt/beta-catenin signaling and is required for Xenopus myogenesis*. Dev Cell. Oct;7(4):525-34.

van Kempen et al., 2012 van Kempen LC, van den Hurk K, Lazar V, Michiels S, Winnepenninckx V, Stas M, Spatz A, van den Oord JJ (2012) *Loss of microRNA-200a and c, and microRNA-203 expression at the invasive front of primary cutaneous melanoma is associated with increased thickness and disease progression*. Virchows Arch. Oct;461(4):441-8. doi: 10.1007/s00428-012-1309-9.

Kim et al., 2002 Kim K, Lu Z, Hay ED (2002) *Direct evidence for a role of beta-catenin/LEF-1 signaling pathway in induction of EMT*. Cell Biol Int.;26(5):463-76.

Kim et al., 2006 Kim KA, Zhao J, Andarmani S, Kakitani M, Oshima T, Binnerts ME, Abo A, Tomizuka K, Funk WD (2006) *R-Spondin proteins: a novel link to beta-catenin activation*. Cell Cycle. Jan;5(1):23-6.

Kim et al., 2008 Kim KA, Wagle M, Tran K, Zhan X, Dixon MA, Liu S, Gros D, Korver W, Yonkovich S, Tomasevic N, Binnerts M, Abo A (2008) *R-Spondin family members regulate the Wnt pathway by a common mechanism*. Mol Biol Cell. Jun;19(6):2588-96. doi: 10.1091/mbc.E08-02-0187.

Kim et al., 2011 Kim NH, Kim HS, Kim NG, Lee I, Choi HS, Li XY, Kang SE, Cha SY, Ryu JK, Na JM, Park C, Kim K, Lee S, Gumbiner BM, Yook JI, Weiss SJ (2011) *p53 and microRNA-34 are suppressors of canonical Wnt signaling*. Sci Signal. Nov 1;4(197):ra71. doi: 10.1126/scisignal.2001744.

Kim, Oh et al., 2011 Kim SJ, Oh JS, Shin JY, Lee KD, Sung KW, Nam SJ, Chun KH (2011) *Development of microRNA-145 for therapeutic application in breast cancer*. J Control Release. Nov 7;155(3):427-34. doi: 10.1016/j.jconrel.2011.06.026.

Kinner et al., 2002 Kinner B, Zaleskas JM, Spector M (2002) *Regulation of smooth muscle actin expression and contraction in adult human mesenchymal stem cells*. Exp Cell Res. Aug 1;278(1):72-83.
Kleinberg, 1997 Kleinberg DL (1997) *Early mammary development: growth hormone and IGF-1*. J Mammary Gland Biol Neoplasia. Jan;2(1):49-57.
Knudsen, Wheelock, 2005 Knudsen KA, Wheelock MJ (2005) *Cadherins and the mammary gland*. J Cell Biochem. Jun 1;95(3):488-96.
Koledova, 2017 Koledova Z (2017) *3D Coculture of Mammary Organoids with Fibrospheres: A Model for Studying Epithelial–Stromal Interactions During Mammary Branching Morphogenesis.* Methods Mol Biol. 1612:107-124. doi: 10.1007/978-1-4939-7021-6_8.
Komiya and Habas, 2008 Komiya Y, Habas R (2008) *Wnt signal transduction pathways*. Organogenesis. Apr;4(2):68-75.
Kruitwagen et al., 2017 Kruitwagen HS, Oosterhoff LA, Vernooij IGWH, Schrall IM, van Wolferen ME, Bannink F, Roesch C, van Uden L, Molenaar MR, Helms JB, Grinwis GCM, Verstegen MMA, van der Laan LJW, Huch M, Geijsen N, Vries RG, Clevers H, Rothuizen J, Schotanus BA, Penning LC, Spee B (2017) *Long-Term Adult Feline Liver Organoid Cultures for Disease Modeling of Hepatic Steatosis*. Stem Cell Reports. Apr 11;8(4):822-830. doi: 10.1016/j.stemcr.2017.02.015.
Kuhl, Schneider, 2013 Kuhl H, Schneider HP (2013) *P4--promoter or inhibitor of breast cancer*. Climacteric. Aug;16 Suppl 1:54-68. doi: 10.3109/13697137.2013.768806.

L

de Lau et al., 2011 de Lau W, Barker N, Low TY, Koo BK, Li VS, Teunissen H, Kujala P, Haegebarth A, Peters PJ, van de Wetering M, Stange DE, van Es JE, Guardavaccaro D, Schasfoort RB, Mohri Y, Nishimori K, Mohammed S, Heck AJ, Clevers H (2011) *Lgr5 homologues associate with Wnt receptors and mediate R-spondin signalling*. Nature. Jul 4;476(7360):293-7. doi: 10.1038/nature10337
Lawrie et al., 2008 Lawrie CH, Gal S, Dunlop HM, Pushkaran B, Liggins AP, Pulford K, Banham AH, Pezzella F, Boultwood J, Wainscoat JS, Hatton CS, Harris AL (2008) *Detection of elevated levels of tumour-associated microRNAs in serum of patients with diffuse large B-cell lymphoma*. Br J Haematol. May;141(5) :672-5. doi: 10.1111/j.1365-2141.2008.07077.x..
LeBlanc, Morin, 2015 LeBlanc VC, Morin P (2015) *Exploring miR-Associated Signatures withcDiagnostic Relevance in Glioblastoma Multiforme and Breast Cancer Patients*. J Clin Med. Aug 14;4(8):1612-30. doi: 10.3390/jcm4081612.
Leung et al., 2015 Leung WK, He M, Chan AW, Law PT, Wong N (2015) *Wnt/β-Catenin activates MiR-183/96/182 expression in hepatocellular carcinoma that promotes cell invasion*. Cancer Lett. Jun 28;362(1):97-105. doi: 10.1016/j.canlet.2015.03.023.
Lee et al., 1993 Lee RC, Feinbaum RL, Ambros V (1993) *The C. elegans heterochronic gene lin-4 encodes small RNAs with antisense complementarity to lin-14*. Cell. Dec 3;75(5):843-54.
Li et al., 2009 Li Y, Guessous F, Zhang Y, Dipierro C, Kefas B, Johnson E, Marcinkiewicz L, Jiang J, Yang Y, Schmittgen TD, Lopes B, Schiff D, Purow B, Abounader R (2009) *MicroRNA-34a inhibits glioblastoma growth by targeting multiple oncogenes*. Cancer Res. Oct 1;69(19):7569-76. doi: 10.1158/0008-5472.CAN-09-0529.
Li et al., 2011 Li H, Bian C, Liao L, Li J, Zhao RC (2011) miR-*17-5p promotes human breast cancer cell migration and invasion through suppression of HBP1*. Breast Cancer Res Treat. Apr;126(3):565-75. doi: 10.1007/s10549-010-0954-4.
Li et al., 2012 Li VS, Ng SS, Boersema PJ, Low TY, Karthaus WR, Gerlach JP, Mohammed S, Heck AJ, Maurice MM, Mahmoudi T, Clevers H (2012) *Wnt signaling through inhibition of β-catenin degradation in an intact Axin1 complex*. Cell. Jun 8;149(6):1245-56. doi: 10.1016/j.cell.2012.05.002.
Li et al., 2013 Li Y, Ma X, Zhao J, Zhang B, Jing Z, Liu L (2013) *microRNA-210 as a prognostic factor in patients with breast cancer: meta-analysis*. Cancer Biomark. Jan 1;13(6):471-81. doi: 10.3233/CBM-130385.
Li et al., 2014: Li P, Sheng C, Huang L, Zhang H, Huang L, Cheng Z, Zhu Q (2014) *MiR-183/-96/-182 cluster is up-regulated in most breast cancers and increases cell proliferation and migration.* Breast Cancer Res. Nov 14;16(6):473. doi: 10.1186/s13058-014-0473-z.

Li et al., 2015 Li J, Gao B, Huang Z, Duan T, Li D, Zhang S, Zhao Y, Liu L, Wang Q, Chen Z, Cheng K (2015) *Prognostic significance of microRNA-203 in cholangiocarcinoma*. Int J Clin Exp Pathol. Aug 1;8(8):9512-6.

Liang & Xi, 2016 Liang Z, Xi Y (2016) *MicroRNAs mediate therapeutic and preventive effects of natural agents in breast cancer*. Chin J Nat Med. Dec;14(12):881-887. doi: 10.1016/S1875-5364(17)30012-2.

Lin et al., 2000 Lin SY, Xia W, Wang JC, Kwong KY, Spohn B, Wen Y, Pestell RG, Hung MC (2000) *Beta-catenin, a novel prognostic marker for breast cancer: its roles in cyclin D1 expression and cancer progression*. Proc Natl Acad Sci U S A. Apr 11;97(8):4262-6.

Lin et al., 2010 Lin H, Dai T, Xiong H, Zhao X, Chen X, Yu C, Li J, Wang X, Song L (2010) *Unregulated miR-96 induces cell proliferation in human breast cancer by downregulating transcriptional factor FOXO3a*. PLoS One. Dec 23;5(12):e15797. doi: 10.1371/journal.pone.0015797.

Livak & Schmittgen, 2001 K.J. Livak and T.D. Schmittgen (2001) *Analysis of Relative Gene Expression Data Using Real-Time Quantitative PCR and the* $2^{-\Delta\Delta C}T$ *Method.* Elsevier Science (USA) Methods. Dec;25(4):402-8.

Liu et al., 2014 Liu D, Xiong H, Ellis AE, Northrup NC, Rodriguez CO,Jr, O'Regan RM, Dalton S, Zhao S (2014) *Molecular homology and difference between spontaneous canine mammary cancer and human breast cancer.* Cancer Res, 74(18):5045-5056.

Liu et al., 2016 Liu Y, Dong Z, Liang J, Guo Y, Guo X, Shen S, Kuang G, Guo W (2016) *Methylation-mediated repression of potential tumor suppressor miR-203a and miR-203b contributes to esophageal squamous cell carcinoma development*. Tumour Biol. Apr;37(4):5621-32. doi: 10.1007/s13277-015-4432-9.

Lombardi et al., 2014 Lombardi S, Honeth G, Ginestier C, Shinomiya I, Marlow R, Buchupalli B, Gazinska P, Brown J, Catchpole S, Liu S, Barkan A, Wicha M, Purushotham A, Burchell J, Pinder S, Dontu G (2014) *Growth hormone is secreted by normal breast epithelium upon P4 stimulation and increases proliferation of stem/progenitor cells*. Stem Cell Reports. Jun 3;2(6):780-93. doi: 10.1016/j.stemcr.2014.05.005.

Lowery et al., 2009 Lowery AJ, Miller N, Devaney A, McNeill RE, Davoren PA, Lemetre C, Benes V, Schmidt S, Blake J, Ball G, Kerin MJ (2009) *MicroRNA signatures predict oestrogen receptor, P4 receptor and HER2/neu receptor status in breast cancer*. Breast Cancer Res.;11(3):R27. doi: 10.1186/bcr2257.

Lowery et al., 2010 Lowery AJ, Miller N, Dwyer RM, Kerin MJ (2010) *Dysregulated miR-183 inhibits migration in breast cancer cells*. BMC Cancer. Sep 21;10:502. doi: 10.1186/1471-2407-10-502.

Lydon et al., 1995 Lydon JP, DeMayo FJ, Funk CR, Mani SK, Hughes AR, Montgomery CA Jr, Shyamala G, Conneely OM, O'Malley BW (1995) *Mice lacking P4 receptor exhibit pleiotropic reproductive abnormalities*. Genes Dev. Sep 15;9(18):2266-78.

Luo et al., 2013 Luo D, Wilson JM, Harvel N, Liu J, Pei L, Huang S, Hawthorn L, Shi H (2013) *A systematic evaluation of miR:mRNA interactions involved in the migration and invasion of breast cancer cells*. J Transl Med. Mar 5;11:57. doi: 10.1186/1479-5876-11-57.

M

Macedo et al., 2017 Macedo T, Silva-Oliveira RJ, Silva VAO, Vidal DO, Evangelista AF, Marques MMC (2017) *Overexpression of miR-183 and miR-494 promotes proliferation and migration in human breast cancer cell lines*. Oncol Lett. Jul;14(1):1054-1060. doi: 10.3892/ol.2017.6265.

Macias, Hinck, 2012 Macias H, Hinck L (2012) *Mammary gland development*. Wiley Interdiscip Rev Dev Biol. Jul-Aug;1(4):533-57.

Madhavan et al., 2016 Madhavan D, Peng C, Wallwiener M, Zucknick M, Nees J, Schott S, Rudolph A, Riethdorf S, Trumpp A, Pantel K, Sohn C, Chang-Claude J, Schneeweiss A, Burwinkel B (2016) *Circulating miRs with prognostic value in metastatic breast cancer and for early detection of metastasis*. Carcinogenesis. May;37(5):461-70. doi: 10.1093/carcin/bgw008.

Mall et al., 2013 Mall C, Rocke DM, Durbin-Johnson B, Weiss RH (2013) *Stability of miR in human urine supports its biomarker potential*. Biomark Med. Aug;7(4):623-31. doi: 10.2217/bmm.13.44.

McDermott et al., 2014 McDermott AM, Miller N, Wall D, Martyn LM, Ball G, Sweeney KJ, Kerin MJ (2014) *Identification and validation of oncologic miR biomarkers for luminal A-like breast cancer*. PLoS One. Jan 31;9(1):e87032. doi: 10.1371/journal.pone.0087032.
Meister et al., 2004 Meister G, Landthaler M, Patkaniowska A, Dorsett Y, Teng G, Tuschl T (2004) *Human Argonaute2 mediates RNA cleavage targeted by miRs and siRNAs*. Mol Cell. Jul 23;15(2):185-97.
Merlo et al., 2008 Merlo DF, Rossi L, Pellegrino C, Ceppi M, Cardellino U, Capurro C, Ratto A, Sambucco PL, Sestito V, Tanara G, Bocchini V (2008) *Cancer incidence in pet dogs: findings of the Animal Tumor Registry of Genoa, Italy*. J Vet Intern Med. Jul-Aug;22(4):976-84. doi: 10.1111/j.1939-1676.2008.0133.x.
Milanese et al., 2006 Milanese TR, Hartmann LC, Sellers TA, Frost MH, Vierkant RA, Maloney SD, Pankratz VS, Degnim AC, Vachon CM, Reynolds CA, Thompson RA, Melton LJ 3rd, Goode EL, Visscher DW (2006) *Age-related lobular involution and risk of breast cancer*. J Natl Cancer Inst. Nov 15;98(22):1600-7.
Mitchell et al., 2008 Mitchell PS, Parkin RK, Kroh EM, Fritz BR, Wyman SK, Pogosova-Agadjanyan EL, Peterson A, Noteboom J, O'Briant KC, Allen A, Lin DW, Urban N, Drescher CW, Knudsen BS, Stirewalt DL, Gentleman R, Vessella RL, Nelson PS, Martin DB, Tewari M (2008) *Circulating microRNAs as stable blood-based markers for cancer detection*. Proc Natl Acad Sci U S A. Jul 29;105(30):10513-8. doi: 10.1073/pnas.0804549105.
Moazzeni et al., 2017 Moazzeni H, Najafi A, Khani M (2017) *Identification of direct target genes of miR-7, miR-9, miR-96, and miR-182 in the human breast cancer cell lines MCF-7 and MDA-MB-231*. Mol Cell Probes. Aug;34:45-52. doi: 10.1016/j.mcp.2017.05.005.
Mote et al., 2002 Mote PA, Bartow S, Tran N, Clarke CL (2002) *Loss of co-ordinate expression of P4 receptors A and B is an early event in breast carcinogenesis*. Breast Cancer Res Treat. Mar;72(2):163-72. 1.
Mote et al., 2006 Mote PA, Arnett-Mansfield RL, Gava N, deFazio A, Mulac-Jericevic B, Conneely OM, Clarke CL (2006) *Overlapping and distinct expression of P4 receptors A and B in mouse uterus and mammary gland during the estrous cycle*. Endocrinology. Dec;147(12):5503-12.
Mukhina et al., 2004 Mukhina S, Mertani HC, Guo K, Lee KO, Gluckman PD, Lobie PE (2004) *Phenotypic conversion of human mammary carcinoma cells by autocrine human growth hormone.* Proc Natl Acad Sci USA. Oct 19;101(42):15166-71.
Mulac-Jericevic et al., 2003 Mulac-Jericevic B, Lydon JP, DeMayo FJ, Conneely OM (2003) *Defective mammary gland morphogenesis in mice lacking the P4 receptor B isoform*. Proc Natl Acad Sci U S A. Aug 19;100(17):9744-9.

N

Nissan et al., 2011 Nissan X, Denis JA, Saidani M, Lemaitre G, Peschanski M, Baldeschi C (2011) *miR-203 modulates epithelial differentiation of human embryonic stem cells towards epidermal stratification*. Dev Biol. Aug 15;356(2):506-15. doi: 10.1016/j.ydbio.2011.06.004.
Nusse, Clevers, 2017 Nusse R, Clevers H (2017) *Wnt/β-Catenin Signaling, Disease, and Emerging Therapeutic Modalities*. Cell. Jun 1;169(6):985-999. doi: 10.1016/j.cell.2017.05.016.

O

O'Bryan et al., 2017 O'Bryan S, Dong S, Mathis JM, Alahari SK (2017) *The roles of oncogenic miRs and their therapeutic importance in breast cancer*. Eur J Cancer. Feb;72:1-11. doi: 10.1016/j.ejca.2016.11.004.
Onyido et al., 2016 Onyido EK, Sweeney E, Nateri AS (2016) *Wnt-signalling pathways and microRNAs network in carcinogenesis: experimental and bioinformatics approaches*. Mol Cancer. Sep 2;15(1):56. doi: 10.1186/s12943-016-0541-3.

P

Pai et al., 2017 Pai SG, Carneiro BA, Mota JM, Costa R, Leite CA, Barroso-Sousa R, Kaplan JB, Chae YK, Giles FJ (2017) *Wnt/beta-catenin pathway: modulating anticancer immune response*. J Hematol Oncol. May 5;10(1):101. doi: 10.1186/s13045-017-0471-6.

Peña et al., 2014 Peña L, Gama A, Goldschmidt MH, Abadie J, Benazzi C, Castagnaro M, Díez L, Gärtner F, Hellmén E, Kiupel M, Millán Y, Miller MA, Nguyen F, Poli A, Sarli G, Zappulli V, de las Mulas JM (2014) *Canine mammary tumors: a review and consensus of standard guidelines on epithelial and myoepithelial phenotype markers, HER2, and hormone receptor assessment using immunohistochemistry*. Vet Pathol. Jan;51(1):127-45. doi: 10.1177/0300985813509388.

Perou et al., 2000 Perou CM, Sørlie T, Eisen MB, van de Rijn M, Jeffrey SS, Rees CA, Pollack JR, Ross DT, Johnsen H, Akslen LA, Fluge O, Pergamenschikov A, Williams C, Zhu SX, Lønning PE, Børresen-Dale AL, Brown PO, Botstein D (2000) *Molecular portraits of human breast tumours*. Nature. Aug 17;406(6797):747-52.

Piao, Ma, 2012 Piao HL, Ma L (2012) *Non-coding RNAs as regulators of mammary development and breast cancer*. J Mammary Gland Biol Neoplasia. Mar;17(1):33-42.

Pinho et al., 2012 Pinho SS, Carvalho S, Cabral J, Reis CA, Gärtner F (2012) *Canine tumors: a spontaneous animal model of human carcinogenesis.* Transl Res. Mar;159(3):165-72. doi: 10.1016/j.trsl.2011.11.005.

Przybyla et al., 2016 Przybyla L, Lakins JN, Weaver VM (2016) *Tissue Mechanics Orchestrate Wnt-Dependent Human Embryonic Stem Cell Differentiation*. Cell Stem Cell. Oct 6;19(4):462-475. doi: 10.1016/j.stem.2016.06.018.

Pulikkan et al., 2010 Pulikkan JA, Peramangalam PS, Dengler V, Ho PA, Preudhomme C, Meshinchi S, Christopeit M, Nibourel O, Müller-Tidow C, Bohlander SK, Tenen DG, Behre G (2010) *C/EBPα regulated microRNA-34a targets E2F3 during granulopoiesis and is down-regulated in AML with CEBPA mutations*. Blood. Dec 16;116(25):5638-49. doi: 10.1182/blood-2010-04-281600.

Q

Qiao et al., 2011 Qiao Y, Jiang X, Lee ST, Karuturi RK, Hooi SC, Yu Q (2011) *FOXQ1 regulates epithelial-mesenchymal transition in human cancers*. Cancer Res. Apr 15;71(8):3076-86. doi: 10.1158/0008-5472.CAN-10-2787.

Qu et al., 2013 Qu Y, Li WC, Hellem MR, Rostad K, Popa M, McCormack E, Oyan AM, Kalland KH, Ke XS (2013) *MiR-182 and miR-203 induce mesenchymal to epithelial transition and self-sufficiency of growth signals via repressing SNAI2 in prostate cells*. Int J Cancer. Aug 1;133(3):544-55. doi: 10.1002/ijc.28056.

R

Rakha et al., 2013 Rakha EA, Teoh TK, Lee AH, Nolan CC, Ellis IO, Green AR (2013) *Further evidence that E-cadherin is not a tumour suppressor gene in invasive ductal carcinoma of the breast: an immunohistochemical study*. Histopathology. Apr;62(5):695-701. doi: 10.1111/his.12066.

Rao et al., 2009 Rao NA, van Wolferen ME, Gracanin A, Bhatti SF, Krol M, Holstege FC, Mol JA (2009) *Gene expression profiles of progestin-induced canine mammary hyperplasia and spontaneous mammary tumors*. J Physiol Pharmacol. May;60 Suppl 1:73-84.

Rathod et al., 2014 Rathod SS, Rani SB, Khan M, Muzumdar D, Shiras A (2014) *Tumor suppressive miR-34a suppresses cell proliferation and tumor growth of glioma stem cells by targeting Akt and Wnt signaling pathways*. FEBS Open Bio. May 22;4:485-95. doi: 10.1016/j.fob.2014.05.002.

Reya et al., 2001 Reya T, Morrison SJ, Clarke MF, Weissman IL (2001) *Stem cells, cancer, and cancer stem cells*. Nature. Nov 1;414(6859):105-11.

Reya & Clevers, 2005 Reya T, Clevers H (2005) *Wnt signalling in stem cells and cancer*. Nature. Apr 14;434(7035):843-50.

Rheinwald & Green, 1975 Rheinwald JG, Green H (1975) *Serial cultivation of strains of human epidermal keratinocytes: the formation of keratinizing colonies from single cells*. Cell. Nov;6(3):331-43.

Rossouw et al., 2002 Rossouw JE, Anderson GL, Prentice RL, LaCroix AZ, Kooperberg C, Stefanick ML, Jackson RD, Beresford SA, Howard BV, Johnson KC, Kotchen JM, Ockene J (2002) *Risks and benefits of estrogen plus progestin in healthy postmenopausal women: principal results From the Women's Health Initiative randomized controlled trial*. JAMA. Jul 17;288(3):321-33.

S

Sachdeva, Mo, 2010 Sachdeva M, Mo YY (2010) *miR-145-mediated suppression of cell growth, invasion and metastasis*. Am J Transl Res. Mar 25;2(2):170-80.

Sánchez-Bailón et al., 2012 Sánchez-Bailón MP, Calcabrini A, Gómez-Domínguez D, Morte B, Martín-Forero E, Gómez-López G, Molinari A, Wagner KU, Martín-Pérez J (2012) *Src kinases catalytic activity regulates proliferation, migration and invasiveness of MDA-MB-231 breast cancer cells*. Cell Signal. Jun;24(6):1276-86.

Santos et al., 2009 Santos SJ, Aupperlee MD, Xie J, Durairaj S, Miksicek R, Conrad SE, Leipprandt JR, Tan YS, Schwartz RC, Haslam SZ (2009) *P4 receptor A-regulated gene expression in mammary organoid cultures*. J Steroid Biochem Mol Biol. Jul;115(3-5):161-72. doi: 10.1016/j.jsbmb.2009.04.001.

Sato et al., 2011 Sato T, Stange DE, Ferrante M, Vries RG, Van Es JH, Van den Brink S, Van Houdt WJ, Pronk A, Van Gorp J, Siersema PD, Clevers H (2011) *Long-term expansion of epithelial organoids from human colon, adenoma, adenocarcinoma, and Barrett's epithelium*. Gastroenterology. Nov;141(5):1762-72. doi: 10.1053/j.gastro..07.050.

Schneider et al., 1969 Schneider R, Dorn CR, Taylor DO (1969) *Factors influencing canine mammary cancer development and postsurgical survival*. J Natl Cancer Inst. Dec;43(6):1249-61.

Shamir, Ewald, 2014 Shamir ER, Ewald AJ (2014) *Three-dimensional organotypic culture: experimental models of mammalian biology and disease*. Nat Rev Mol Cell Biol. Oct;15(10):647-64. doi: 10.1038/nrm3873.

Shan et al., 2016 Shan NL, Wahler J, Lee HJ, Bak MJ, Gupta SD, Maehr H, Suh N (2016) *Vitamin D compounds inhibit cancer stem-like cells and induce differentiation in triple negative breast cancer*. J Steroid Biochem Mol Biol. Dec 5. pii: S0960-0760(16)30340-5. doi: 10.1016/j.jsbmb.2016.12.001.

Shao et al., 2017 Shao Y, Gu W, Ning Z, Song X, Pei H, Jiang J (2017) *Evaluating the Prognostic Value of microRNA-203 in Solid Tumors Based on a Meta-Analysis and the Cancer Genome Atlas (TCGA) Datasets*. Cell Physiol Biochem. Mar 24;41(4):1468-1480. doi: 10.1159/000470649.

Shen et al., 2012 Shen Z, Zhan G, Ye D, Ren Y, Cheng L, Wu Z, Guo J (2012) *MicroRNA-34a affects the occurrence of laryngeal squamous cell carcinoma by targeting the antiapoptotic gene survivin*. Med Oncol. Dec;29(4):2473-80. doi: 10.1007/s12032-011-0156-x.

Shi et al., 2011 Shi W, Gerster K, Alajez NM, Tsang J, Waldron L, Pintilie M, Hui AB, Sykes J, P'ng C, Miller N, McCready D, Fyles A, Liu FF (2011) *MicroRNA-301 mediates proliferation and invasion in human breast cancer*. Cancer Res. Apr 15;71(8):2926-37. doi: 10.1158/0008-5472.CAN-10-3369.

Shi et al., 2017 Shi Y, Zhao Y, Shao N, Ye R, Lin Y, Zhang N, Li W, Zhang Y, Wang S (2017) *Overexpression of microRNA-96-5p inhibits autophagy and apoptosis and enhances the proliferation, migration and invasiveness of human breast cancer cells*. Oncol Lett. Jun;13(6):4402-4412. doi: 10.3892/ol.2017.6025.

Siegel et al., 2013 Siegel R, Naishadham D, Jemal A (2013) *Cancer statistics, 2013*. CA Cancer J Clin. Jan;63(1):11-30. doi: 10.3322/caac.21166.

Skibinski, Kuperwasser, 2015 Skibinski A, Kuperwasser C (2015) *The origin of breast tumor heterogeneity*. Oncogene. Oct 16;34(42):5309-16. doi: 10.1038/onc.2014.475.

Soler et al., 2002 Soler AP, Russo J, Russo IH, Knudsen KA (2002) *Soluble fragment of P-cadherin adhesion protein found in human milk*. J Cell Biochem ;85(1):180-4.

Sorenmo et al., 2011 Sorenmo KU, Rasotto R, Zappulli V, Goldschmidt MH (2011) *Development, anatomy, histology, lymphatic drainage, clinical features, and cell differentiation markers of canine mammary gland neoplasms*. Vet Pathol. Jan;48(1):85-97. doi: 10.1177/0300985810389480.

Spender et al., 2016 Spender LC, Ferguson GJ, Liu S, Cui C, Girotti MR, Sibbet G, Higgs EB, Shuttleworth MK, Hamilton T, Lorigan P, Weller M, Vincent DF, Sansom OJ, Frame M, Dijke PT, Marais R, Inman GJ (2016) *Mutational activation of BRAF confers sensitivity to transforming growth factor beta inhibitors in human cancer cells*. Oncotarget. Dec 13;7(50):81995-82012. doi: 10.18632/oncotarget.13226.

Sun et al., 2008 Sun F, Fu H, Liu Q, Tie Y, Zhu J, Xing R, Sun Z, Zheng X (2008) *Downregulation of CCND1 and CDK6 by miR-34a induces cell cycle arrest*. FEBS Lett. Apr 30;582(10):1564-8. doi: 10.1016/j.febslet.2008.03.057.

T

Tamai et al., 2000 Tamai K, Semenov M, Kato Y, Spokony R, Liu C, Katsuyama Y, Hess F, Saint-Jeannet JP, He X (2000) *LDL-receptor-related proteins in Wnt signal transduction*. Nature. Sep 28;407(6803):530-5.

Taube et al., 2013 Taube JH, Malouf GG, Lu E, Sphyris N, Vijay V, Ramachandran PP, Ueno KR, Gaur S, Nicoloso MS, Rossi S, Herschkowitz JI, Rosen JM, Issa JP, Calin GA, Chang JT, Mani SA (2013) *Epigenetic silencing of microRNA-203 is required for EMT and cancer stem cell properties*. Sci Rep.;3:2687. doi: 10.1038/srep02687.

Thatcher et al., 2008 Thatcher EJ, Paydar I, Anderson KK, Patton JG (2008) *Regulation of zebrafish fin regeneration by microRNAs*. Proc Natl Acad Sci U S A. Nov 25;105(47):18384-9. doi: 10.1073/pnas.0803713105.

U

Uva et al., 2009 Uva P, Aurisicchio L, Watters J, Loboda A, Kulkarni A, Castle J, Palombo F, Viti V, Mesiti G, Zappulli V, Marconato L, Abramo F, Ciliberto G, Lahm A, La Monica N, de Rinaldis E (2009) *Comparative expression pathway analysis of human and canine mammary tumors*. BMC Genomics. Mar 27;10:135. doi: 10.1186/1471-2164-10-135.

Uyama et al., 2006 Uyama R, Nakagawa T, Hong SH, Mochizuki M, Nishimura R, Sasaki N (2006) *Establishment of four pairs of canine mammary tumour cell lines derived from primary and metastatic origin and their E-cadherin expression*. Vet Comp Oncol 4: 104–113.

V

Valastyan, Weinberg, 2010 Valastyan S, Weinberg RA (2010) *miR-31: a crucial overseer of tumor metastasis and other emerging roles*. Cell Cycle. Jun 1;9(11):2124-9.

Van Leeuwen et al., 1996 Van Leeuwen IS, Hellmen E, Cornelisse CJ, Van den Burgh B, Rutteman GR (1996) *P53 mutations in mammary tumor cell lines and corresponding tumor tissues in the dog*. Anticancer Res 16: 3737–3744.

Vascellari et al., 2009 Vascellari M, Baioni E, Ru G, Carminato A, Mutinelli F (2009) *Animal tumour registry of two provinces in northern Italy: incidence of spontaneous tumours in dogs and cats*. BMC Vet Res. Oct 13;5:39. doi: 10.1186/1746-6148-5-39.

Vieira, Paredes, 2015 Vieira AF, Paredes J (2015) *P-cadherin and the journey to cancer metastasis.* Mol Cancer.; 14: 178. Oct 6. doi: 10.1186/s12943-015-0448-4 PMCID: PMC4595126

Vos et al., 1993 Vos JH, van den Ingh TS, Misdorp W, Molenbeek RF, van Mil FN, Rutteman GR, Ivanyi D, Ramaekers FC (1993) *Immunohistochemistry with keratin, vimentin, desmin, and alpha-smooth muscle actin monoclonal antibodies in canine mammary gland: normal mammary tissue*. Vet Q. Sep;15(3):102-7.

W

Walden et al., 1998 Walden PD, Ruan W, Feldman M, Kleinberg DL (1998) *Evidence that the mammary fat pad mediates the action of growth hormone in mammary gland development.* Endocrinology. Feb;139(2):659-62.

Wagner et al., 2013 Wagner S, Willenbrock S, Nolte I, Murua Escobar H (2013) *Comparison of non-coding RNAs in human and canine cancer*. Front Genet. Apr 8;4:46. doi: 10.3389/fgene.2013.00046.

Wang et al., 2008 Wang G, Mao W, Zheng S (2008) *MicroRNA-183 regulates Ezrin expression in lung cancer cells*. FEBS Lett. Oct 29;582(25-26):3663-8. doi: 10.1016/j.febslet.2008.09.051.

Wang et al., 2012 Wang C, Zheng X, Shen C, Shi Y (2012) *MicroRNA-203 suppresses cell proliferation and migration by targeting BIRC5 and LASP1 in human triple-negative breast cancer cells*. J Exp Clin Cancer Res. Jun 19;31:58. doi: 10.1186/1756-9966-31-58.

Wang et al., 2013 Wang D, Huang B, Zhang S, Yu X, Wu W, Wang X (2013) *Structural basis for R-spondin recognition by LGR4/5/6 receptors*. Genes Dev. Jun 15;27(12):1339-44. doi:10.1101/gad.219360.113.

Wang, Zhang, 2015 Wang K, Zhang ZW (2015) *Expression of miR-203 is decreased and associated with the prognosis of melanoma patients*. Int J Clin Exp Pathol;8: 13249-13254. PMCID: PMC4680470

Weber-Hall et al., 1994 Weber-Hall SJ, Phippard DJ, Niemeyer CC, Dale TC (1994) D*evelopmental and hormonal regulation of Wnt gene expression in the mouse mammary gland*. Differentiation. Sep;57(3):205-14
Willert et al., 2003 Willert K, Brown JD, Danenberg E, Duncan AW, Weissman IL, Reya T, Yates JR 3rd, Nusse R (2003) *Wnt proteins are lipid-modified and can act as stem cell growth factors*. Nature. May 22;423(6938):448-52.

Y
Yang et al., 2013 Yang S, Li Y, Gao J, Zhang T, Li S, Luo A, Chen H, Ding F, Wang X, Liu Z (2013) *MicroRNA-34 suppresses breast cancer invasion and metastasis by directly targeting Fra-1*. Oncogene. Sep 5;32(36):4294-303. doi: 10.1038/onc.2012.432.
Yoshiba et al., 2012 Yoshiba N, Yoshiba K, Ohkura N, Shigetani Y, Takei E, Hosoya A, Nakamura H, Okiji T (2012) *Immunohistochemical analysis of two stem cell markers of α-smooth muscle actin and STRO-1 during wound healing of human dental pulp*. Histochem Cell Biol. Oct;138(4):583-92. doi: 10.1007/s00418-012-0978-4.

Z
Zhang et al., 2011 Zhang H, Meng F, Liu G, Zhang B, Zhu J, Wu F, Ethier SP, Miller F, Wu G (2011) *Forkhead transcription factor foxq1 promotes epithelial-mesenchymal transition and breast cancer metastasis*. Cancer Res. Feb 15;71(4):1292-301. doi: 10.1158/0008-5472.CAN-10-2825.
Zhang et al., 2015 Zhang W, Qian P, Zhang X, Zhang M, Wang H, Wu M, Kong X, Tan S, Ding K, Perry JK, Wu Z, Cao Y, Lobie PE, Zhu T (2015) *Autocrine/Paracrine Human Growth Hormone-stimulated MicroRNA 96-182-183 Cluster Promotes Epithelial-Mesenchymal Transition and Invasion in Breast Cancer*. J Biol Chem. May 29;290(22):13812-29.
Zhang et al., 2017 Zhang K, Wang YW, Wang YY, Song Y, Zhu J, Si PC, Ma R (2017) *Identification of microRNA biomarkers in the blood of breast cancer patients based on microRNA profiling*. Gene. Jul 1;619:10-20. doi: 10.1016/j.gene.2017.03.038.
Zhang, Ma et al., 2017 Zhang M, Ma F, Xie R, Wu Y, Wu M, Zhang P, Peng Y, Zhao J, Xiong J, Li A, Kequan C, Zhang Y, Liu S, Wang J, Chen X (2017) *Overexpression of Srcin1 contributes to the growth and metastasis of colorectal cancer*. Int J Oncol. May;50(5):1555-1566. doi: 10.3892/ijo.2017.3952.
Zhu et al., 2005 Zhu T, Starling-Emerald B, Zhang X, Lee KO, Gluckman PD, Mertani HC, Lobie PE (2005) *Oncogenic transformation of human mammary epithelial cells by autocrine human growth hormone*. Cancer Res. Jan 1;65(1):317-24.

Governmental advice report
Koëter et al. (2016) *Koëter H, Bout H, Hendriksen C, Prins J, Roelfsema P, de Leeuw W, Hameleers R, 2016 Transitie naar proefdiervrij onderzoek over mogelijkheden voor het uitfaseren van dierproeven en het stimuleren van proefdiervrije innovatie (https://www.rijksoverheid.nl/documenten/rapporten/2016/12/15/advies-transitie-naar-proefdiervrij-onderzoek)*

Books
Meuten, 2016 Meuten DJ (2016) *Tumors in Domestic Animals*, 5th Edition, Wiley-Blackwell, ISBN: 978-0-8138-2179-5

General discussion

For decades now, SCs have proven their significance with regard to neoplastic formations. Their undifferentiated nature, their capability of cellular proliferation, and their ability to shift towards a cancer stem cell phenotype has doomed them the primary suspects of cancer research. In this study, investigations performed on canine mammary tumour cell lines have contributed to the knowledge on the Wnt pathway signalling, and prepositions have been made concerning promising targets of this pathway. Although the cluster miR-96/182/183 did not yield the hypothesized results, it did show an interesting and highly significant response to the Src inhibitor Dasatinib. Both miR-182 and miR-183 were stimulated drastically by Dasatinib, and although miR-96 did not yield significant data it clearly followed the same pattern. Accordingly, correlation analysis of the 3 miRs only reinforces the believe that the miRs function as a cluster, and the lack of significance in miR-96 is most likely to be explained by its relatively low expression level. However, for now we are kept in the dark regarding the exact connection between Dasatinib treatment and the miR cluster, but due to the high significance this remains an intriguing concept for future research.

With miR-34a's reputation of being a tumour suppressor related miR, treatment with Wnt was expected to lower miR-34a levels. However, contradictory data was obtained. MiR-34a levels rose tremendously in response to Wnt stimulation, but did not respond to either Dasatinib or RSPO1. Thus, from this study the supposed tumour suppressor abilities of miR-34a were not substantiated, and its exact connection with the Wnt pathway should be further investigated before any definitive statements can be made.

Of all 5 investigated miRs, it was miR-203 that came up most promising with regard to the Wnt signalling pathway. Starting off with the irrefutable upregulation of this miRs in uniquely the high basal Wnt cell lines, it then continued yielding relevant and significant data during Wnt stimulation experiments. Concluding from these results, miR-203 is proposed to be the most suitable marker for Wnt activity as can be derived from this study. Yet again, extensive in-depth research should uncover what mechanism, or which mechanisms, are responsible for this connection. However, with this being the first data on canine mammary cancer research in relation to miR-203, we do believe to have unmasked a participant in carcinogenic developments of the mammary gland that has until now gone unnoticed.

Another objective of this study was to aid mammary cancer-related research by improving on mammary stem cell derived organoids. These could then subsequently be utilized for elucidating disease-related pathways and mechanisms, and could be further optimized to employ in drug testing, with the ultimate goal of developing a tool for personalized cancer treatment investigations. We have elucidated the effect of varying Wnt conditions on organoid differentiation and proliferation, and have therefrom selected concentrations that seemed most fit to either keep the organoid in a high proliferating, undifferentiated state, or contrarily, to promote stem cell differentiation into more specialized cell types. Against our own expectations, we have managed to culture the organoids over a surprisingly long period of time, thus yielding promising results for future organoid investigations to be performed at our laboratory. Additionally, organoid stainings have provided with knowledge on the exact cell types and their locations that can be found in stem cell derived structures, and how these develop over time and in relation to Wnt3a and RSPO1 concentrations. Overall, in this study a step forward in the development of mammary stem cell derived organoids has been achieved. This will hopefully aid the quest of finding a cure for both human and canine mammary gland cancer, a common disease that is all too often related to a grim prognosis with fatal results.

Acknowledgements

We greatly acknowledge Prof Dr Hellmen, SLU, Uppsala, Sweden and Prof. Sasaki, Laboratory of Veterinary Surgery, University of Tokyo, Japan for providing the tumour cell lines. Furthermore, we would like to acknowledge Hans Clevers, Hubrecht Institute, Utrecht, The Netherlands for providing the TOPflash and FOPflash reporter constructs. Furthermore we would like to acknowledge Calvin J. Kuo, Stanford University, California, for providing the Rspo1-Fc-expressing cell line, and Monique van Wolferen for preparing the RSPO CM therefrom.

Additionally, I would like to thank my supervisors Jan Mol and Elpetra Timmermans-Sprang for teaching me all laboratory skills required, and for guiding me through this year of research with ceaseless support and commitment. I would also like to acknowledge the CTO group for their support, and for sharing their thoughts and contributions. Also, special thanks to CTO group member Adri Slob for educating me in the skill of IHC stainings and cutting of the IHC slides (in cooperation with Saskia van Essen-van Dorresteijn, Department of Pathobiology) used for the performed stainings, and Ronald Kisjes (Veterinary Pathology Diagnostic Centre, Utrecht University) for processing the canine mammary tissues. Finally, a great thank you to many of the employees and students at the second floor of the Jeannette Donker-Voet building, Utrecht University, for creating such a pleasant atmosphere, for answering my questions and aiding me whenever assistance was required.

Attended courses

Presenting in English

On March 3 and 10, 2017, I attended the course *Presenting in English*, taught by Erick van den Bercken. I had signed up for this course due to my uncertainty when speaking for an audience, to improve upon my presenting skills and to learn a few tricks on how to make the presentation more interesting for the audience. I truly learned a lot from this course, I now know what to focus on when preparing the presentation, I've learned about body language, about figures and text colour in the PowerPoint. Also we focused on what language to employ when presenting, and how to deal with the 'Q&A' section at the end of a presentation. In conclusion, I'm very satisfied with the course, the atmosphere was pleasant, the teacher was highly educated, with more than sufficient knowledge on the subject and with the proper skills to pass some of his knowledge on to the students.

Academic Writing in English

From May 1, 2017, I attended the course *Academic Writing in English* by Hanneke van Nes. The course comprised 10 sessions, and throughout the course the entire structure of an academic English publication was discussed. Additionally, we focused on grammar, vocabulary and mistakes often made in academic publications. Also, the feedback we received on sections of our own work was very valuable, since one never learns as much as from his or her own mistakes.

Appendices

Appendice A: Abbreviations

Abbreviation	Description
αSMA	Alpha smooth muscle actin
AR	Antigen Retrieval
APC	Adenomatous polyposis coli
BSA	Bovine serum albumin
CCND1	Cyclin D1
CK	Cytokeratin
CK1	Casein kinase 1
CM	Conditioned medium
CMT	Canine mammary tumour
CTNNB1	β-catenin gene
DMPC	Dutch Molecular Pathology Centre
E-cad	Epithelial cadherin
EGFR	Epidermal growth factor receptor
EMT	Epithelial mesenchymal transition
EtOH	Ethanol
FBS	Fetal bovine serum
FZD	Frizzled
GH	Growth hormone
GSK3β	Glycogen synthase kinase 3β
HRP	Horseradish Peroxidase
IHC	Immunohistochemistry
LEF	Lymphoid enhancer-binding factor
LGR	Leucine-rich repeat-containing G-protein-coupled receptor
LRP	Low-density-lipoprotein-related protein
mQ	MilliQ, DNase- & RNase-free water
miR	MicroRNA
mRNA	MessengerRNA
MTT	3-[4,5-dimethylthiazol-2-yl]-2,5-diphenyltetrazolium bromide
NCBI	National Centre for Biotechnology Information
NGS	Natural Goat Serum
P#	Passage number
P4	Progesterone
P-cad	Placental cadherin
PBS	Phosphate Buffered Saline
Rpm	Rounds per minute
RSPO1	R-spondin-1
SC	Stem cell
SEM	Standard error of the mean
SRC	Proto-oncogene SRC
siRNA	Small interfering RNA
TBS	Tris-buffered saline
TNBC	Triple-negative breast cancer
Wnt	Wingless-type

Appendice B: Figures

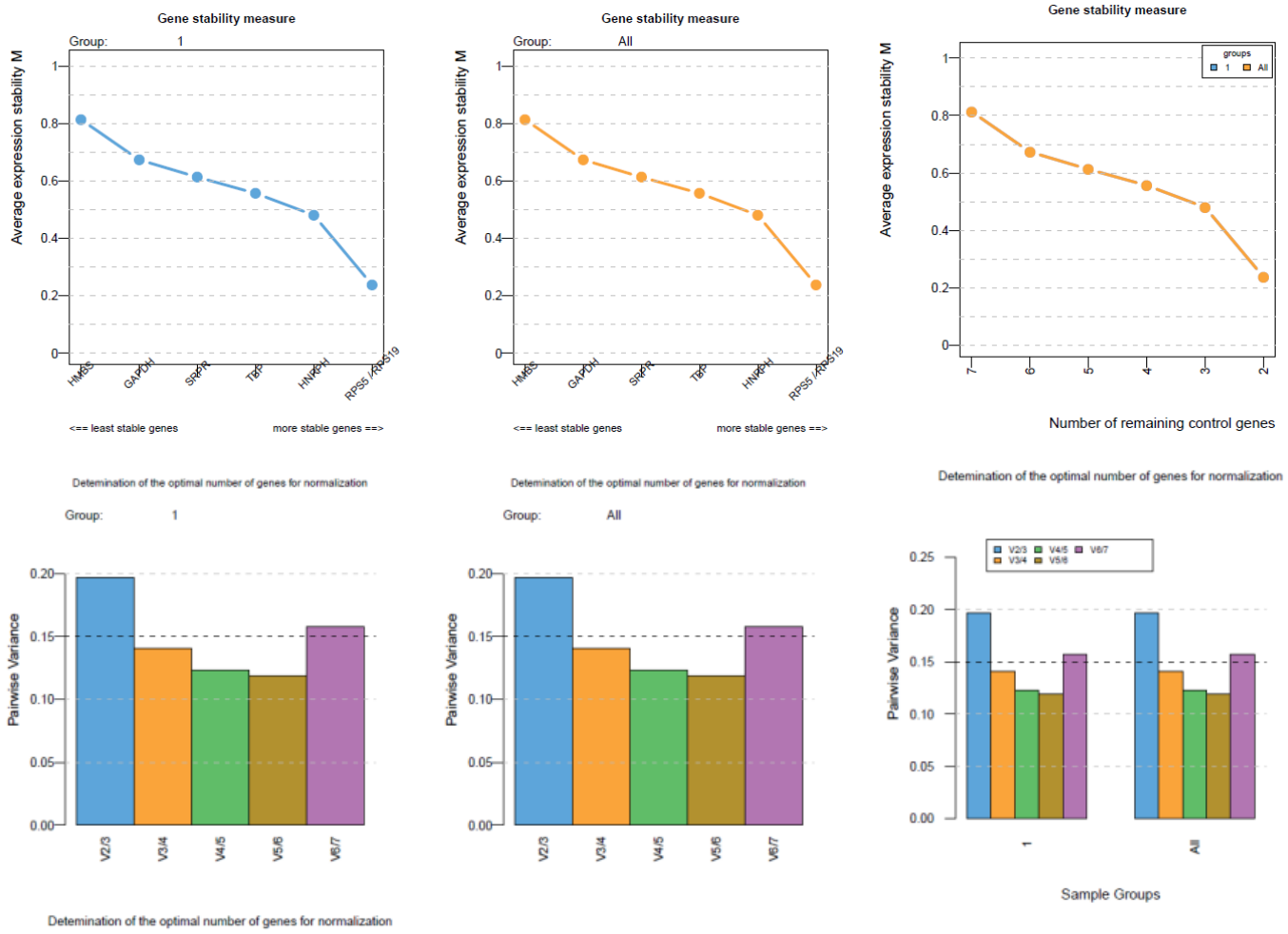

Figure 33 Stability and Variance, as obtained by geNorm.

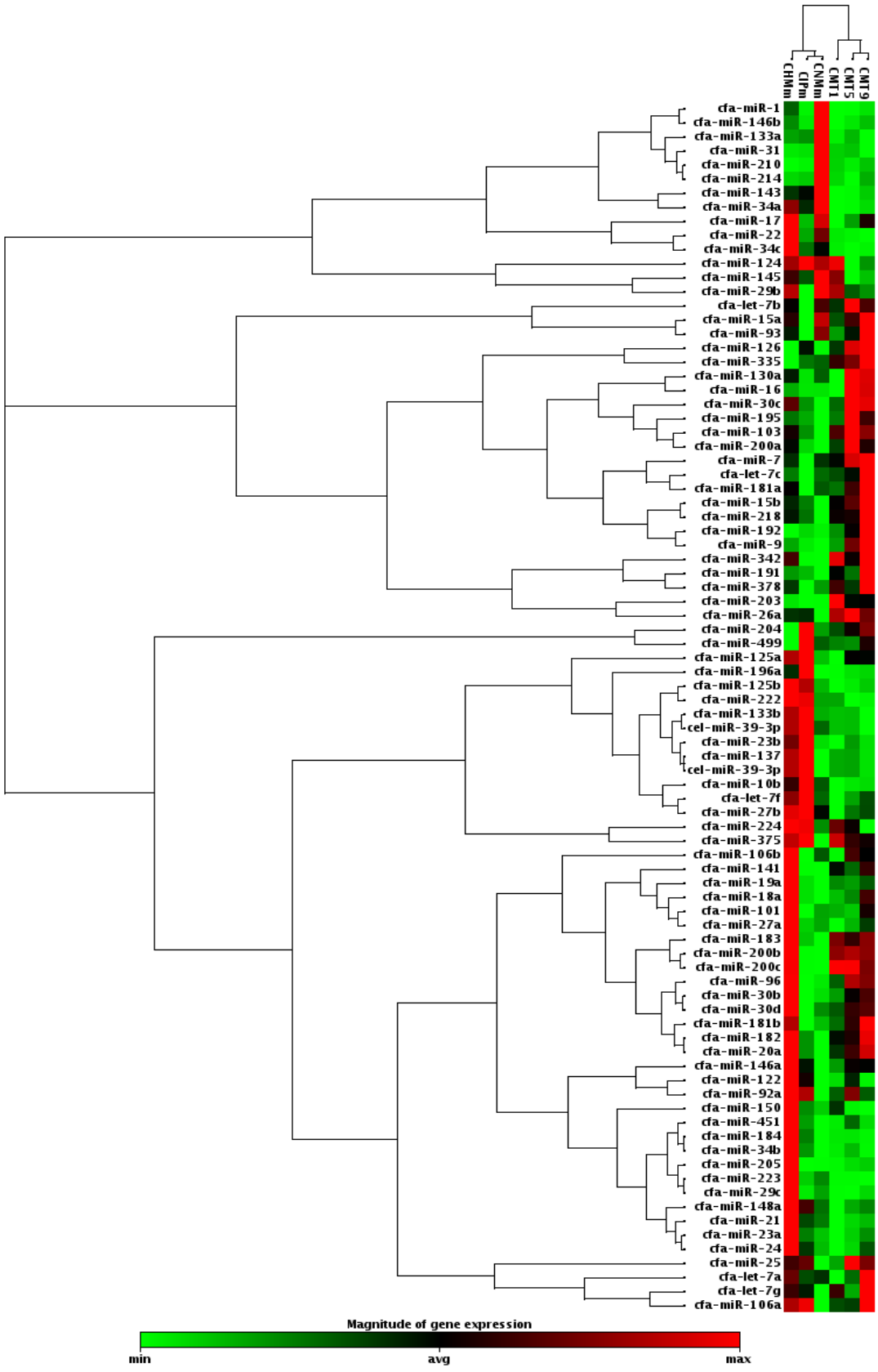

Figure 34 Clustergram for miFinder PCR Array
(http://pcrdataanalysis.sabiosciences.com/miR/arrayanalysis.php?target=clustergram)

Appendice C: Protocols

Protocol I *miRNA pipetting protocol*

Part I Reverse Transcription for Quantitative, Real-Time PCR

Procedure

1. **Thaw template RNA on ice. Thaw 10x miScript Nucleics Mix, RNase free water, and 5x miScript HiSpec Buffer at RT (15–25°C).**
   Mix solutions by flicking the tubes. Centrifuge briefly, store on ice.
2. **Prepare the reverse transcription master mix on ice (Table 3).** Gently mix, store on ice.
   Note: Remove miScript Reverse Transcriptase Mix from the –20°C freezer just before master mix preparation, mix gently, place on ice. Return mix to the freezer immediately after use.
   Note: If setting up more than one reaction, prepare a volume of master mix 10% greater than that required for the total number of reactions to be performed.

Spike-In control

3. Dilute 10 pmol dry stock in 300 µl RNase free water = 2 x 10^{10} copies/µl
4. Vortex gently, spin down → make aliquots, 10 µl per tube and store @ -20°C.
5. Dilute 3 µl stock with 12 µl RNase free water = 4 x 10^{9} copies/µl

Standard Curve

6. Add 2 µl of 4 x 10^{9} copies/µl dilution to 6 µl RNase free water as a carrier

Table 2. Spike-In Control - Reverse transcription reaction components
(p.27 miRNeasy Serum/Plasma Handbook 02/2012)

Component	Volume
miRNeasy Serum/Plasma Spike-In Control from step 6/7 (1 x 10^{9} copies/µl)	1.1 µl (1.1 x 10^{9} copies)
Total RNA sample*	1.25 µl (~100 ng)
5x miScript HiSpec Buffer	2 µl
10x miScript Nucleics Mix	1 µl
RNase-free water	3.65 µl
miScript Reverse Transcriptase Mix	1 µl
Total volume	**10 µl**

* Complex RNA background = *CMT-U27 Control*

Samples

7. Add 6 µl of 4 x 10^{9} copies/µl dilution to 144 µl RNase free water.

Table 3. Reverse transcription reaction components

Component	Volume/reaction	Mix
5x miScript HiSpec Buffer	1 µl	22 µl
10x miScript Nucleics Mix	0.5 µl	11 µl
RNase-free water	Variable → 1.5 µl	33 µl
miScript Reverse Transcriptase Mix	0.5 µl	11 µl
miRNeasy Spike-In Control (1.6 x 10^{8} copies/µl)	0.875 µl	19.25 µl
Template RNA (added in step 3)	Variable → 0.625 µl (Table 2)†	
Total volume	**5 µl**	**96.25 µl**

† If using RNA from serum or plasma samples prepared using the QIAGEN Supplementary Protocol: Purification of total RNA, including small RNAs, from serum or plasma using the miRNeasy Mini Kit, we recommend using 5 µl of the RNA preparation as a starting point.

8. Dilute RNA to 100 ng/µl → add 4.4 µl mix to each well, add 0.625 µl template RNA. Gently mix, briefly centrifuge, store on ice.

9. Incubate 4 strips for 60' at 37°C.
10. Incubate 5' at 95°C to inactivate miScript Reverse Transcriptase Mix, place on ice.
11. Proceed with real-time PCR, dilute 5 µl sample cDNA in 50 µl RNase-free water.
12. Add 100 µl in total of RNase-free water to the Standard Curve sample
    Note: If you wish to store the reverse transcription reactions prior to real-time PCR, transfer the undiluted cDNA to a –20°C freezer, or dispense the diluted cDNA into aliquots and transfer to a –20°C freezer.

Part II Real-Time PCR for Detection of Mature miRNA or Noncoding RNA

Procedure

1. Thaw 2x QuantiTect SYBR Green PCR Master Mix, 10x miScript Universal Primer, 10x miScript Primer Assay, template cDNA, and RNase-free water at RT (15–25°C). Mix the individual solutions.

Spike-In: Standard curve

2. Use the diluted reverse transcription reaction to prepare serial dilutions according to **table 4**.

Table 4. cDNA serial dilutions

Tube	cDNA	Water	Concentration spike-in control	Use in PCR
1	10 µl diluted cDNA	10 µl	5 x 10^6 copies/µl	2 µl (1 x 10^7 copies)
2	2.5 µl from tube 1	22.5 µl	5 x 10^5 copies/µl	2 µl (1 x 10^6 copies)
3	2.5 µl from tube 2	22.5 µl	5 x 10^4 copies/µl	2 µl (1 x 10^5 copies)
4	2.5 µl from tube 3	22.5 µl	5 x 10^3 copies/µl	2 µl (1 x 10^4 copies)

3. Using 2 µl from each tube in Table 4, set up separate PCRs according to Table 5.

Table 5. Reaction set up for real-time PCR – Spike-In Control

Component	Volume/reaction
2x QuantiTect SYBR Green PCR Master Mix	*5 µl*
10x miScript Universal Primer	*1 µl*
10x miScript Ce_miR-39_1 Primer Assay	*1 µl*
RNase-free water	*1 µl*
Template cDNA from table 5	*2 µl*
Total volume	***10 µl***

4. Add 8 µl mix to 4 wells in an 8-well strip, add 2 µl of S1 to well 1, S2 to well 2 etc. Mix thoroughly and proceed with PCR using the cycling conditions in Table 7.

5. Prepare a reaction mix (Table 6) for a 10 µl per well reaction volume (384-well plates).
   Reaction mix contains everything except the template cDNA. It is not necessary to keep samples on ice during reaction setup or while programming the real-time cycler.

Table 6. Reaction setup for real-time PCR Target miR genes

Component	Volume/reaction
2x QuantiTect SYBR Green PCR Master Mix	*5 µl*
10x miScript Universal Primer	*1 µl*
10x miScript Primer Assay	*1 µl*
RNase-free water	*Variable → 2 µl*
Template cDNA (added at step 3)‡	*≤1 µl*
Total volume	***10 µl***

‡ The volume of diluted cDNA should not exceed 10% of the final reaction volume. Volumes refer to cDNA prepared using the miScript II RT Kit with miScript HiSpec Buffer, and diluted according to Table 4. The final concentration of cDNA should be within 50 pg–3 ng per reaction.

6. Mix the reaction mix thoroughly but gently, add 9 µL into the individual wells (white plate).
7. Add 1 µl template cDNA to the wells with reaction mix.

8. Carefully, tightly seal the plate or disc with caps or film.
9. Centrifuge for 1' at 1000 g at RT to remove bubbles.
10. Program the real-time cycler according to Table 7.

Table 7. Cycling conditions for real-time PCR

Step	Time	Temperature	Additional comments
PCR Initial activation step	15 min	95°C	To activate HotStarTaq DNA Polymerase
3-step cycling:*			
Denaturation	15 s	94°C	
Annealing	30 s	55°C	
Extension	30 s	70°C	Perform fluorescence data collection.
Cycle number	45 cycles		

***** For Bio-Rad models CFX96™ and CFX384™: adjust the **ramp rate to 1°C/s.**

11. Place the plate in the real-time cycler and start the cycling program.

Protocol II *3D Mammary Gland Derived Organoid Isolation & Culturing*

November 25, 2016

Organoid selection

1 ml suspension from Dogs 1 - 5, 10072013 series from liquid nitrogen = column 2, box 8/9 (10-07-2013)
Turn on incubator at 37°C. Put 24-well culture plates from Greiner, cover removed, in the incubator at 37°C, > 24 h before plating the organoids.

*Solutions for organoid culturing**

Medium solution

DMEM/F12	40 ml
FBS (Gibco)	5 ml
Gentamycin (Gibco)	100 µl
Insulin (Sigma)	50 µl
Trypsin (Gibco, 10X Trypsin)	5 ml

Collagenase solution

Collagenase Type IV (Sigma, #C5138)	0,2 g in 25 ml DMEM/F12
Collagenase MIX IA (#C9891) 0.2 g, and #C9407 (for epithelial tissue), make a pool for all types, 0.13 g per type	
Shake at RT until dissolved (10 min)	

BSA solution

HBSS	100 ml
BSA	2.5 g
Shake at RT until dissolved (10 min), filter through 0,22 µm filter. Rinse all plastic pipettes (10 ml and the small tips) before pipetting the cell/organoid suspension	

BSA solution for dissolving additives

HBSS	100 ml
BSA	0.1 g

DNase solution

Prepare 10 tubes:	
200 units in 10 ml, final add 4 ml /tube	40 ml
DMEM/F12	100 ml
DNase	0.73 mg (2000 u)
Sigma, #D4138, 80 kU in 29.3 mg	

Basic organoid growth medium, 100 ml

Advanced DMEM/F12 (*Gibco, #12634-010*)	97.6 ml
P/S (100 times diluted)	1 ml
Glutamax (*#35050-038, (100X), Gibco*)	1 ml
HEPES (1M stock)	1.5 ml

Protocol **

1. Take the mammary gland tissue out of the liquid nitrogen, thaw as fast as possible using a 37°C water bath, and wash away the Cell Culture Freezing Medium (Gibco™ Recovery™, #12648-010, LOT 1808010) in a Petri Dish (#663161, LOT# F161233Q, Greiner Bio-one) with *Medium solution*, repeat twice.
2. Cut <0.5 cm^3 tissue into pieces until all clump together.
3. Add the tissue to a 50 ml tube (Greiner Bio-one) with 15 ml medium solution and put on ice.
4. Isolate all mammary tissue and collect in 50 ml tubes (max. 1 portion) on ice.
5. Add 0,5 cm^3 in 5 ml to a 15 ml tube (Greiner Bio-one) and add 5 ml collagenase. 10 tubes with Collagenase type IV and 10 tubes with Collagenase type IA and collagenase for epithelial tissue (mixed).
6. Shake the collagenase solution at 200 rpm and 37°C for 30 min. After every 5 min in the incubation step, take the tube out and shake it top/down. Shake the tube in the incubator top over top until there is a wave in the solution visible.
7. Incubate until the solution becomes unclear, +/- 25 min.
8. Centrifuge the tube at 1500 rpm for 10 min at RT. The tube will contain 3 layers: a fatty layer on top, an aqueous layer in middle and a pellet of epithelial cells on the bottom.
9. Remove the aqueous layer and the fatty layer. Make sure to keep the supernatant until the end of the experiment.
10. Add 10 ml DMEM/F12 to the pellet, pipette up and down to resuspend the pellet in the 10 ml solution.
11. Spin tube for 10 min at 1500 rpm.
12. Aspirate the supernatant and add 12 ml *DNase solution*, shake by hand for 5 min.
13. Spin tube at 1500 rpm for 10 min.
14. Aspirate the supernatant and resuspend the pellet in 6 ml DMEM/F12.
15. Put a 100 µm filter in a 50 ml tube and add the suspensions for each collagenase (final 2 50 ml tubes, one with collagenase type IV and one with 1A and epithelial tissue)
16. Differentially centrifuge to wash out the enzymes and to separate unwanted single cells from organoids; do a total of more than 4 times, until there are no single cells left in the supernatant (most of them are fibroblast). Plate the single cells apart, in matrigel (#354230, Corning, BD Biosciences, Breda, the Netherlands)
17. Aspirate supernatant, save supplement in 50 ml tube, make a suspension from the first supernatant with the single cells
18. Resuspend the pellet in 10 ml DMEM/F12
19. Pulse to 1500 rpm, then stop as fast as possible (+/- 30 sec)
20. Most organoids are left over in the pellet, so pool the pellets in an Eppendorf tube and spin 1 min at 1500 rpm to remove the remaining supernatant.
21. Cell count:
    Single cells
    A = 3.6 x 10^6 cells/ml

4 = 3.2 10^6 cells/ml

22. Spin down and take off the supernatant till there is ± 20 µl left
23. Calculate the desired amount of matrigel (60-80% matrigel final to the volume of the pellet (e.g. a 20 µl pellet with 80 µl matrigel)) and mix the matrigel by pipetting up and down before adding it to the organoids. 500 fragments per 25 µl matrigel, pipette the entire volume in one go and make droplets: 4 droplets per well on a 24-well Cell Culture Plate (Greiner Bio-one), try to avoid the formation of air bubbles.
24. *1st Plate setup*:

4O	4O	4O	4O	4O	A SC
AO	AO	AO	AO	AO	A SC
A Sup	A Sup	A Sup	A Sup	A Sup	A SC
4 SC	4 SC	4 SC	4 SC	4 SC	4 SC

25. Rotate the plates upside down and leave for a few min at RT so that the droplet can solidify with the least matrigel - plastic contact possible. When organoids attach to plastic this enables fibroblast growth.
26. Carefully place the plates upside down in the incubator, incubate at 37°C for 20 min.
27. Add 300 µl *Basic organoid growth medium* to the organoids (Table 3 Culture medium for Organoid culturing, 25/11/2016)

* *Culture medium also from: Huch et al., 2013; Boj et al., 2015; Sato et al., 2011*

** *Protocol based on basis protocol from mw. dr. R. (Renée) van Amerongen*
Adjustments by A. Gracanin

Protocol III *Organoid Passaging*

1. Discard medium, add 1.5 ml ice-cold *Basic organoid growth medium* to each well of a 24 well plate, pipette up-down 2 times, transfer organoids to 15 ml tubes (1 condition per tube)
2. Spin down 1' @ 1000 rpm @ 4°C, discard/pipette off supernatant
3. Wash once with 3 ml *Basic organoid growth medium*, spin down 1' @ 1000 rpm @ 4°C, discard supernatant. (if necessary, repeat this washing step once)
4. Add 60% (usually 0.5 ml) TrypLE Ex, resuspend 2 – 40 times with pipette volume selected at 150 µl, incubate for 2 min.
5. Spin down 1' @ 1800 rpm @ 4°C, discard supernatant
6. Wash 1 – 2 times with 3 – 15 ml *Basic organoid growth medium*, spin down 1' @ 1800 rpm @ 4°C
7. Transfer pellet to microcentrifuge tube, rinse the 15 ml tube with 1 ml *Basic organoid growth medium*, transfer to same microcentrifuge tube → spin down 1' @ 1800 rpm
8. Discard supernatant, leave as small a rest volume as possible without removing any organoids. (if necessary spin down 1' @ 1800 rpm again)
9. Add 4 times the rest volume of ice-cold matrigel to the microcentrifuge tube (so dilute organoids 5 times), resuspend the pellet without forming bubbles, pipette 4 droplets per well on a clean 37°C 24 Well plate (Greiner Bio-one). Leave for 20' upside down in stove, add 350 µl medium to corresponding wells.

Protocol IV *Tissue Obtainment*

Preparations

- Thaw Cell Culture Freezing Medium
- Attain Cutting Set with scalpel holder, tweezers and scissors
- Ensure access to sufficient number of Petri Dishes, scalpels and cryovials (Corning)
- Prepare sufficient HBSS+ PBS solution

Collecting sample

1. Preferably shave mammary tissue, wash with 70% EtOH
2. Collect at least mammary gland numbers 2 and 3, both left and right gland (Fig 35), keep on ice during transport
3. Collect corresponding blood sample, 1 ml minimum, in a heparin tube for P4 level

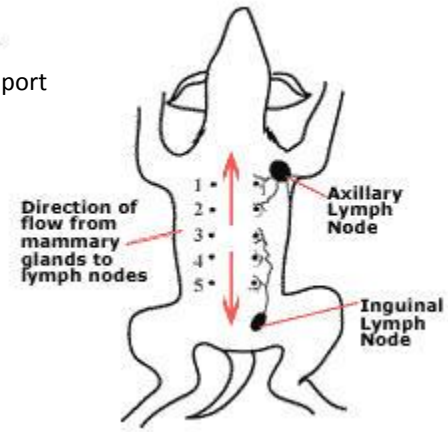

Figure 35 **Mammary gland numbering in dogs** http://www.lowchensaustralia.com/health/mammarytumors.htm

Dissection

1. Remove as much non-mammary tissue from mammary gland as possible (including hairs, fat, skin)
2. Collect up to 10 tissue pieces of 1 mm^3 in a 1.6 ml cryovial, add 1.0 ml Cell Culture Freezing Medium
3. Store the cryovials at -80°C in a Mr. Frosty (Nalgene®, Thermo Scientific)
4. Collect +/- ½ a gland in fixative (?) 10-20 x tissue volume, keep at RT for 2 days, discard fixative and add 70% EtOH
5. Collect +/- 2 cm^2 in a cryovial for RNA isolation

Protocol V *Organoid Embedding in Paraffin*

Note*: you will lose some organoids during washing, try using a full well/combine 2 wells*
Note*: when preparing organoids for storage in HBSS (up to a month), follow protocol up to and including* ***step 4***
Note*: 1 ml for relatively large amounts of organoids. When embedding fewer, adjust amount accordingly*

1. Discard medium, add 1.5 ml ice-cold Advanced DMEM. Spin down at 800 rpm for 5' at 4°C, discard supernatant.
2. Fix the organoids with 4% (500 µl) paraformaldehyde (PFA) + 1% (5 µl) eosin for 30' at RT.
   Note*: eosin for visualizing the organoids during the next steps.*
3. After fixation, wash 2x with HBSS.
4. Dehydrate the organoids using 1 ml :

- 25% EtOH 15'
- 50% EtOH 15'
- 70% EtOH 15'

Note*: Pipette off EtOH, make sure not to remove any organoids.*
Note*: Resuspend w/ pipette in between dehydration steps*
Organoids can be stored in 70% EtOH for up to a month.

5. Dehydrate the organoids in 1 ml 96% EtOH + 1% eosin for 30' at RT.
6. Continue dehydration with 1 ml :
   - 3x 20' 100% EtOH
   - 3x 20' n-butanol
     - After two rounds with n-butanol transfer the pellet + n-butanol to polystyrene 5 ml tube, dehydrate for 20'

○ Turn on Tek plate at 60°C

7. Add 1 ml histowax with a preheated plastic Pasteurs pipette, seal the styrene tubes with parafilm and impregnate 3 x 20 mins using a 65°C water bath.
8. Preheat a glass Pasteur pipette with a Bunsen burner. Transfer the organoids with the pipette to a small Tissue-Tek mold, move the organoids with the pipette to the middle of the block. Divide over 2 molds if many coupes are needed.

9. Once the organoids are in place, pour a little more paraffin on top of the organoids, carefully move the mold on ice to harden the paraffin a little.
10. Put the cassette on the mold and top up with warm paraffin. Harden the paraffin on ice and remove the mold.

Protocol VI *Organoid Staining – CK7*

Step	Additional information	Time (in minutes, unless indicated otherwise
Deparaffinize	**5 – 5 – 3 – 3 – 2 – 2**	30
mQ		5
Proteinase-K	**Dako**	40
TBS/T 0.1%		2 x 2
Peroxidase block	**Dako Ready to use**	10
TBS/T 0.1%		3 x 5
NGS 10%		30
1st AB	**In AB-diluent, DAKO), K7 – 1:25 (mouse**)	o/n @ 4°C
TBS/ T0.1%		3 x 5
2nd Antibody	**Goat anti-mouse, HRP**	45
TBS	**No Tween**	3 x 5
DAB		5
mQ		3 x 5
Haematoxylin	**QS-Dako**	30 sec
Running tap water		10
Dehydrate	**2 – 2 – 3 – 3 – 5 – 5 – 5**	30
Vectamount		
CK7:	*Dako, #M7018, 1:25*	
Neg. Control:	*Normal mouse IgG1, sc-3877 Lot# A1712*	

Protocol VII *Organoid Staining – CK19*

Step	Additional information	Time (in minutes, unless indicated otherwise
Deparaffinize	**5 – 5 – 3 – 3 – 2 – 2**	30
mQ		5
AR	**Proteinase K**	15
Buffer	**TBS/T**	2 x 2
Peroxidase block	**Dako Ready to use**	10
Buffer		3 x 5
NGS 10%	**in 90% TBS/T**	30
1st Antibody	**1:300**	o/n at 4°C
Buffer		3 x 5
2nd Antibody	**Goat anti-mouse, HRP**	45
Buffer	**TBS**	3 x 5
DAB		5
mQ		3 x 5
Haematoxylin	**QS-Dako**	30 sec
Running tap water		10
Dehydrate	**2 – 2 – 3 – 3 – 5 – 5 – 5**	30
VectaMount		

CK19:	*Novocastra, NCL-CK19 – Dilution 1:300*
	Mouse, in AB-diluent
Neg. Control:	*Normal mouse IgG1, sc-3877 Lot# A1712*
	AB-diluent

Protocol VIII *Organoid Staining – αSMA*

Step	Additional information	Time (in minutes, unless indicated otherwise
Deparaffinize	**5 – 5 – 3 – 3 – 2 – 2**	30
mQ		5
Peroxidase block	**Dako Ready to use**	30
PBS/T		3 x 5
NGS	**10% in PBS**	15
1st AB	**1:200, in PBS**	60
PBS/T		3 x 5
2nd AB	**Goat anti-mouse, HRP**	45
PBS		3 x 5
DAB		5
mQ		3 x 5
Haematoxylin	**QS-Dako**	30 sec
Running tap water		10
Dehydrate	**2 – 2 – 3 – 3 – 5 – 5 – 5**	30
Vectamount		

αSMA:	*1:200, IgG2a, MU128-UC, BioGene, Mouse anti-αSMA*
Neg. Control:	*Normal mouse IgG2a*
	AB-diluent

Protocol IX *Organoid Staining – E-cad*

Step	Additional information	Time (in minutes, unless indicated otherwise
Deparaffinize	**5 – 5 – 3 – 3 – 2 – 2**	30
MQ		2x5
AR	**Citrate**	20
Cool		20
Buffer	**PBS/T**	3 x 4
Peroxidase block	**Dako Ready to use**	10
Buffer		3 x 4
NGS 10%	**in PBS/T**	30
1st Antibody	**1:50, Diluted in 10% NGS in PBS/T**	o/n at 4°C
Buffer		3 x 4
2nd Antibody	**Goat anti-mouse, HRP**	30
Buffer	**PBS**	3 x 4
DAB		5
mQ		2 x 4
Haematoxylin	**QS-Dako**	30 sec
Tap water		10
Dehydrate	**2 – 2 – 3 – 3 – 5 – 5 – 5**	30
VectaMount		

E-cad:	*Mouse anti-Ecad*
Neg. Control:	*Normal mouse IgG1, sc-3877 Lot# A1712*
	AB-diluent

Protocol X *Organoid Staining – P-cad*

Step	Additional information	Time (in minutes, unless indicated otherwise
Deparaffinize	**5 – 5 – 3 – 3 – 2 – 2**	30
Buffer	**TBS**	2x5
AR	**TE**	20
Cool		20
Buffer		2x5
Peroxidase block	**Dako Ready to use**	10
Buffer		2 x 5
NGS	**10% + 90% buffer + 1% BSA**	30
1st Antibody	**First drawer bottom freezer, Pcad in mice, 1:100 In TBS + 10% BSA**	o/n at 4°C
Buffer		2 x 5
2nd Antibody	**Goat anti-mouse, HRP**	45
Buffer		2 x 5
DAB		5
mQ		2 x 5
Haematoxylin	**QS-Dako**	30 sec
Tap water		10
Dehydrate	**2 – 2 – 3 – 3 – 5 – 5 – 5**	30
VectaMount		

P-cad:	*First drawer bottom freezer, Pcad in mice, 86078945*
Neg. Control:	*Normal mouse IgG1, sc-3877 Lot# A1712*
	AB-diluent

Appendice D: Tables

Table 1 **Primer sequences used in quantitative RT-PCR**

miR	Primer	Sequence
miR-34a	SLR	UGGCAGUGUCUUAGCUGGUUGUUGUGAGUAAUAGUGAAGGAAGCAAUCAGCAAGUAUACUGCCCUA
	Probe	5'UGGCAGUGUCUUAGCUGGUUGU
Product #	218300	
Cat.	MS00030457	
miR-96	SLR	CUGCUUGGCCGAUUUUGGCACUAGCACAUUUUUGCUUGUGUCUCUCCGCUCUGAGCAAUCAUGUGCAGUGCCAAUAUGGGAAAAGCGGG
	Probe	5'UUUGGCACUAGCACAUUUUUGCU
Product #	218300	
Cat.	MS00031192	
miR-182	SLR	GCUUGCCUCCCGCCGUUUUUGGCAAUGGUAGAACUCACACUGGUGAGGUAAUGGGAUCCGGUGGUUCUAGACUUGCCAACUAUGGUGCGAGG
	Probe	5'UUUGGCAAUGGUAGAACUCACACU
Product #	218300	
Cat.	MS00029743	
miR-183	SLR	UAUGGCACUGGUAGAAUUCACUGUGAACAGUCUCGGUCAGUGAAUUACCGAAGGGCCAUAAA
	Probe	5'UAUGGCACUGGUAGAAUUCACU
Product #	218300	
Cat.	MS00029750	
miR-203	SLR	CCCGGCGCGCUGGGUCCAGUGGUUCUUAACAGUUCAACAGUUCUGUAGCGCAAUUGUGAAAUGUUUAGGACCACUAGCCCCGGCGGGCCCGGCG
	Probe	5'GUGAAAUGUUUAGGACCACUAG
Product #	218300	
Cat.	MS00029988	
miR-39	SLR	UAUACCGAGAGCCCAGCUGAUUUCGUCUUGGUAAUAAGCUCGUCAUUGAGAUUAUCACCGGGUGUAAAUCAGCUUGGCUCUGGUGUC
	Probe	5'UCACCGGGUGUAAAUCAGCUUG
Product #	218300	
Cat.	MS00019789	
	SLR = Stem-loop reverse	

Table 2 **Gene table for Q-PCR primers**

Gene	Forward/Reverse	Genbank Acc. #	Product length	Tm (°C)	Sequence 5' → 3'
CCND1	F	NM_001005757.1	117	60	GCCTCGAAGATGAAGGAGAC
	R				CAGTTTGTTCACCAGGAGCA
GSK3β	F	XM_851518.2	105	64	CGGAAACAGTATACAGAGTTGC
	R				TAGGCTAAACTTCGGAACAG
LEF1	F	XP_863334.2	137	60	AGACATCCTCCAGCTCCTGA
	R				GATGGATAGGGTTGCCTGAA
GAPDH	F	NM_001003142	100	58	TGTCCCCACCCCCAATGTATC
	R				CTCCGATGCCTGCTTCACTACCTT
HNRPH	F	XM_538576	151	61[2]	CTC-ACT-ATG-ATC-CAC-CAC-G
	R				TAGCCTCCATAACCTCCAC
RPS5	F	XM_533568	141	62[5]	TCACTGGTGAGAACCCCCT
	R				CCTGATTCACACGGCGTAG
RPS19	F	XM_533657	95	61/63	CCTTCCTCAAAAAGTCTGGG
	R				GTTCTCATCGTAGGGAGCAAG
SRPR	F	XM_546411	81	61[2]	GCTTCAGGATCTGGACTGC
	R				GTTCCCTTGGTAGCACTGG
TBP	F	XM_849432	96	57	CTATTTCTTGGTGTGCATGAGG
	R				CCTCGGCATTCAGTCTTTTC

Table 3 **Culture medium for Organoid culturing, 25/11/2016**

	1 ml	**High**	**Medium**	**Low**
Medium	*900 µl*	300 µl	650 µl	930 µl
WCM **5%**	*50 µl*	500 µl	250 µl	50 µl
RSPO1 medium **2%**	*20 µl*	200 µl	100 µl	20 µl
hNoggin	*1 µl*	1 µl	1 µl	1 µl
hEGF	*0.5 µl*	0.5 µl	0.5 µl	0.5 µl
P	*1 µl*	1 µl	1 µl	1 µl
A83	*1 µl*	1 µl	1 µl	1 µl
Nico	*10 µl*	10 µl	10 µl	10 µl
Y-27632/ROCK	*1 µl*	1 µl	1 µl	1 µl
FGF10	*1 µl*	1 µl	1 µl	1 µl
N-Acetyl Cysteine	*2 µl*	2 µl	2 µl	2 µl
GH	*4 µl*	4 µl	4 µl	4 µl
B27	*20 µl*	20 µl	20 µl	20 µl
SB20219*	*0.33 µl*	0.33 µl	0.33 µl	0.33 µl

* First added *16 / 12 / 2016*

Table 4 **Staining, Antibody properties**

Staining	**Target location**	**Target cells**	**Positive control**	**IgG**	**Dilution**	**Negative control**	**Antibody**
E-Cad	Luminal epithelium	Glandular cells	Colon	Mouse IgG1	1/100	Colon	Invitrogen,180223
P-Cad	Basal part of myoepithelial cells	Just below epidermis	Skin	Mouse IgG1	1/100	Mammary tissue	BD, 610227
CK7	Luminal epithelium and basal cells	Mainly glandular epithelium	Liver	Mouse IgG1	1/25	Mammary carcinoma	DAKO, M7018
CK19	Luminal epithelium	Glandular cells	Colon	Mouse IgG1	1/300	Mammary carcinoma	Novocastra, NCL-CK19
αSMA	Myoepithelial cell	Smooth muscle cells, stromal cells and myoepithelial cells	Colon	Mouse IgG2a	1/200	Mammary carcinoma	BioGenex, MU128-UC

Table 5 **Transfection solutions**

Solution	*WCM, µl*	*(%)*	*RSPO1, µl*	*(%)*
1	450	5		
2	1800	20		
3			180	2
4			900	10
5	450	5	180	2
6	450	5	900	10
7	1800	20	180	2
8	1800	20	900	10